Departament de Teoria
del Senyal i Comunicacions

UNIVERSITAT POLITÈCNICA DE CATALUNYA

PHILOSOPHY DOCTOR THESIS

INVESTIGATION OF REFLECTIVE OPTICAL NETWORK UNITS FOR BIDIRECTIONAL PASSIVE OPTICAL ACCESS NETWORKS

Author
Cristina Arellano Pinilla

Advisor
Josep Prat Gomà

JUNE 2007

Philosophy Doctor Thesis

Optical Communications Group
Department of Signal Theory and Communications
Universitat Politecnica de Catalunya

INVESTIGATION OF REFLECTIVE OPTICAL NETWORK UNITS FOR BIDIRECTIONAL PASSIVE OPTICAL ACCESS NETWORKS

Author

Cristina Arellano Pinilla

Advisor

Josep Prat Gomà

Thesis presented in fulfilment of the doctorate program of the signal theory and communication department
Polytechnic University of Catalonia
June 2007

To everyone who believed in me
A todos los que creyeron en mi

Acknowledgments

There are many people who I would like to thank for accompanying me during the last four years.

First of all, I want to express my gratitude to my advisor Professor Josep Prat for having given to me the opportunity to develop my PhD. within the Optical Communications Group (GCO). He was always a reference to me and a guide throughout the thesis work.

These investigations would not have been possible without the active involvement of the full team of the GCO. I am indebted to Victor Polo for his laboratory assistance and for teaching me his practical experience. Special thanks to Carles Bock with whom I shared most of the time and experiences during this period. A warm thank to all the colleagues for making every day an enjoyable atmosphere at the office, also to those who do not belong to the GCO anymore.

I sincerely appreciate very much the kind welcome at the Heinrich-Hertz-Institut in Berlin. I would like to thank my advisors there Klaus-Dieter Langer, Ronald Freund and Godehard Walf. Also to all who helped me in the laboratory, Lutz Molle, Christian Paul and to the memory of Fritz Raub. And of course, thanks to all the colleagues of the Photonics Networks department, especially to Matthias Seimetz and my lovely friend Jelena Grubor.

I would like to thank the University College of London, especially Ed Burr for his laboratory assistance. Moreover, I am grateful to Antonio Teixeira and Tiago de Silveiro for their support. Thanks to the University of Essex and to Manoj Thakur for the good experiments preformed there and their hospitality.

Thanks to the people at Tellabs and especially to Muneer Zuhdi for the interest that he has always demonstrated.

On the personal level, I would like to thank to my family. Thanks to my parents and to the unconditional Sonia and Wolfgang, for multiple forms of support.

The last four years have been a great experience for me. I had the pleasure to meet and talk with many admirable persons from around the world. I learnt to compete and to defend my work; I laughed and I cried. Definitely -I would do it again.

The performed work was funded by the Spanish Ministry of science and education by the FPI grant associated to the investigation project TIC2002-00053 and supported by the European e-Photon/ONe Network of Excellence.

Abstract

This research was conducted to deal with the problem of finding cost-effective solutions for Fibre-to-the-Home (FTTH) network deployment. In the FTTH network, the transceiver at the user premises and the deployment of fibre at the last mile are the major barriers.

A single-fibre topology to address each user reduces the amount of fibre required; passive optical components alleviate maintenance requirements in the access network.

The Rayleigh backscattering effect is identified as the most critical crosstalk in such transmission, the effect on the system performance and the investigations of possible solutions are presented in this thesis. The studies reveal that despite the Rayleigh backscattering crosstalk can not be totally eliminated, several techniques can mitigate the effect.

The use of the semiconductor optical amplifiers to feature transceiver tasks at the user premises adds simplicity to the network design in terms of wavelength transparency and amplification capabilities. We propose implementations with semiconductor amplifiers and test modulation and detection potentials inside the optical network.

The experimental results successfully demonstrate modulation and detection at 1Gbit/s and 2.5Gbit/s with semiconductor-based devices, in links of 30km and even though of 50km length; bit rate of 10Gbit/s is feasible with novel prototypes as well.

Reflective structures based on reflective semiconductor optical amplifiers are potential candidates, as they perform transmission functions efficiently and provide adequate amplification however, it is necessary the design of further structures capable of transmitting at a higher bit rates.

Table of Contents

Chapter 1

Introduction

1.1 Network Evolution Driving Context

Fibre-to-the-Home technology is one of the main research objectives of the lasts years in optical fibre communication. The increasing development of data communications and the emerging of applications demand a redesign of the access networks in order to accomplish new bandwidth and latency requirements. Wireless communications are a good alternative for quick deployments and low cost implementations but this technology can not compete against optical communications in terms of available bandwidth, latency and robustness. Access optical networks are capable of solving those requirements for present and future applications.

The recent explosive growth of the internet has triggered the introduction of broadband access network based on FTTH. This trend will dramatically accelerate from now due to further progress in services. To deal with various demands, access and metro networks require scalability in terms of capacity and accommodation and flexibility with regard to physical topology. The introduction of technically mature WDM technologies, that are cost effective in core networks, to support access and metro is expected to offer new scalable and flexible access networks. Therefore, new specific components are required. The advanced high speed technology of core networks is expected to provide cost-effective migration of the component solutions towards access applications; however, improvements in terms of the integration of functions and low cost packaging have to be made.

In order to achieve cost effective solutions for FTTH, present investigations are centred in access networks which mainly use passive optical components to avoid the use of power sources and costly control equipment between the central office (Optical Line Termination - OLT) and the user premises (Optical Network Unit - ONU). The ONU has a direct impact en the cost capital expenditures (CAPEX) per customer, that is the amount used during to acquire or improve long term assets.

The size of the outside plant is also critical when deploying an access network. The number of kilometres of fibre that are deployed and the number of optical fusions needed to connect the ONUs to the OLT depends not only on the network topology but also on the number of fibres used for the transmission. Therefore, in the direction of a cost affordable FTTH system, it is reasonable to consider a single-fibre outside plant for reducing the amount of fibre to deploy the access network. Despite this architecture is very attractive, it presents an important limiting effect which is the Rayleigh Backscattering. Due to signals propagating in opposite directions, there is a crosstalk between the signal travelling in one direction and the backscattering from the signal that travels in the opposite direction.

1.2 Motivation

Bidirectional single-fibre strategy seams to be the most interesting architecture in terms reducing the CAPEX though this requires new ONU designs hence the ONU becomes a key element in access networks and an interesting area of investigation. For a total successful FTTH deployment the network unit model should be simple, robust, flexible and cost-available for the final customer.

The translation of the requirements mentioned above into technical specifications establish the following guidelines for the design of the FTTH ONU as

- Single-Fibre Solution Design to reduce network size
- Wavelength Independency (Colourless) to allow transparent in WDM operation
- Without Active Light Source to prevent stabilization and provisioning at the customer premises
- Amplification to increase the number of users and achieve longer distances

These are the fundamental drivers of this thesis work.

1.3 Objectives

The main objective of this thesis is the investigation of reflective optical network units, especially those based on semiconductor optical amplifiers, as well as

their performance into a FTTH solution, based on WDM-PON access technology. This basically implies

- to identify the proposed architectures and devices by means of the investigation of the related published work and highlight limitations and requirements of the current systems
- to evaluate the different alternatives for implement the ONU and propose improved solutions through simulations and experiments
- to investigate possible limitations in bidirectional single-fibre transmission systems and present solutions to deal with bidirectional transmission impairments
- to develop analytical descriptions for the signals involved in the transmission and for the system performance.

1.4 Thesis Overview

This dissertation can be divided into two general topics. Chapters two to five treat aspects concerning to the optical network unit and the implementation with semiconductor amplifiers. The second part, chapters six to nine, covers features of bidirectional transmission. The thesis is organized as follows.

In chapter two, an overview of the state of the art of WDM-PON is exposed. There is established the network framework of this research as well as the actual standardization of passive optical networks.

The next chapters, three and four, are devoted to the investigation of the optical network unit. First, we review and evaluate the existing techniques and architectures and then we propose and study advanced configuration based on reflective SOA devices.

The fifth chapter investigates semiconductor amplifiers. The basic characteristics of SOAs are analytically studied in order to setup laboratory prototypes for the characterization of the principal parameters involved in the transmission. The characterization of the integrated SOA saturated-absorber was due to the collaboration with the HHI and the laboratory assistance of W. Brinker, from HHI. The charactherization of the RSOA was in part due to the collaboration with the UCL and the laboratory assistance of E. Burr for the time measurements.

In chapter six, we give an overview of general aspects of bidirectional transmission. Following, in chapter seven there is set up the analytical model for the transmission impairments, characteristic from the transmission over a single fibre, which are Rayleigh backscattering and single reflections.

After, in chapter eight, we propose and experimentally demonstrate techniques capable of mitigating the Rayleigh backscattering crosstalk. The experiment of Ethernet transmission with subcarrier multiplexing modulation

over the RSOA was carried out at the University of Essex. V. Polo from UPC assisted in the network experiments performed at UPC.

In the end, chapter nine covers the influence of the amplification applied at the ONU in the system performance. The upstream interferences are defined and analytically described and the evolution of the interferences regarding significant parameters is studied. Then, a general expression for the crosstalk-to-signal ratio including all the interferences is given. Furthermore, simplifications considering the system exempt of reflections and only affected by RB and the influence of the location of the distribution element are treated in this chapter. Afterwards, we deduce an expression for the Q-parameter function of the gain at the ONU. And finally the influence of the gain at the ONU is experimentally verified.

Finally, the last chapter summarizes the knowledge gained throughout the research and present conclusions and recommendations for further research as well as some remarks on the findings.

The performed work was funded by the Spanish Ministry of science and education by the FPI grant associated to the investigation project TIC2002-00053 and supported by the European e-Photon/ONe Network of Excellence.

Chapter 2

State of the Art

This chapter summarizes the current state of the art of the aspects concerning this thesis work. WDM-PON technology and basic architectures are first described. Following, aspects with reference to the standardization as well as differences between the two main trends Ethernet-PON and Gigabit-PON are exposed. Then we illustrate with a brief explanation about FTTH deployment around the world. And at the last section we expose the history and the state of the art on semiconductor optical amplifiers technology applied to the access network.

2.1 WDM-PON

In recent years, power splitting Passive Optical Networks (PONs), active optical networks and direct point-to-point (p2p) optical links have become very popular for provisioning broadband access to communication networks. They benefit from highly sharing of either the OLT or a meshed access network with active remote nodes, or from a simple link design. The choice strongly depends on the conditions present in the area to be supplied. These systems usually offer aggregated data rates of up to few Gbit/s (GPON, EPON) or provide point-to-point (p2p) links according to the Ethernet standard (Ethernet in the first mile). Recent EPON developments are directed towards 10Gbit/s. The traditional role of WDM in these systems is to enable single fibre solutions by means of band-wise direction division multiplexing (BWDM). The major aim of using WDM to a larger extent is to provide cost-efficient virtual p2p links in a clearly arranged access network layout, while avoiding the major drawbacks of the above

mentioned solutions. Thus, the drivers are sharing of fibre infrastructure and independent multi-speed multi-protocol links operating continuously (non-burst mode). Such links offer high privacy and enable speed-up of single ONUs (bandwidth on demand). Further issues are unbundling of services/networks and extension/upgrade of standard optical networks. Fig.2.1 illustrates the corresponding development of WDM in the access network domain.

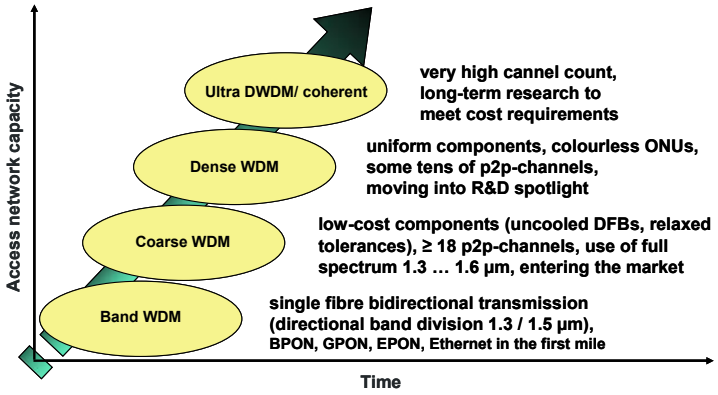

Fig.2.1 Evolution of WDM technology in optical access networks

Thus, WDM will be initially used for overlay or upgrade of already existing systems, or will be introduced directly in green-field deployment scenarios. CWDM technology is ready for such applications and is currently entering the market. Soon, we expect a more extensive use of wavelengths channels in terms of DWDM technology. Most crucial then is to avoid wavelength specific equipment as far as possible, at least at the ONU. In the more distant future, ultra dense WDM or coherent systems may appear in the access domain if they can further enhance cost-efficiency. In a nutshell, the present R&D on WDM-PON technology aims to achieve very simple, cost-efficient, easy-to-operate, and future-proof solutions using passive access networks based largely on uniform components.

2.2 Network Reference Scenario

Passive optical network is an access technology based on the specification developed by the Full Service Access Network (FSAN) [1]. PON networks elements consist of Optical Line Terminals (OLT) located in the central office or in the head end of the CATV provider, Optical Network Units (ONU) which are the interface between optical fibre and copper-based wiring near the user's level. In a FTTH scenario, the ONU is positioned at the home user. Passive splitters divide the downstream signal from the OLT at the network edge into multiple, identical signals that are broadcast to the subtending ONUs. Each OLT/ONU is responsible for determining which data are intended for it, and for

ignoring all others. Upstream signals are supported by a Time-Division Multiple Access (TDMA) scheme, with the transmitters in the ONUs operating in burst mode.

The purpose of the FTTx access network is to bring optical fibre to the final customer. Depending on the applications supported and on the distance between the OLT and the ONU, there are defined different configurations for the FTTx technology: Fibre-to-the-Home (FTTH), Fibre-to-the-Building/Curb (FTTB/C) and Fibre-to-the-Cabinet (FTTCab).

The network reference scenario comprising this dissemination is a Fibre-to-the-Home configuration, illustrated in Fig.2.2. The OLT provides the network-side interface of the access network and is connected to one or more optical distribution networks (ODNs); the ONU provides (directly or remotely) the user-side interface of the access network and is connected to the ODN. Thus, each home is connected with a fibre to the backbone network. A fibre to the home network offers a bandwidth for carry out applications that require a high bit rate as high definition music, photo sharing, research, learning, gaming, movies, punctual sport matches or work at home. In order to achieve cost effective solutions at present investigations are centred in access networks which mainly use passive optical components to avoid the use of power sources and costly control equipment between the OLT and the ONU.

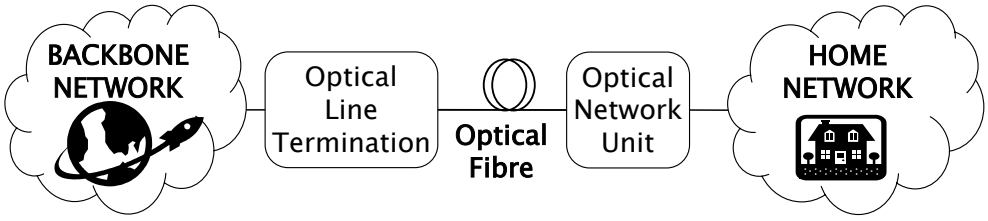

Fig.2.2 Network reference scenario

2.3 Basic WDM-PON Architectures

To roughly classify WDM-PON architectures we have to distinguish between two cases: using identical wavelengths for downstream and upstream transmission and using different ones. In the first case, the transmission performance is mainly limited by reflections (Rayleigh backscattering and discrete reflections). One way to overcome this problem is to use dual fibre transmission on at least the dominant section of the link (usually the feeder, which implies sharing of the directional coupler), see Fig.2.3a, b. Low-cost electronics employing either sub-carrier multiplexing (SCM) or forward error correction (FEC) can efficiently mitigate these effects [2], [3], thus enabling pure single fibre solutions (Fig.2.3 d). Alternatively, the backscatter subject can be

bypassed by using different wavelengths for downstream and upstream transmission. However, the splitting or accumulation of signals at the remote node (RN) then needs a special solution. One way is to use an arrayed waveguide grating (AWG) as a splitter/combiner and to exploit its free spectral range by choosing the matching upstream and downstream wavelengths.

From an easy (and low-cost) deployment and installation point of view, it is beneficial to use a single fibre solution (Fig.2.3c, d). However, there may be technical reasons (such as a special ONU design) for using two fibres on the distribution segment (Fig.2.3e).

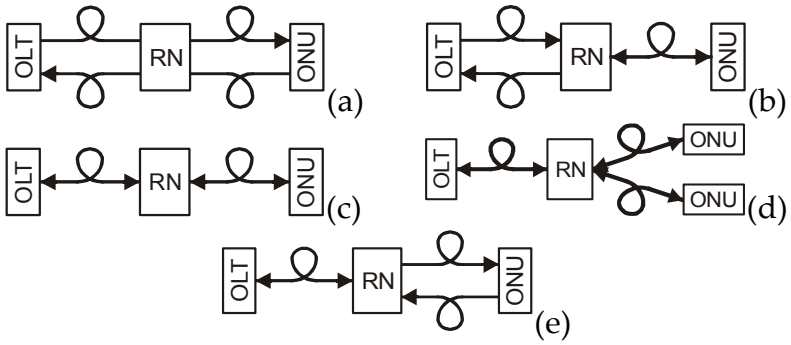

Fig.2.3 Options with dual or single fibre links in the feeder and distribution sections

With respect to simple and uniformly designed WDM-capable optical interfaces, there are two key techniques to create WDM carriers. At the OLT spectral slicing can be used, whereas at the ONU (besides reflective elements) wavelength agile devices such as injection-locked Fabry-Perot lasers (FP-LD) are considered.

2.4 Standardization

There are several recommendations concerning passive optical networks (PONs); the ITU-T G.983 Broadband Passive Optical Network (BPON) [4], the ITU-T G.803.2ah Ethernet Passive Optical Network (EPON) [5] and ITU-T G.984 Gigabit-capable Passive Optical Network GPON [6]. They offer different degrees of service and network performance. The next chart resumes the principle characteristics of the actual standards (Table 1).

The GPON recommendation shows unprecedented performance and flexibility with respect to the BPON and EPON standards, since different combinations of bit rate for up and downstream are feasible; as well a larger number of subscribers with guaranteed quality of service (QoS) are possible. The EPON recommendation, which concerns Ethernet traffic networks, is not so flexible and the number of users is limited.

Moreover, there are specific recommendations for coarse WDM networks (CWDM) enclosed in the ITU-T G.695 Optical interfaces for Coarse Wavelength Division Multiplexing applications, and the ITU-T G.694.2 Spectral grids for WDM applications: CWDM wavelength grid standards.

	BPON	EPON	GPON
Standard	**ITU G.983**	**IEEE803.2ah**	**ITU G.984**
Data Packet cell Size	53 bytes (48 payload and 5 overload)	1518 bytes	Variable size, from 53 bytes up to 1518 bytes
Maximum Bandwidth	Downstream: 1.2Gbit/s Upstream: 622Mbit/s	Up to symmetric 1.25Gbit/s	Downstream: configurable from 1.2Gbit/s up to 2.5Gbit/s. Upstream: configurable in 155Mbit/s, 622Mbit/s, 1.25Gbit/s or 2.5Gbit/s
Wavelength	Downstream: 1480nm to 1500nm Upstream: 1260nm to 1360nm	Downstream: 1550nm Upstream: 1310nm	Downstream: 1480nm to 1500nm Upstream: 1260nm to 1360nm
Maximum logical reach	20 km	20km	60km
Traffic Modes	ATM	Ethernet	ATM, Ethernet, TDM
Voice	TDM	VoIP or TDM	Native TDM
Video	1550nm overlay	1550nm overlay	Either as RF or over IP
ODN Classes Supported	A, B and C	A and B	A, B, and C
Max. PON Splits	32	16	64

Table 1 Basic PON characteristics

Nevertheless, following the trends, the natural step is 10GPON, enlarging the link up to 100km and removing the metro network, thus the access network could be directly connected to the core network but it is still not clear which of the techniques will remain.

Regarding the two main families GPON and EPON, there are several differences between the standards. Even though both technologies are capable of offering similar services, on the whole, GPON offers more facilities but it's more complex, EPON is more cost-effective and simple but it has less facilities. For instance, an EPON system supports symmetric bit rate for the up and downlink, whilst the GPON standard considers both, symmetric and asymmetric configuration. Moreover, EPON supports Ethernet traffic and GPON is able to carry three different types: ATM, Ethernet (data) and TDM (voice). Additionally, GPON can arrive to more users and longer distances.

GPON or EPON? This is a difficult question to answer since few years ago. A large number of documents have been written and discussions made in order

to clarify the future of PONs. There are extreme positions. Ones say that EPON will not be in the future and GPON groups believe the opposite. The main inconvenient in GPON system is the costs of components; however it is decreasing and being comparable with Ethernet equipment. On the other hand, the major drawback in EPON is that IP traffic does not carry high quality audio and video traffic by nature, but new protocols as GMPLS appears to deal with this fact. Therefore there is no clear evidence of which technology will remain. It could be reasonable to think than in a residential FTTH environment GPON would fit better due to its capability of triple play services, whilst in business areas EPON could be more suitable. In contrast, the market tendencies do not match exactly with the last reasoning. The FTTH system in Japan employs EPON systems and in the USA the deployment is BPON/GPON.

The subsequently question is then 10-GPON or 10-EPON upgrading? Which will be the most cost-effective? In [7] two different upgrading scenarios are exposed for EPON: wavelength upgrade and spatial-upgrading. In [8] a 10-EPON system using WDM is proposed. To allow incremental upgrade cost, only a subset of ONUs may be upgraded to operate at higher rates. Thus, there will be an intermediate step where some ONU operate at 1Gbit/s and some at 10Gbit/s. In the following it is exposed some upgrading scenarios.

EPON upgrading scenarios

Wavelength-upgrade scenario: some of the EPON ONUs will migrate to new wavelengths for both upstream and downstream traffic. While data rate on each wavelength will remain the same, there will be a small number of ONUs for sharing that bandwidth capacity. This procedure can be repeated again in the future and eventually will lead to a WDM-PON system where each subscriber is allocated its individual wavelengths. This, denoted as WDM-EPON system, could maintain the ranging protocol. The OLT should process more data but it is not difficult. Besides, it is requires an ONU more complex, capable of generating data in different wavelengths.

Spatial upgrade scenario: some ONUs migrate to a new PON network. Thus, a 1:32 EPON may become two 1:16 EPONs, leading to a p2p architecture with an independent fibre running to each subscriber. In this spatial upgrading no different equipment neither protocols are required, however the cost of migration of the fibres could be difficult to carry out.

GPON upgrading scenarios

In a GPON system the problem for increasing the bit rate and the number of users at the last loop is the power consumption, as much users, much power is required [9]. Passive amplification can be obtained with Semiconductor Optical Amplifiers (SOAs) and Erbium Doped Fibre Amplifiers (EDFAs). As well, novel modulators can solve this fact. Semiconductor amplifiers (EAM+SOA, RSOA) can be used for both, modulation and amplification at 2.5Gbit/s or 10Gbit/s. In [10], a Super PON with 512 users at 2.5Gbit/s and 128 users at 10Gbit/s in the upstream transmission is evaluated achieving good performances. The SARDANA network, reported in [11] supports transmission up to 100Km and 1024 users with RSOA at bit rate 1.25Gbit/s; or transmission up to 50Km and 1024 users with RSOA at bit rate 2.5Gbit/s. However, it should be mentioned that the important issue in GPON upgrading remains in upstream synchronization of dynamic band sources, denoted as dynamic bandwidth allocation.

2.5 FTTx Deployment

FTTH began with several field trials around the world: *Broadband* in Sweden, *Fastweb* in Italy, and *Canet2* in Canada. The technology used on first field trials was conventional; two fibres for each user and point-to-point connexions. Although this is a straightforward solution, the costs of the outside plan increase with the numbers of users.

In order to reduce network size and complexity several research projects have been running on this field: GIANT (GIgapon Access NeTwork), PLANET (Photonic Local Access Networks), RAFOH (Redes Avanzadas de Fibra Óptica hasta el Hogar), Harmonics, Planet, Sonata, Cobra, Darpa or MUSE (Multi Service Access Everywhere). All with the common of developing passive optical networks where only passive optical components are used and the wide fibre bandwidth is shared.

Nowadays, the leader countries on FTTH development, regarding the number of subscribers, are Japan with seven million users, USA and Korea. In Europe, FTTH is also a reality in some lands like Sweden, Italy, France or Denmark, where it is planed to build the first 10Gbit/s FTTH network. In Spain there are recent initiatives in the region of Asturias; also in Viladenans, a town near Barcelona will offer fibre services to twenty-six mil homes. Moreover, countries which traditionally base their economy in the petrol industry are now focusing in tourism services, since they realize the petrol is a finite recourse. Countries like Arabia Saudi and Dubai offer FTTH services as an additional value of tourism resorts.

2.6 SOA Technology

One of the main objectives of current projects is to propose and develop high speed WDM 10Gbit/s components suitable for low-cost standard photonic packages necessary for migration of the flexibility and high bit rates in access, metro and similar networks. Even though these components should integrate several functionalities such as simultaneously modulation, detection and equalisation, or modulation, wavelength-tuning and switching, the fabrication, packaging and using are assumed to be simple.

Optical communication with semiconductor amplifiers has been successfully demonstrated from the past, achieving appropriate transmission results. The first works date of the middle '90s [12]-[14]; the earliest use of a laser amplifier for modulation in local access is reported [12]. There, a reflective semiconductor is employed for modulation of the uplink signal in a passive network at bit rate of 100Mbit/s. Similarly performance results are reported in [13] where bit rate is increased to 155Mbit/s. In [15] is reported the first re-modulation scheme. A downlink signal, modulated at 2.5Gbit/s, is re-modulated at 900Mbit/s in the upstream direction by means of a reflective SOA. However downlink reception achieves successful error rate results, the detection of the upstream was still not completely satisfactory; BER was in the order of 10^{-7} and 10^{-9} at a 600Mbit/s.

Further improvements are described in [16] and [17]. There, two cascaded SOAs are employed, the first saturates the incoming downlink data (at 2.5Gbit/s); the second is modulated with the upstream data signal at 622Mbit/s. However error free operation is accomplished in these new experiments, the proposed topology implies a two-fibre solution. Meanwhile, the capability of a SOA operating as a photo-detector was verified in [18] and [19].

In [20] we first reported modulation and detection with reflective SOA at 1.25Gbit/s in a TDM scheme, employing intensity modulation in both up- and down transmission. Lately, in [21] we described the re-modulation of a downstream FSK-modulated signal with a RSOA, at 1.25Gbit/s, as well. And in [3] we experimented with electrical sub-carrier multiplexing over the RSOA. A list of our contributions to this topic is found in *Appendix C*.

In the recent years, the number of active groups working in colourless solutions for the ONU based on RSOA increased. Companies and universities develop new devices with the aim to achieve best transmission performance. Some of the most representative active groups are Samsung in collaboration with Yonsei University in Korea; Alcatel Thales III-V labs joint with France Telecom, France; CIP and Cork University in Ireland.

Chapter 3

Next Generation PON Configurations

In this chapter we establish the premises for the design of the ONU for the FTTH network and review several architectures for WDM-PON technology implementation in the access network.

3.1 Drivers and Requirements for FTTH-PON

Fibre-to-the-home technology is one of the main research objectives in the 'Broadband for all' concept that encourages the development of optical access infrastructures. In order to fulfil this concept, cost effective solutions must be developed to be able to offer future-proof broadband connections to the end users at a reasonable cost [22]. A key element in access networks is the ONU of the Customer Premises Equipment (CPE), having a direct impact on the cost per customer, whereas the access part represents the main segment of the total capital cost; to set up a low cost ONU is a key factor to achieve effective solutions for FTTH access networks. Other key requirements for the access network are

- the use of one single fibre for both upstream and downstream transmission, in order to reduce network size and connection complexity of the outside plant
- the elimination of the laser source at the ONU, thus avoiding its stabilization and provisioning

- uniform and wavelength independent components (colourless) at the ONU, to fit in a transparent WDM-PON scenario

In [23], a techno-economic comparison of optical access networks demonstrated a reduction of the access network CAPEX cost when WDM technology is combined with a reflective ONU topology compared to a point-to-point (homerun) network. In such approach, the ONU is a key element owing to its direct impact on the cost per customer. For a successful FTTH deployment, the ONU design should be simple, robust, flexible, and inexpensive. Additionally, reflective configuration allows the use of a single-light source for each ONU, located at the OLT in the central office, which optimizes the final design.

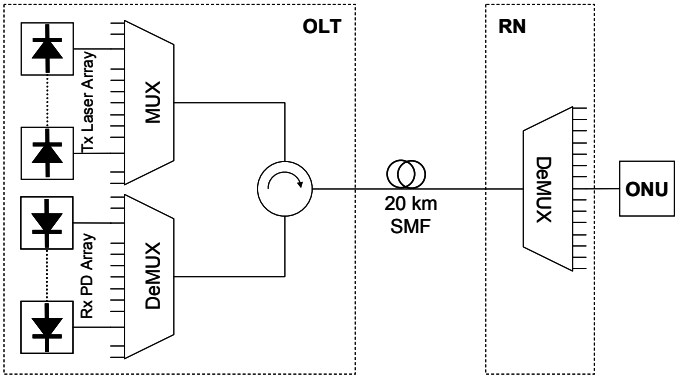

Fig.3.1 Passive optical access network scenario providing point-to-point links

Bidirectional single-fibre single-wavelength (BSFSW) transmission schemes are cost-effective designs for FTTH networks. They have the potential to offer a low cost solution to the end user [23]. BSFSW systems optimize the use of optical resources and reduce the network outside plant, since a single fibre is used to transmit in both directions. The use of a reflective device at the ONU provides wavelength independence to it, thus the light source is centralized at the OLT. Further, the identical design of all ONUs reduces provisioning costs and simplifies network deployment. A natural scenario for the BSFSW approach is a WDM-PON access network, which according to the ITU G.984 GPON and IEEE 803.2ah EPON standards, covers distances up to 20km. In this scenario, a laser stack at the OLT provides the transmission wavelengths and establishes point-to-point connections to the ONUs, as depicted in Fig.3.1 Wavelength routing at the Remote Node (RN) can be achieved using an Arrayed Waveguide Grating (AWG). The ONU reflects the incoming downstream signal and modulates the upstream data. The use of a single-fibre solution in the scenario presented in Fig.3.1 offers the advantage that the entire outside plant, including the number of splices and AWG-ports, is reduced by 50% as compared to a dual-fibre implementation [24]. Multiplexing in the time

domain can also be implemented when adding a secondary stage of optical power splitters in the RN. Then a higher density of users can be reached by using a combined WDM/TDM access scheme [25].

In the mentioned scheme, no additional light is injected at the ONU for uplink transmission. Thus, the power budget is a critical parameter. Amplification is essential for traversing sufficiently large distances and serving a large number of users by power splitting at the RN. Bidirectional amplification is possible by EDFAs but an additional high pump power is required. To this end, Semiconductor Optical Amplifiers (SOAs) are suitable candidates for deployment at the ONU, since they not only carry out modulation tasks, but also offer additional gain by amplifying the incoming signal. SOAs hence improve the power budget and are wavelength independent by design. Line rate and wavelength range depend mainly on the SOA manufacturing process. The modulation speed of commercially available devices is as high as 2.5Gbit/s in wide wavelength bands in the range of 50-100nm. Recent SOA developments can cover as many as 10 CWDM channels [26].

The main limiting factor of the proposed network approach is that light is being transmitted in both directions over the same fibre at the same wavelength, causes both coherent and incoherent crosstalk. These effects arise both from Rayleigh backscattering, an important and unavoidable limiting interference in bidirectional single-fibre systems [27], and from possibly lumped reflections. The effect of Rayleigh backscattering and single reflections on a BSFSW topology is extensively studied in further chapters.

3.2 Basic Techniques for WDM-PON

The main basic techniques applied in WDM-PONs in order to reduce the cost of components and thus simplify the network are spectral slicing, injection and self-injection locking, remote modulation and re-modulation. In the following, we take a closer look at those basic principles.

Spectral Slicing

The aim of spectral slicing is to exploit a single light source for transmission on a large number of (dense) wavelength channels (carriers) by means of identical modulators. For this purpose the spectrum of a broadband or multi-mode light source (e.g. LED, SLED) is sliced by a filter and the slices are used for transmission. The spectrum, with at least full width half-maximum (FWHM) spectral width equal to the wavelength band of the WDM system, is band-pass filtered by an AWG. Spectral slicing can be employed in many applications; some are illustrated in Fig.3.2. By placing the light source at the OLT this

technique can be used for both local modulation the downlink data and as a source for remote modulation at the ONU with uplink data signals. At the ONU, it can be use as a local light source for to generate uplink data signals.

As a broadband source (BLS) there are several alternatives like a white source, an ASE noise source or a multi-mode laser. The available power will depend on the slice-width. A larger slice will increase the resultant power but also increase dispersion problems and therefore a decrement in the number of the available channels.

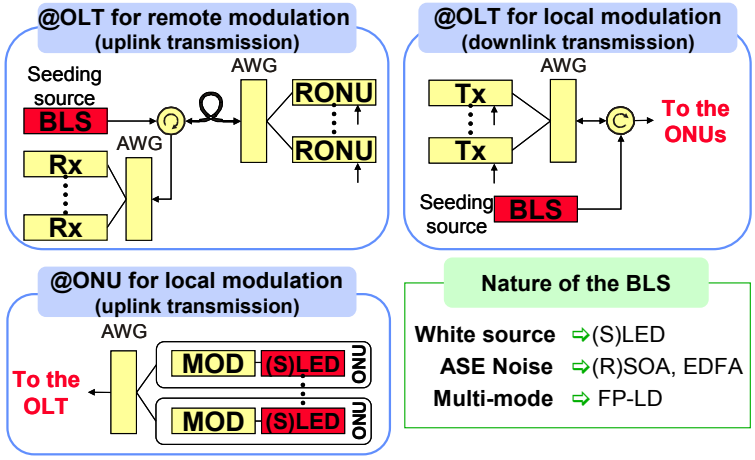

Fig.3.2 Applications of Spectral Slicing in WDM-PONs

Injection and self-injection locking

The idea behind injection locking is to employ a low-cost Fabry-Perot (slave) laser emitting light at a certain wavelength within a WDM band that is sufficiently large to host an adequate number of channels. This is achieved by injecting low-power and low-noise seeding light at the desired frequency into the high-power slave laser through a partially transparent cavity mirror Fig.3.3a. By maintaining the frequency of the seeding source sufficiently close to the slave laser, the injection forces the slave to operate only on the injected frequency with relatively little noise. The injection locking can strongly reduce the side-mode suppression ratio (SMSR) of an FP-LD, which is essential for DWDM operation. The self-injection locking technique is similar, but instead of a master device, the seed signal is taken from the slave itself. The laser cavity receives some optical feedback that is spectrally filtered, usually by a narrow-band fibre Bragg grating Fig.3.3b.

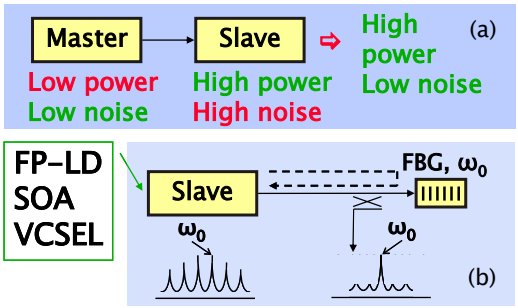

Fig.3.3 Injection and self-injection locking

Remote modulation and re-modulation

In remote modulation the signal for modulate with the uplink data is sent from the OLT to the ONUs. This allows employing different wavelengths in the up and down transmission. Re-modulation consists on reusing the downlink signal to imprint on it the uplink data, which allows different alternatives for modulation format for the uplink and downlink: intensity modulation in uplink and downlink, modulation constant amplitude for downlink (FSK or PSK), or different sub-carrier for upstream and downstream (SCM).

3.3 Architectures for Downstream Modulation

The conventional downstream modulation format in WDM is intensity modulation (IM). Nevertheless, alternative modulation formats as optical FSK, PSK or electrical SCM may be employed. These present advantages in front of bidirectional crosstalk impairments. Additionally, FSK and PSK can be easily re-modulated in IM at the ONU owing to they are constant in amplitude [28]. When using SCM, up and down data is carried on different electrical frequencies, thus the interference is reduced by electrically filtering after detection [3].

Fast tuneable lasers

A remarkable approach for WDM is the new generation of fast tuneable multi-electrode semiconductor lasers, with switching time in the range of ns. That allows the lasers to be employed to both, downlink data transmission and for the generation of CW bursts to be used in the ONUs for upstream data modulation. Tuneable lasers and receivers at the OLT can be shared by all ONUs and thus the total number of transceivers is reduced. With fast tuneable lasers optical FSK modulation can be performed at suitable bit rates (2.5Gbit/s). For FSK demodulation at the ONU an optical interferometer or a tuneable filter can be used in together with a photo detector [28].

Homodyne / Heterodyne detection

Homodyne detection in the optical domain is also a recent approach to be mentioned [29]. It is based on an optical phase locked loop (OPLL) to detect the signals that is not a cost-effective solution as it requires an optical oscillator at the ONU side and infringes one of the basic premises we establish at the beginning of this chapter. Several investigations are carrying on this matter; optical homodyne is a promising solution for future Dense WDM architectures (DWDM) however it is nowadays a not mature technology.

Optical heterodyne detection schemes are proposed [30] due to its high sensitivity and spectral density properties. A power splitter at the remote nodes broadcasts downstream signals to all ONUs that select arbitrary wavelength channels by tuning the wavelength of a local laser diode. To lower system costs, upstream signal generation is accomplished by the same directly modulated laser diode. Maximum data rate downstream is 1.25Gbit/s and upstream 622Mbit/s with channel spacing of 12.5GHz.

3.4 Architectures for Upstream Modulation

In this section we introduce several alternatives for upstream network architectures. It is worth mentioning that in most cases discussed transport mechanisms are also used to create downstream paths. In the first step, we distinguish between remotely working schemes and local generation at the ONU. In a further step, the kind of generating the optical signal for upstream transmission is used to divide the systems for a more detailed discussion. Here, we take the type of light source at the OLT as criterion for differentiation.

3.4.1 Remote-seeded light ONUs

They are the called reflective structures owing to the need for an optical source at the ONU is eliminated. Light is remotely generated at the OLT and sent to the ONU where the signal is modulated with the corresponding upstream data. From the ONU perspective these structures are wavelength independent which enables to use uniform, so called colourless, ONUs. Wavelength supplier at the OLT can be divided into broadband or multi-mode light sources (which employ spectrum slicing techniques) and coherent laser sources. Fig.3.4 indicates a generic WDM-PON architecture with alternatives commonly used as remote light source as well as different ONU-designs. It illustrates examples is of colourless ONU with centrally generated seeding light. The seeding light coming from the OLT can be generated by a BLS in combination with an AWG, implementing thus Spectral Slicing; or from a coherent laser. At the ONU the

modulation is performed by a laser operating with injection-locking, an RSOA, or a combination with an SOA and an external modulator.

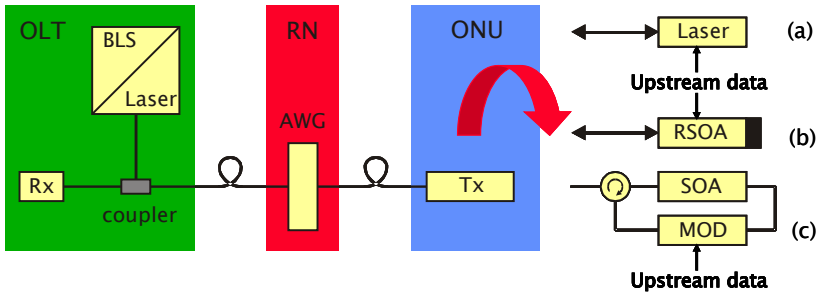

Fig.3.4 Generic upstream configuration with remote spectrum-sliced/routed BLS or laser source at the OLT and colourless ONU. (a)Injection-locked laser; (b)Reflective SOA; (c)SOA-modulator loop

3.4.1.1 ONU using injection locking FP–LD

In order to gain light to seed the ONU, in some cases downstream signals are partially tapped for data receiving purposes, while the rest is injected into the FP-LD. However, mostly reported are WDM-PON designs using different wavelengths for up- and down-stream transmission. In any case, careful dimensioning of the injected light and of the laser parameters is required for efficient laser operation.

Spectrum slicing light sources

Several types of broadband (BLS) or multi-mode light sources can be spectrum-sliced by narrow-band filters including SLED, EDFA and FP-LD. However, beyond power issues, this type of seed light inherently implicates limitations on the modulation speed due to diverse noise sources including mode-partition noise, intensity noise and optical beat noise. Moreover, spectrally–sliced BLS injections cause FP-LD output spectra with broad linewidth. Spectrally-sliced FP-LDs acting as seed light source are proposed in [31] potentially permitting gigabit Ethernet data rates in upstream direction. Rayleigh backscattering induced noise affecting the performance of one-fibre transmission systems using wavelength-locked FP-LD is investigated comprehensively [32].

BLS in the form of amplified spontaneous emission (ASE) light at the OLT and wavelength-locked FP-Laser diodes (FP-LD) at each ONU are described in [33]. Using the periodic property of AWGs, 35 signals at 155Mbit/s can be transmitted bidirectional. Optimised FP-LDs injection-locked by ASE light are investigated in [34]. This scheme works well within a 60°C temperature range without wavelength detuning effects over 10km at data rates up to 622Mbit/s. By incorporating 1:8 power splitters behind the AWG at the remote node, the number of maximum subscribers is boost to 128. To mitigate intensity noise effects, SOA-based broadband light sources are proposed in [35]. Colourless

operation over 25km fibre for up- and downstream signals is demonstrated at 155Mbit/s within the temperature range -20°C to 80°C using uncooled FP-LD.

Coherent light sources

An alternative to broadband or multi-mode light sources are OLT-based coherent light sources e.g. DFB lasers, potentially providing much higher data rates compared to spectrum-sliced light sources. Injection-locked VCSELs operating as stable, uncooled ONU transmitters for upstream data rates up to 2.5Git/s over 25km fibre length are proposed in [36]. Injection-locking is furnished by tapping the downstream signal. A unique design using FP-LDs that are injection-locked by a polarisation insensitive super continuum pulse source supports upstream transmission up to 2.5Gbit/s over 10km [37]. In order to minimize any modulation speed limiting effects potentially associated with spectrum-sliced BLS, FP-LD or tapped downstream data signals, coherent light generated by OLT-based CW-lasers are injection-locked to FP-LD located at the ONU [38]. As a result, data rates up to 10Gbit/s can be generated and transmitted over 10km.

3.4.1.2 ONU using semiconductor optical amplifier

Semiconductor optical amplifiers (SOA) are used for two basic functions, namely amplification and modulation. Different configurations are possible in SOA-based ONUs.

As it occurs with FP lasers, mentioned in the previous section, the type of source used to remotely feed the semiconductor may come from a broadband source [39] or from a coherent laser (DFB, ECL, GCSR). When using a broadband source or the spectrum slicing technique results in an error floor at the receiver due to dispersion and beat noise interference. Both reach and bit rate are limited by chromatic dispersion. The most straightforward configuration consists of a reflective SOA (RSOA) as shown in Fig.3.4b. Here, the downstream signal is partly coupled to the RSOA branch where it is amplified while upstream data is imprinted and the signal is back-reflected towards the OLT. Direct modulation of SOAs is limited to the semiconductor electrical response which is band limited. A loop structure, which combines a SOA and an external modulator (Fig.3.4c) allows for higher bit rates, up to 10Gbit/s.

3.4.2 Local-generated light ONUs

WDM-PON architectures using remotely generated light are vulnerable to degraded external seed signals. For example, wavelength drifts in both upstream and downstream paths may cause detuning effects resulting in

malfunctioning ONUs. In order to ensure proper upstream path generation and signal transmission, seed light generation can be realised locally at the subscriber side.

Light generation using injection locking

Fig.3.5 sketches a WDM-PON scheme using directly modulated, self-injection locked FP-LD [40]. Here, the lasing wavelength of the injection-locked FP-LD tracks the reflected FBG peak wavelength. For upstream transmission purposes the continuous wavelength from the FP-LD output is modulated by an external modulator. Signals at 1.25Gbit/s can be transmitted over 10km without active temperature control (20°C to 50°C) at both remote node and ONU. Note that this is a two-fibre solution and consequently a no cost-efficient approach as two fibres are required to address each ONU and moreover, two ports of the AWG at the remote node are occupied.

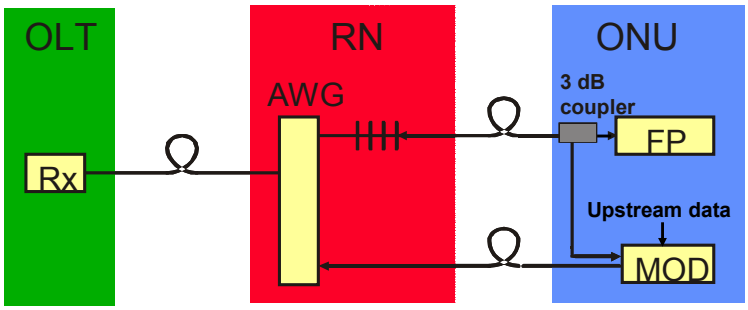

Fig.3.5 Upstream transmission configuration with locally generated seed light and self-injection locked FP-LD located at the ONU

Light generation using optical amplifier

A more efficient approach using locally generated seed light in conjunction with directly modulated self-seeding RSOAs is described in [41]. Broadband ASE from each RSOA is spectrally sliced by an AWG, and a proper designed band-pass filter ensures that only one sliced light per output port is reflected back to each SOA, Fig.3.6. There is no need for temperature tracking between AWG and BPF. Distances up to 20km can be bridged at 1.25Gbit/s.

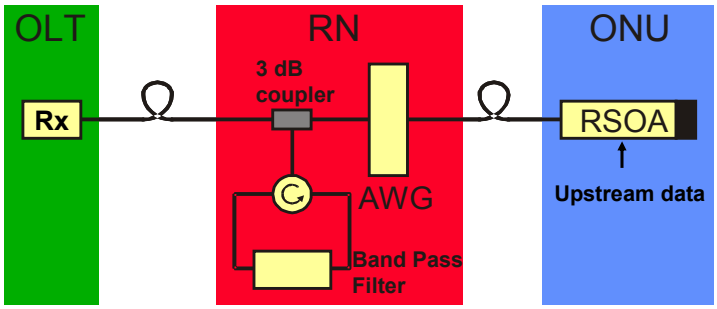

Fig.3.6 Upstream transmission configuration with ONU-based amplifiers

3.5 Conclusion for the FTTH-ONU

Subsequent to the revision of the several alternatives and based on the premises established at the beginning of this chapter which plead for a cost-effective solution for the end customer, a single fibre topology, no active light components at the ONU and, to employ uniform components, one can ending that the best solution to implement the ONU in a FTTH access network is an RSOA-based ONU.

Semiconductor optical amplifiers are a potential candidate for modulation and detection tasks at the ONU thanks to their capabilities for detection, modulation, and amplification at the same time. Cost effective designs are possible employing a single device at the ONU. The result design is self-amplified, wavelength-independent, and suitable for a bidirectional single-fibre topology. Other known low-cost solution, which directly competes, consists in using injection-locked Fabry-Perot lasers diodes but this solution is distance and temperature sensitive and the modulation rate is a function of the incoming locking power level and the optical mode spectrum is temperature dependent, which places this solution in a secondary position.

Chapter 4

RSOA-based ONUs

Definitely, SOA-based reflective ONUs present a step towards unique and simple wavelength independent ONUs for WDM-PON application.

Several ONU configurations can be implemented using SOAs. Half-duplex or full-duplex transmission can be achieved, depending on the modulation format and the multiplexing scheme selected. The simplest technique for half-duplex transmission is data modulation using Amplitude Shift Keying (ASK) for both uplink and downlink directions in a Time Division Multiplexing (TDM) mode. Full-duplex transmission can be performed by combining Frequency Shift Keying (FSK) for the downstream data and ASK for the upstream data, or by using SCM in the electrical domain for both the upstream and downstream directions.

4.1 Half-Duplex Configuration

In Fig.4.1, a half-duplex configuration using either an RSOA or an SOA is depicted. An electrical switch is used to select the operation mode, which can be either modulation or detection. Additionally, it is shown that the incoming signal at the ONU is divided into two timeslots: the downstream slot containing the data sent by the OLT, and an optical signal used to imprint the upstream data. When detection mode is selected, the variation of the carrier density produced by the incoming modulated signal is detected through the bias electrode. In the other time-slot, modulation is performed by acting on the device current. In Fig.4.1a, the incoming light is reflected towards the OLT at the high reflection face of the RSOA, while in Fig.4.1b, the light passes through

the SOA and then is coupled back to the transport fibre. An isolator or a circulator must be used to prevent the signals from entering the SOA output port.

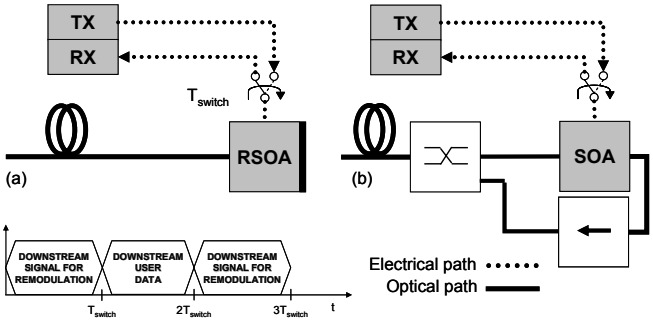

Fig.4.1 Half-duplex structures using (a)Reflective SOA; (b)SOA

4.2 Full-Duplex Configuration

Full-duplex transmission can be achieved by combining an ordinary photo-receiver and an RSOA. In such a scheme, the downstream signal is partly coupled with the RSOA branch where it is amplified, while upstream data is imprinted and the signal is reflected back towards the OLT. Three different configurations are illustrated in Fig.4.2.

The system of Fig.4.2a uses an ASK modulated downlink signal with a constant offset, which can be ASK re-modulated by the RSOA (biased for operating in the saturation region).

In the design of Fig.4.2b, FSK modulation is used for downstream transmission. For detection at the ONU, an optical filter converts the FSK signal into an intensity modulated (IM) symbol by selecting the frequency that corresponds to the logical 'one' of the data stream. The signal for upstream use is coupled with the RSOA, where it is orthogonally ASK re-modulated. In order to be wavelength-agnostic the optical FSK discriminator should be periodic, e.g. as in an MZ interferometer. In Fig.4.2c, the uplink and downlink data are carried on different electrical sub-carrier frequencies. The downlink spectrum is shifted to an electrical frequency at least three times higher than the uplink sub-carrier frequency, in order to prevent spectral overlapping. By locating the downstream sub-carrier outside the electrical bandwidth of the RSOA (~1.5GHz), it acts as an electrical low pass filter. Then the remained power carried into the base band is up-converted and modulated with the uplink data. The sub-carrier multiplexing scheme can also be implemented by using only a single optical device at the ONU. In that case, the bit rate must be decreased in order to be able to detect the signal with the highest electrical frequency.

In next sections, when we talk about bidirectional transmission impairments, it will see that configurations 4.2b and 4.2c present an advantage in front Rayleigh backscattering and reflection interference. In the first case, interference is significantly reduced by employing a broad-spectrum signal. In 4.2c, the interference is reduced by separating the signal from the crosstalk by electrical filtering.

Similar configurations can be implemented by using an SOA with a coupler and an isolator instead of the RSOA (as shown in Fig.4.1b), though it is preferred to operate with a single device.

Experimental details related to those configurations are given in Chapter 8. As an example, with 0dBm launched optical power at the OLT, experimental results demonstrate an adequate power budget for networks according to Fig.3.1. In the uplink (which is the critical direction), sensitivities of -20dBm are achieved for both the ASK-ASK and FSK-ASK schemes at 1.25Gbit/s while the SCM system arrived at -30dBm at 155Mbit/s. In all systems error correction techniques (FEC) improve the link budget.

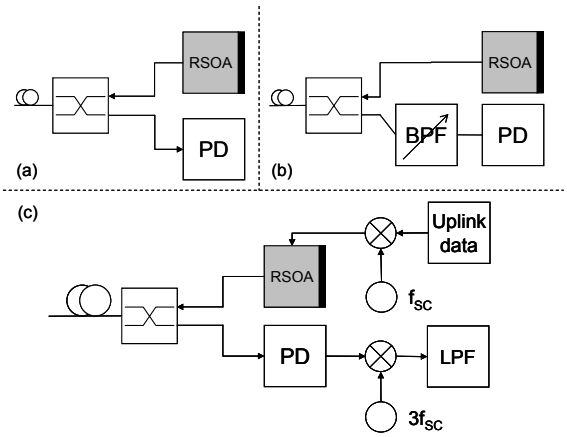

Fig.4.2 Configurations of reflective ONUs using different modulation schemes. (a)Downlink ASK, uplink ASK; (b)Downlink FSK, uplink ASK; (c)SCM uplink and downlink

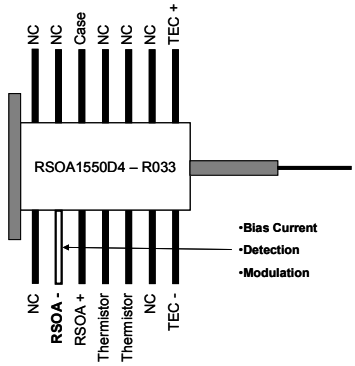

Fig.4.3 RSOA pinout

4.4 ONU Prototypes

The first prototype of reflective ONU developed at UPC is dated on February 2004. For illustrating, the block diagram of the employed RSOA is in Fig.4.3. At the laser cathode (RSOA-) are connected the bias current circuit and the two RF ports. In the second prototype, designed a year later, we improved electrical aspects in order to achieve higher bit rate and include an electrical switch in the board. A recent prototype comprises a second generation RSOA; the achieved modulation bit rate is 2.5Gbit/s. A future step is a new product in a TO-CAN package which does not require an internal temperature controller that is an interesting option for FTTH solution.

Chapter 5

Semiconductor Optical Amplifiers in the Access Network

Semiconductor Optical Amplifiers (SOAs) have several applications. They are rarely used as in-line amplifiers due to its high level of noise. Otherwise, no lineal applications like, detection, modulation, commutation, wavelength conversion or signal regeneration are well performed by such devices. In addition, SOAs present some advantages: low fabrication cost, small dimensions, possible integration, wide bandwidth, low insertion loss and fast time response. So SOAs are a potential candidate as an electro-optic transceiver in PON networks; they are able to carry on with the transmission and, at the same time, with the amplification of signals at the user premises.

5.1 Basic Characteristics

Semiconductor amplifiers are similar to conventional semiconductor lasers except that they have no feedback. This is accomplished by blocking cavity reflections using both an antireflection (AR) coating and the technique of angle cleaving the chip facets (angle of about 7^{o}). For example, by using titanium-oxide/silicon-oxide (TiO2/SiO2) layers for the AR coating, it is possible to achieve a reflectivity in the order of 10^{-5} and thus gain ripples as low as 0.5 dB.

A schematic diagram is sketched in Fig.5.1. An SOA consists of a central active region (typically 300-500μm) of a semiconductor material between two semiconductor layers of different compositions, Fig.5.1a. When the device is driven by an electrical current, the electrons are excited in the active region. The photons travelling through the active region cause the electrons to lose part of their extra energy in the form of more photons with the wavelength as the initial ones (stimulated emission) generating thus an amplification of the incoming signal, Fig.5.1b.

Such an SOA structure is inherently polarization sensitive, as the transverse-electric (TE) mode gain is greater than the transverse-magnetic (TM) mode gain. The polarization dependent gain effect can be reduced to an acceptable value of 0.5dB by designing the active waveguide nearly square (0.4μm x 0.6μm), having thus almost the same confinement factor for both TE and TM polarization states.

A special type of SOA is the Reflective Semiconductor Optical Amplifier (RSOA). In this structure, one of the facets is high reflection-coated with reflectivity close to 100%. Thus, when the light enters into the cavity it is reflected towards the input port. Both structures present similar behaviour in terms of gain, bandwidth, and noise, but a RSOA has only one optical port (Fig.5.1c). This becomes an advantage when used in ONUs for single-fibre topologies because no additional optical element is needed for terminating the downstream path and feeding the upstream signal into the same fibre.

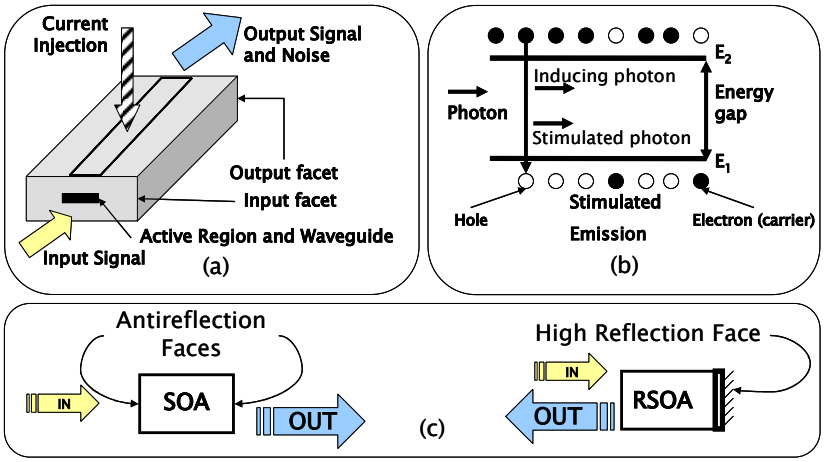

Fig.5.1 (a)SOA block diagram; (b)Spontaneous and stimulated processes; (c)SOA and RSOA transmission diagram

5.2 Analytical Models

5.2.1 Amplifier Gain

The fundamental characteristic of an SOA is the intrinsic gain parameter; that is the ratio of the input signal at the input facet to the signal power at the output

facet. The gain value depends on physical structure of the device, material and fabrication parameters. The gain expression, of a basic Fabry-Perot type structure is given by [42],

$$G_{FP}(\nu) = \frac{(1-R_1)(1-R_2)G(\nu)}{\left(1-G(\nu)\sqrt{R_1R_2}\right)^2 + 4G(\nu)\sqrt{R_1R_2}\sin^2\left[\pi(\nu-\nu_m)/\Delta\nu_L\right]}. \quad (5.1)$$

Where R_1 and R_2 are the input and output facet reflectivity; υ_m are the cavity resonance frequencies; $\Delta\upsilon_L$ is the longitudinal-mode spacing; and $G(\upsilon)$ is the frequency-dependent single-pass amplification factor given by $G(\nu) = e^{g(\nu)\cdot L}$, with L the length of the semiconductor and $g(\upsilon)$ the amplifier factor gain. Note that for an ideal SOA $R_1=R_2=0$ and then the gain is equal to the single-pass gain; moreover, in an ideal RSOA the photons travel twice the cavity length, then $L_{RSOA}=2L_{SOA}$ and

$$G_{RSOA}(\nu) = e^{[g(\nu)L_{RSOA}]} = e^{[g(\nu)2L_{SOA}]} = \left(G_{SOA}(\nu)\right)^2. \quad (5.2)$$

5.2.2 Gain Ripple

In a non-ideal situation, the face reflectivity provokes a ripple on the output signal. From (5.1) it is observed a gain variation depending on the input frequency; there is maxim peak when the frequency of the incident wave coincides with the resonance frequency. The gain ripple can be easily deducted from (5.1) as

$$\Delta G = \frac{G_{FP}^{\max}}{G_{FP}^{\min}} = \left(\frac{1+G\sqrt{R_1R_2}}{1-G\sqrt{R_1R_2}}\right)^2. \quad (5.3)$$

The gain ripple should be lowest possible. For instance, for gain variations less than 3dB, (5.3) fulfils $\Delta G<2$, and therefore $G\sqrt{R_1R_2} < 0.17$. In a second example, for an RSOA with $R_2=1$ and gain G=10dB; if the desired output ripple is less than 0.1dB, then the outcome in that case is much more restrictive so R_1<3e-7.

5.2.3 Gain Bandwidth

From (5.1) the 3dB bandwidth is deduced as [42]

$$\Delta\nu_{3dB} = \frac{2\Delta\nu_L}{\pi}\sin^{-1}\left(\frac{1-G\sqrt{R_1R_2}}{\left(4G\sqrt{R_1R_2}\right)^{1/2}}\right). \quad (5.4)$$

Continuing with the last example of the RSOA, taking $\Delta\upsilon_L$=100GHz as a typical value, one can calculate the optical bandwidth which gives $\Delta\upsilon_{3dB}$<2GHz and can be considered as the upper limit of modulation bandwidth.

This result is considerably lower than the case of laser diode which can have 10GHz modulation bandwidth; the reason is in part, the restriction imposed in the example to the face reflectivity.

5.2.4 Saturation Gain

The saturation gain is deducted from the semiconductor peak gain equation (5.5) and the carrier rate equation (5.6).

$$g(N) = \left(\Gamma \sigma_g / V\right)\left(N - N_0\right) \tag{5.5}$$

$$\frac{dN}{dt} = \frac{I}{q} - \frac{N}{\tau_c} - \frac{\sigma_g (N - N_0)}{\sigma_m h\nu} P . \tag{5.6}$$

Γ is the confinement factor; σ_g is the differential gain; V is the volume of the active zone; N is the number of carrier in the active zone; and N_0 is the value of N required at transparency.

σ_m is the cross-sectional area of the waveguide mode; τ_c is the carrier life time; q is the electron charge and h is the Planck constant.

If the pulse is longer than the carrier life time, then $dN/dt = 0$ and N can be obtained from (5.6). Introducing N in (5.5), one obtain the gain coefficient as

$$g = \frac{g_0}{1 + P/P_{SAT}} . \tag{5.7}$$

Where g_0 is the maximum gain, given by

$$g_0 = \left(\Gamma \sigma_g / V\right)\left(I \tau_c / q - N_0\right) \tag{5.8}$$

and P_{SAT} is the saturation power, defined by

$$P_{SAT} = h\nu \sigma_m / \left(\sigma_g \tau_c\right) \tag{5.9}$$

5.2.5 Noise Factor

The noise factor defines de relation of the signal-to-noise-ratio at the input of the amplifier and the signal-to-noise ratio at the amplifier output. And is given by [42]

$$F_n = 2 n_{sp} (G - 1) / G . \tag{5.10}$$

That is, the power at the output (5.11) is the input power amplified by the gain factor plus an additional term caused by spontaneous emission (P_{ASE})

$$P_{out} = G P_{in} + P_{ASE} . \tag{5.11}$$

Where $P_{ASE} = (G - 1) n_{sp} h\nu B_o$ and n_{sp} is the spontaneous emission coefficient of the amplifier. The ASE noise has degrades the bit error rate and thus in the system performance. The noise figure is usually expressed in dB and is denoted then as

noise factor, typical values of the noise factor in commercial semiconductor optical amplifiers are 8-12dB.

5.2.6 Modulation and Detection Principle

The physical principle for modulation/detection in semiconductors consists of applying/sensing differences in voltage at the bias electrode of the device.

If an optical signal is injected into the semiconductor, the carrier density decreases, as the optical power increases. Then, as the intensity of the input light changes the carrier density also changes. This has a proportional effect on the quasi-Fermi levels and thus the diode voltage. In this phenomenon the main process involved is stimulated emission, however, spontaneous emission is also present. Spontaneous is an unwanted occurrence since it contributes with increasing the noise of the optical signal and so degrades the detection on the electrical output. A reverse mechanism occurs in modulation. A modulated electrical signal injected at the bias electrode produces a variation of the optical power obtaining then the modulation of the light.

The relation between the number of optical carriers inside the SOA cavity and the difference in voltage at the bias electrode of the device is given by [43]

$$\Delta V = \eta\left(\frac{kT}{q}\right)\ln\left(\frac{N+\Delta N}{N}\right), \tag{5.12}$$

where η is the junction ideality factor, k is the Boltzmann constant, T indicates the absolute temperature (300°K), q the electronic charge, and N the carrier density. From (5.12) it is deduced that a modulated signal injected at the bias electrode generates a variation of the optical power and thus performs the modulation of light. Detection is achieved by sensing differences in voltage produced at the same bias electrode. Fig.5.2 illustrates a common circuit used to drive the semiconductor for both modulation and detection functions.

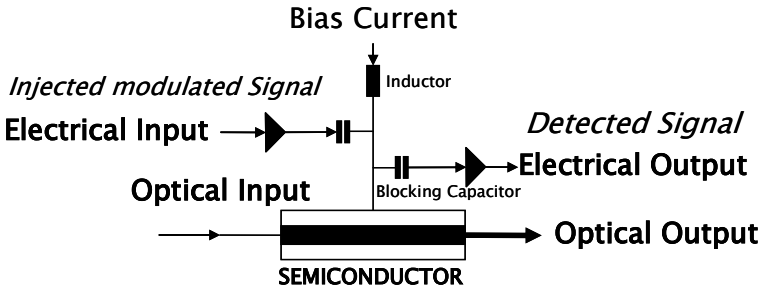

Fig.5.2 Modulation/Detection drive circuit

For illustrating, in a RSOA we experimentally observed optimum performance about 110mA of bias where the semiconductor shows a responsibity about

85volt/watt, and a flat frequency response up to 900MHz. Taken N=1.5 10^{24} m^{-3}, $\Delta N=10^{-4}$, (5.12) gives 65volt/watt, similar magnitude order.

5.3 Experimental Characterization

Previous to the experimentation with semiconductor devices inside the network, this in this part of the work we give details about the experimental characterization of a collection of devices available during the period of the thesis work.

We denoted as first generation devices the ones which were not engineered for modulation and detection, but for the amplification of signals. The main issue is that the operation bit rate is in the region of 1Gbit/s at the optimum, limited by the electrical bandwidth. Moreover, these are relatively long chips and therefore noisy; and also exhibit high Polarization Dependent Gain (PDG) which can be difficult to deal with at the customer premises. A second step approach is two-section structure composed by a semiconductor and an absorber material in the same chip. In the example presented, the potential bit rate is promising but the gain and noise are still not satisfactory. The second generation of reflective SOAs is designed for WDM applications featuring ONU tasks. Gain, noise, PDG and electrical bandwidth are then improved; bit rate of 2.5Gbit/s is feasible in a relaxed way. Future promising devices consisting on two-section structures are capable of achieve higher bit rate.

5.3.1 SOA and RSOA. First Generation

The tested devices are an SOA (*Kamelian OPB-10-15-N-C-FA*) and an RSOA (*Opto-Speed 1550D4-R033*). The semiconductor is InP-InGaAsP metal-organic chemical vapour deposition grown type, the chip lengths are 500μm, and the operation window is at 1550nm.

Optical Gain

The following figure (Fig.5.3) shows the gain response of the amplifiers to a continuous wavelength optical signal.

The curves show a high dependency on the injected bias current and the optical input power. The gain increases with the current until it achieves a maximal saturation gain of about 15dB for the SOA and 16dB for the RSOA. However, for each curve in Fig.5.3a, b, the gain decreases when the optical input power is further increased. The saturation output power is defined as the optical output power for 3dB of gain reduction, $P_{out_{-3dB}} = P_{in_{-3dB}} + G_{-3dB}$. From the curves related to the highest current values, the saturation output power is $P_{out_{-3dB}} = -3\text{dBm} + 12\text{dB} = 9\text{dBm}$ for the SOA and $P_{out_{-3dB}} = -12\text{dBm} + 13\text{dB} = 1\text{dBm}$ for the RSOA.

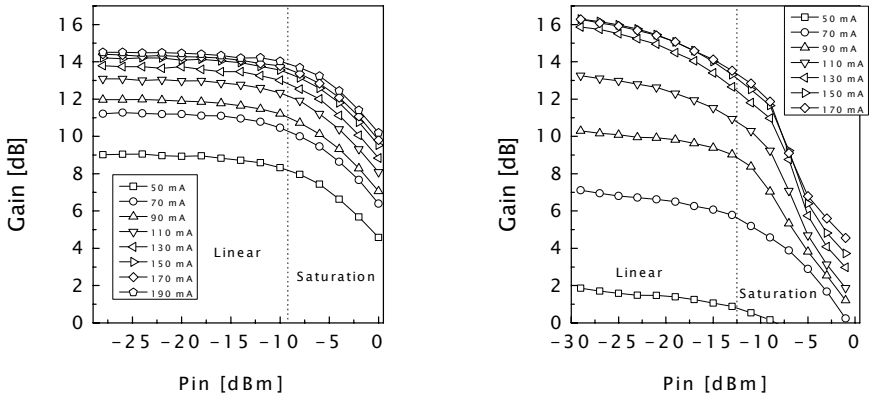

Fig.5.3 Gain as function of the input power for several bias current. (a)SOA; (b)RSOA

Furthermore, each curve can be divided into two distinct regions, separated by a minimum of 1dB of gain reduction: the linear section, where the gain remains virtually constant when increasing the input power, and the saturation region, where the gain varies strongly with the input power.

Bias current selection

The SOA and RSOA presented can be biased with currents up to 250mA. The current selection is critical, as it defines the device response, as shown in previous paragraph. The strategy to modulate SOAs is to vary the input current at the bias electrode. A continuous bias current is set and the modulation varies it around this bias point. For modulation purposes, it is desirable to have a large extinction ratio. This can be achieved by selecting an optimal value for the bias current. This happens in the linear region, where for a fixed optical input power the curves are more separated. In addition, the higher gain at this point is beneficial with respect to the uplink signal. Fig.5.4 shows the extinction ratio, and the corresponding gain at the bias point, when a modulated signal (40mA peak-to-peak) is added to the bias electrode, for the RSOA. The input power is -20dBm. The extinction ratio reaches a maximum value in the linear region of the gain. It can be enlarged by increasing the amplitude of the modulated signal. When the device is in the saturation region, the gain as well as the carrier density varies abruptly, and the gain curve can be approximated linearly. Hence, such a region is proper for detection purposes. The carrier density variations induce voltage variations at the SOA electrode, providing thus the photo-detection operation, analytically described by (5.12).

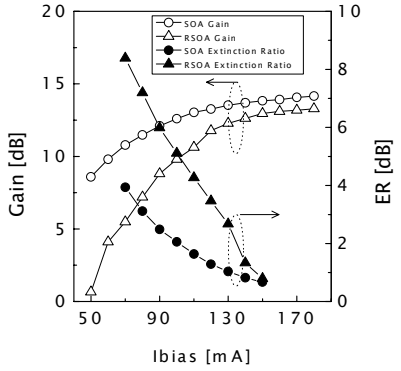

Fig.5.4 Gain and Extinctin Ratio vs Bias Current

A more illustrative example can be seen in Fig.5.5, for the RSOA as well. The input power is -10dBm in this case. It can be clearly seen that for the same amplitude of the modulated current, the output signal has larger extinction ration, when biasing the semiconductor in a lowest point; this is traduced as a more open eye diagram.

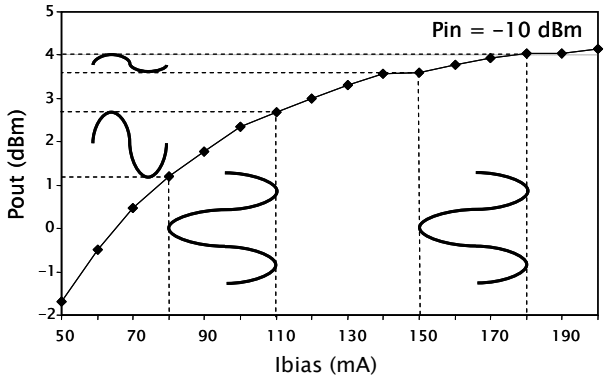

Fig.5.5 Output power as function of the bias current

Spectra and ASE noise

The operation centre frequency and the 3dB optical bandwidth are 1478nm and 63nm for the SOA, and 1552.8nm and 30nm for the RSOA, respectively. The spontaneous emission spectra of the RSOA for several biases current are represented in Fig.5.6a (the SOA has similar spectra figure).

The power of the ASE noise increases considerably with the bias current. The ASE power is given by the area underneath the curves; it can be calculated and also measured with a power meter. The measured power as function of the current is represented in Fig.5.6b.

Regarding again Fig.5.6a, it is observed is a gain ripple which is maxim at the centre wavelength and also increases with the current. The ripple is a critical characteristic as it soils the transmitted signals. The gain ripple measures 0.9dB at the maximum for the highest current. Note that the centre wavelength shifts to lowest lambdas when increasing the bias; this will provokes a chirping of the modulated signal. Since modulation consists on changing the current, the optical frequency will be at the same time modified. This effect reveals that the larger the extinction ratio the more chirped modulation.

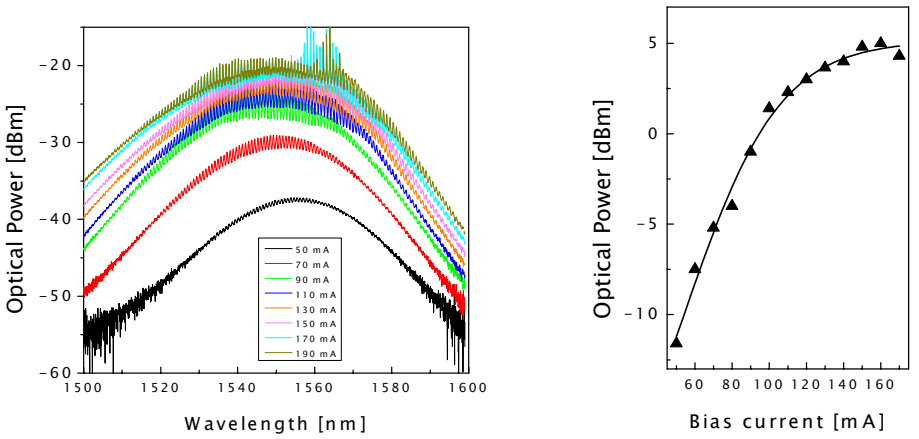

Fig.5.6 (a)Spontaneous emission spectra of the RSOA for different bias current; (b)ASE power

Eventually, the polarization dependent gain can be observed at the curves corresponding with 170mA and 190mA. In the experiments, the fibre connected to the device was deliberately bent; it is observed additional ripple on the spectra.

The gain variation can be measured by adjusting a polarization controller connected at the optical port of the device; the mean variation of the gain was measured 5dB. The high PDG makes mandatory to employ a polarization controller when inserting the RSOA inside the network.

Dynamic Response

The time response of the pair of semiconductors is described following. The pump–probe configuration used to observe the recovery of the SOA from saturation is the same reported in [44]. For the RSOA the recovery time is measured with a similar method, the setup is sketched in Fig.5.7.

The experiment consists on sending a short-pulse train of 2ps pulses to the device under test; the response is captured then by an oscilloscope. The results are shown in Fig.5.8. For the SOA the recovery time is about 200ps which means that it could follow signals up to 5Gbit/s, Fig.5.8a; and for the RSOA the

time is larger, 500ps and in consequence it supports lower bit rate, 2Gbit/s in this case (Fig.5.8b).

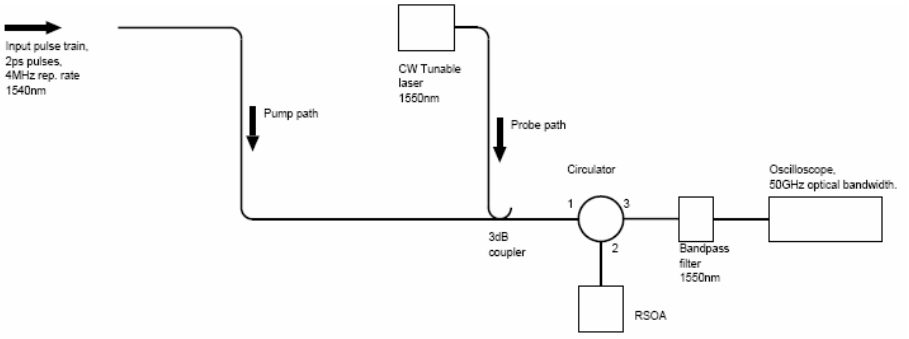

Fig.5.7 Configuration setup for pump–probe measurements of RSOA

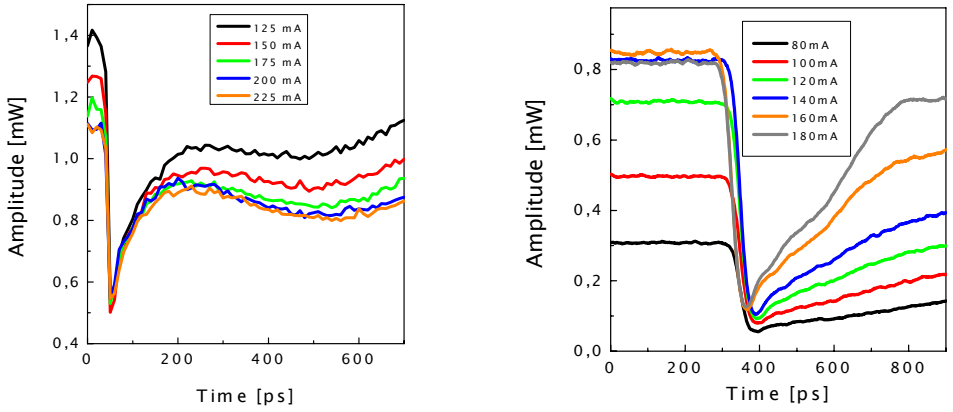

(a) (b)

Fig.5.8 Recovery time response to a short-pulse. (a)SOA; (b)RSOA

The next figure (Fig.5.9) shows the response of the RSOA to a squared pulse train at an intermediate frequency within the electrical bandwidth of the device. The RF signal of 500MHz frequency is applied to the data input; the optical output is photo-detected by means of an APD receiver and the detected signal is recorded by an oscilloscope. Although in this situation it would be expected a high-quality at the output signal, a distortion in the pulses is detected. The lowest current causes a negligible pulse distortion. Also gives wide amplitude, i.e. large extinction ratio that agrees with the statements exposed previously regarding the bias current selection. Furthermore, there is almost no distortion at the low level. In contrast, when increasing the current the pulses are strongly affected, especially from currents above 90mA, the amplitude decreases and the distortion intensifies.

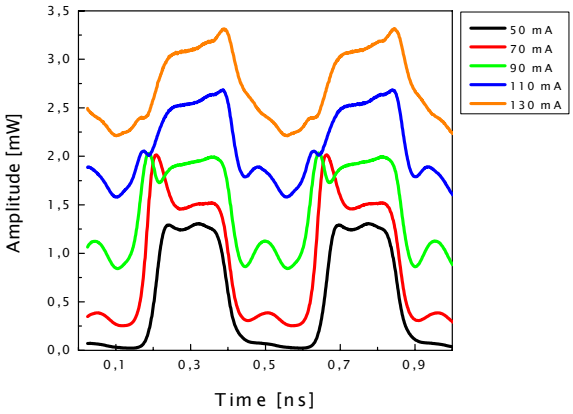

Fig.5.9 Pulse response

5.3.2 Integrated SOA with Saturated Absorber

The following device is a prototype developed at the *Fraunhofer Institute for Telecommunications, Heinrich-Herz-Institut, Berlin (GE)*. It consists of an integrated module formed by a SOA and a saturated absorber (SA) (*HHI-AVT-Stda-V3.0-040/05*). The chip length of the SOA section is 500μm and 100μm for the SA section. The allowed biased current is in the range of 0 to 200mA at the SOA and the operating voltage at the SA is -0.5 to 1.0 V; the schematic is depicted in Fig.5.10. It has two optical ports, one connected to the SOA section and the other one to the SA section; at the same time, there are two electrical ports, connected to each section. Besides, it has a temperature controller port.

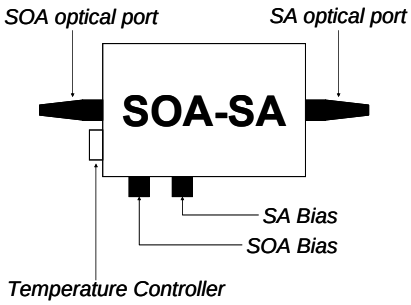

Fig.5.10 Schematic of the SOA-SA module

As in the two previous examples, this chip is not engineered for transmission purposes. The SOA-SA module is designed as an in-line amplifier for long-haul communications system; the SA is integrated with the SOA in order to prevent the accumulation of amplified spontaneous emission in a cascade of optical amplifiers [45]. Nevertheless, since there was no option for

self-manufacturing a specific device and any commercial solution was able at that moment, the transmission capabilities of this module were tested in order to investigate whether the integration of an absorption section could improve the performance offered by a single-section SOA.

Spontaneous Emission Spectrum

The connection for measuring the spontaneous emission is illustrated in Fig.5.11. The spectra are recorded at the two optical ports with an optical spectrum analyzer (OSA); the current and the voltage are adjusted to several values. The results at the absorber port and at the SOA port are represented in Fig.5.12 and Fig.5.13, respectively.

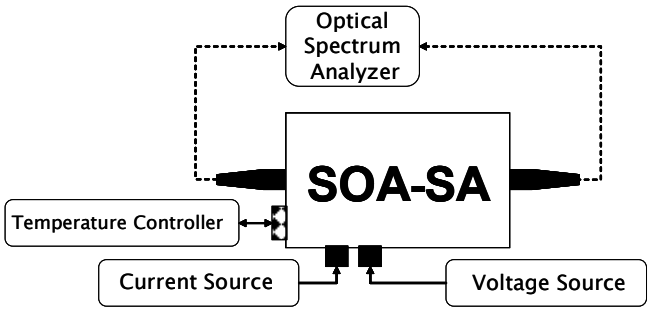

Fig.5.11 Setup of the measurements of Spontaneous Emission Spectra

At the absorber port, despite the spontaneous emission power increases with both the SOA and the SA bias, the total ASE is much lower with respect to the SOA port. Major part of the ASE noise generated at the semiconductor section is absorbed at the SA section, in particular when it is biased with reverse voltage (-1V).

At the SOA port the behaviour is similar to the RSOA device previously analyzed. The wavelength shifts when modifying the bias, although the increment is larger (40nm) than for the RSOA (20nm), see Fig.5.6; this will imply a chirping effect on the modulated signal. In the SOA-SA chip, the gain ripple is present in the entire optical spectral band and it is accentuated at the central wavelength owing to reflections produced inside the module due to imprecations of anti-reflection faces and also to an air gap between the chip and the fibre.

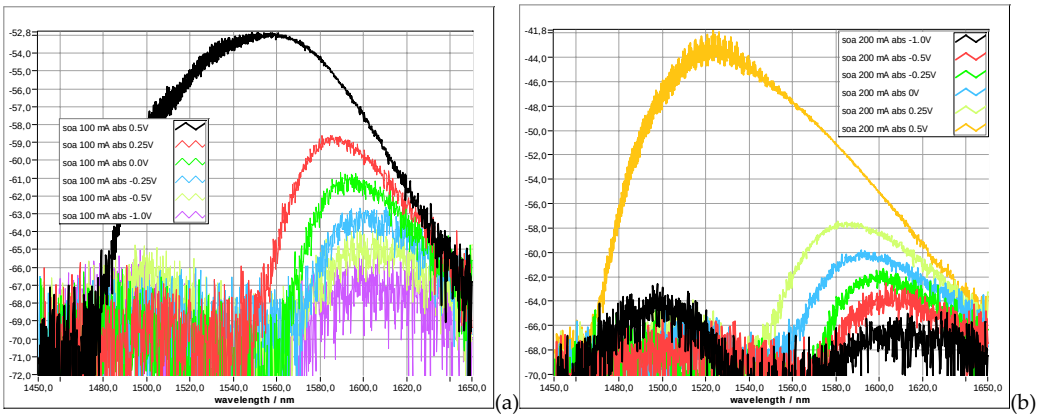

(a) (b)

Fig.5.12 Output Spectra of SOA-SA at the Absorber port. (a)SOA bias: 100mA; (b)SOA bias: 200mA

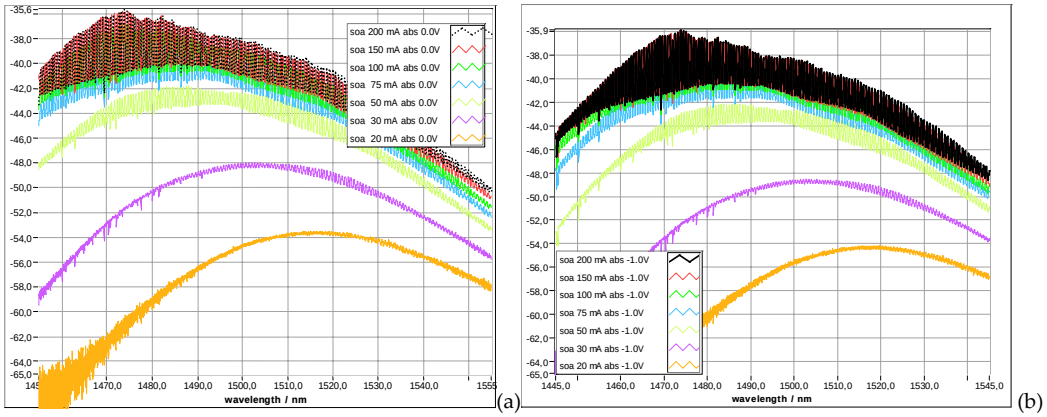

(a) (b)

Fig.5.13 Output Spectra of SOA-SA at the SOA port. (a)Absorber bias: 0.0V; (b)Absorber bias: -1.0V

Gain and Noise Figure

The setup for measuring the gain and noise figure (NF) is illustrated in Fig.5.14. A laser source at 1550nm is used to inject an optical continuous wavelength to the device. The optical power is varied, also the current of the semiconductor input; for measurements the absorbed is biased at -1V. The output power at the SA port is directly measured by a special function of the OSA; the noise figure is also calculated by the OSA. The results are represented in Fig.5.15.

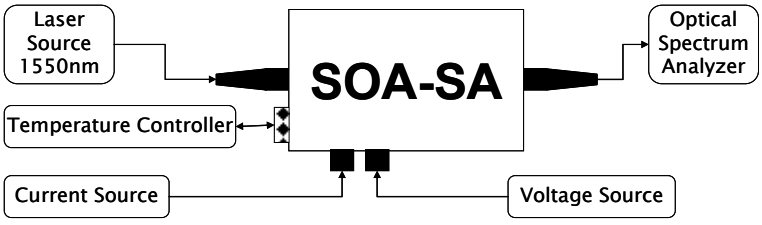

Fig.5.14 Setup of the Gain and Noise Figure measurements

The gain of the module is represented in Fig.5.15a. It is not so high because of the absorber section is absorbing part of the power generated by the amplifier which also explains the negative values. The maximum gain is 3dB. Fig.5.15b shows the noise figure as function of the bias current for different optical input powers. As the gain, the NF increases with the current and decreases for higher input powers. The value of NF is kept in the range of 10-12dB. Fig.5.15c resumes the evolution of the gain and NF with the input power for a current of 200mA and, clearly shows that the highest the gain the highest the noise. In spite of being elevated, the noise figure is inside the range of values offered by commercial devices. On the contrary, the gain can result a bit poor, when amplification is required at the ONU premises.

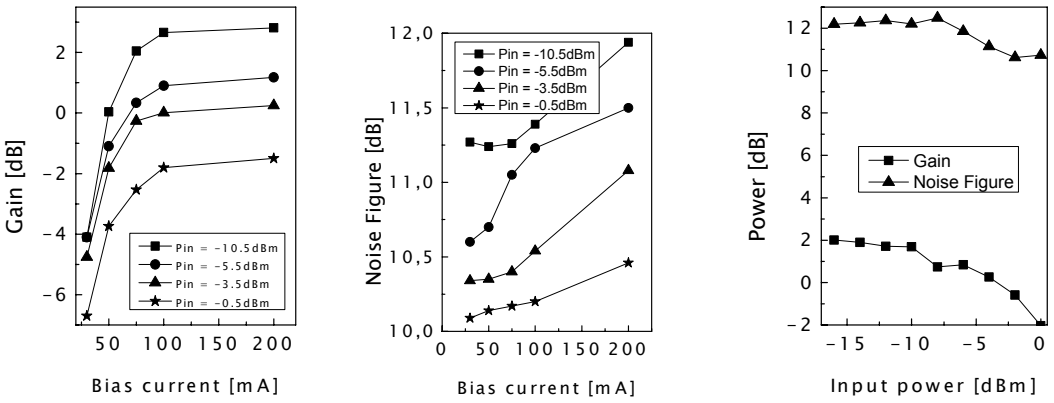

Fig.5.15 (a) Gain as function of the SOA bias; (b)Noise figure as function of the SOA bias; (c)Gain and noise figure as function of the input power

Modulation at the absorber port

In order to investigate the transmission capabilities of the SOA-SA, we first investigate the modulation. A PRBS signal is combined with the bias current with a *Bias-T* and introduced at the SOA electrical port. A photo-detector connected to the SA optical port detects the output signal (Fig.5.16). The detected eye diagram at 1Gbit/s and 1.5Gbit/s is depicted in Fig.5.17a, b, respectively.

The eye diagram is open and clear in both cases, although at the bit rate of 1.5Gbit/s there is an eco. This is caused by the time response to the device to alter from the high to the low level. For higher bit rates, the effect is more accentuated; nevertheless, the modulation response of the SOA-SA is improved compared with the semiconductor studied before.

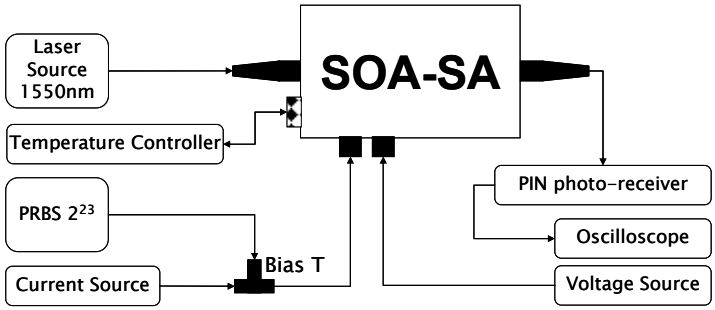

Fig.5.16 Setup of the modulation at the absorber port measurements

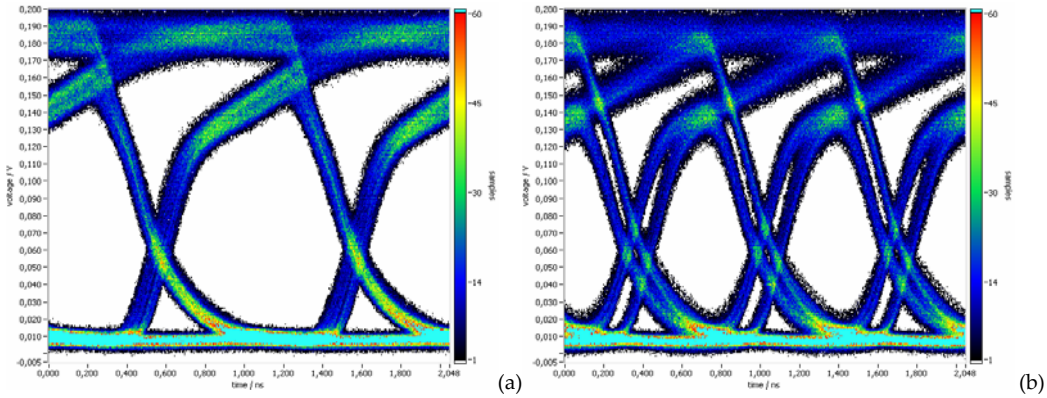

Fig.5.17 Eye diagram of the modulated signal. Optical input power: -5dBm. (a)1Gbit/s; (b)1.5Gbit/s

Detection at the absorber port

The setup for detection test is sketched in Fig.5.18. A modulated optical PRBS signal is introduced at the SOA optical port; the SOA section is biased at 180mA. The absorber section is biased at -0.5V. By means of a *Bias-T*, the RF signal is isolated from the bias and directly monitored at the oscilloscope. The eye diagram of the detected signal is represented in Fig.5.19a, b, for bit rates of 1Gbit/s and 1.5Gbit/s, respectively. The eye diagram is sharp in both cases and demonstrates good properties for detection of the integrated device even though at higher bit rate.

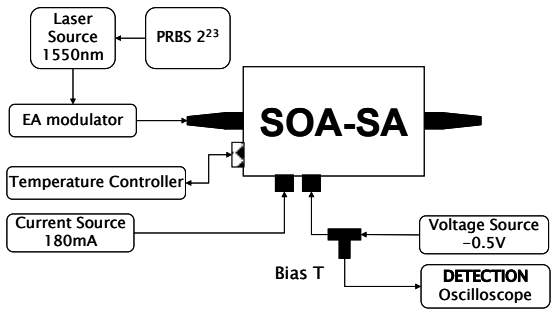

Fig.5.18 Setup of the detection at the absorber port measurements

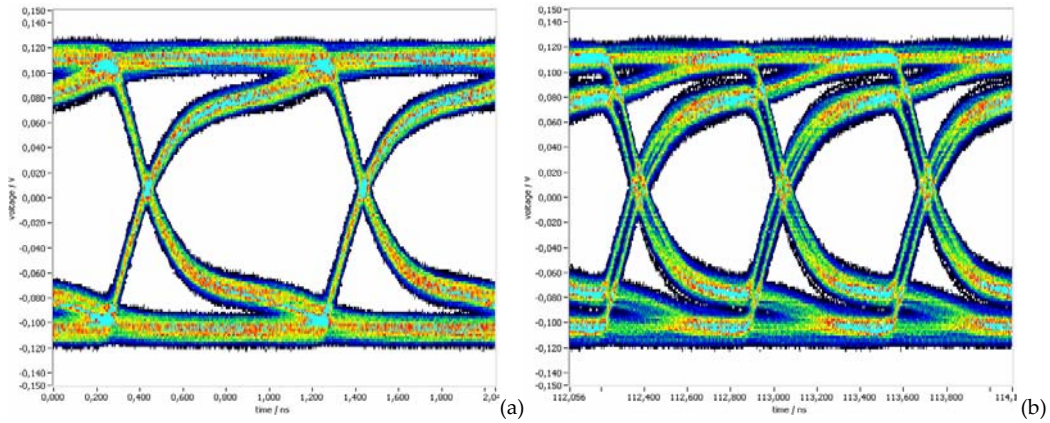

Fig.5.19 Eye diagram of the detected signal. Optical input power: -5dBm. (a)1Gbit/s; (b)1.5Gbit/s

As a conclusion, the integration of two-section material is an step forward with respect to the first generation of semiconductor amplifier but it still needs to be improved in next generation devices, properly designed for featuring the transmission of data signals.

5.3.3 RSOA. Second Generation

After that several investigation pointed up that a colourless reflective ONU is a key component for FTTH network success, some companies realised the RSOA as a competitive device deal with modulation and transmission tasks at the ONU and reengineer their products. Then a new generation of RSOAs appears, this time, specifically designed to be placed at the ONU as a reflective wavelength independent element.

In the next figure (Fig.5.20) we see the main characteristics of one of those new RSOAs; in concrete it corresponds to the model *CIP SOA-RL-OEC-1550* Reflective SOA. Fig.5.20a shows the gain and the electrical bandwidth function of the input power. The maxim gain is measured 22.5dB and the broader electrical bandwidth 2GHz; however both conditions are not present simultaneously. Fig.5.20b shows the entire frequency response for different optical input power. As an illustrating example, an adequate compromise is to set and operation point at optical gain about 10dB together with an electrical frequency bandwidth in the range of 1.5GHz, allowing thus 2.5Gbit/s bit rate. The eye diagram for this example is represented in Fig.5.20c. The detected eye is after transmitting over 25km SMF in error free operation.

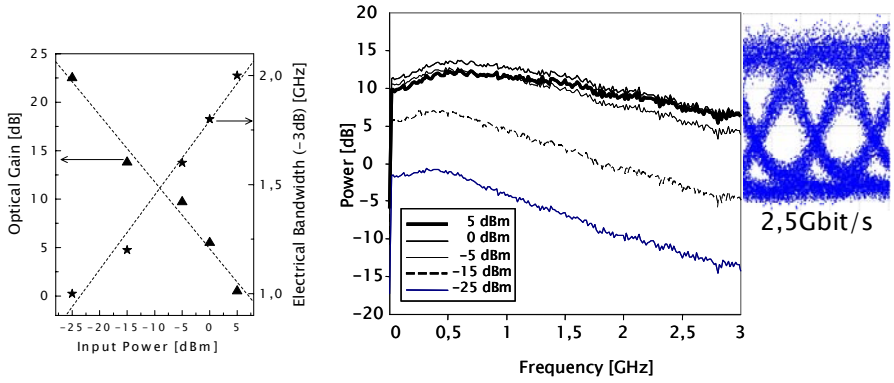

(a) (b) (c)

Fig.5.20 (a)Optical gain and electrical bandwidth as function of input power; (b)Frequency response; (c)Detected eye diagram at 2.5Gbit/s. Bias current: 80mA

A prototype developed at Alcatel-Thales III-IV Lab was also tested. It exhibits broader electrical bandwidth, more than 1.7GHz and allows bit rate up to 5Gbit/s, after electronic equalization.

5.4.4 RSOA–EAM Integration. Next Generation

As a summary, from the previous paragraphs, semiconductor optical amplifiers followed a bit rate evolution 1→2.5→5Gbit/s. Last developments report transmission at bit rate of 7.5Gbit/s [46] and 10Gbit/s [47] with integrated chips. The future generation of devices will consist on the integration of a reflective SOA and electro-absorption modulators (EAM) in a single chip, similar to the type studied in section 5.3.2 and optimise them as 10Gbit/s reflective modulators or detectors in order to benefit from EAM high speed flexibility as well as from power equalisation function of SOA. The RSOA-EAM is a device with an active SOA section monolithically integrated with a passive EAM section. The EAM offers very high bit rate modulation ability and the best compromise between drive and high extinction ratio.

A further approach is a two-section SOA, formed by a SOA section and an RSOA section. The operation is the same as for an RSOA-EAM, except for SOA modulation through injection current, instead of voltage modulation for EAM. The advantage is to have insertion loss free operation. In addition, employing the same structure in both sections leads to a simpler technological process.

Chapter 6

Features of Bidirectional Transmission in PONs

The increasing development of data communications and real-time applications urgently demand for an upgrade of conventional access networks in order to accomplish corresponding bandwidth and latency requirements. As the optical access network technology is considered crucial for solving this task, fibre-to-the-home became one of the main research objectives in the recent years. The share of cost per subscriber for the needed infrastructure and scalability in terms of both number of users and bit rate are fundamental constraints for the development of novel designs. Bidirectional single-wavelength single-fibre transmission is the most interesting scheme for application in the access network domain, mainly because of its cost-efficiency in terms of capital expenditure per customer. In this chapter we give an overview of general aspects involved in bidirectional transmission.

6.1 Modes of Transmission

One of the major barriers of FTTH technologies is the deployment of new fibre infrastructure. The size of the outside plant is then a critical constraint when deploying the access network. The number of kilometres of fibre required and the number of optical fusions needed to connect the ONUs to the OLT depends not only on the network topology but also on the number of fibres used for the

transmission. In Fig.6.1 there are represented the basic options for bidirectional transmission.

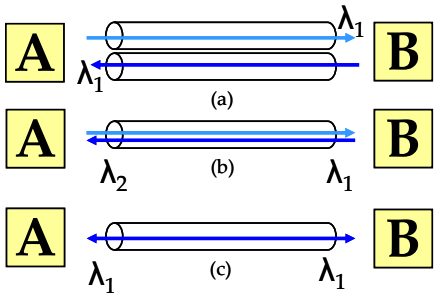

Fig.6.1 Options for bidirectional transmission. (a)Two fibres; (b)one fibre-two wavelengths; (c)one fibre-one-wavelength

A plain option is the two-fibre solution, consisting in one fibre for each direction, Fig.6.1a. Even if this is not a cost-effective design, most of the actual commercial technologies for PONs are based on this architecture. The main reason is that optical components employed are less restrictive and inexpensive laser or even LED sources can be employed achieving correct transmission results. Single fibre transmission presents a more efficient solution because only half of the amount of fibres is necessary; as well, the cost for connectors, splices and other network components decrease. Transmission over a single fibre can be implemented using two strategies. The simplest is to transmit down- and up-link data using different wavelength Fig.6.1b. Thus, the signals do not interfere with each other, as they are carried in separated frequencies. This option requires sources of different wavelength as well as and optical filters to divide up- and down-link channels. The second alternative consists in using the same wavelength in both directions, Fig.6.1c.

The last strategy presents a clear advantage for WDM networks, as wavelengths for both directions are now available especially for Coarse WDM (CWDM) networks where the number of wavelength is limited. However, there is a need of new solutions to deal with potential coherent crosstalk as well as of novel ONU designs.

6.2 Impairments

Definitely, bidirectional single-fibre transmission is the most interesting scheme to be developed in the access network; nevertheless the signal travelling at the same time over the same mean may sever degrade the transmission. Fig.6.2 shows a schematic of the transmission impairments that appears in bidirectional communication.

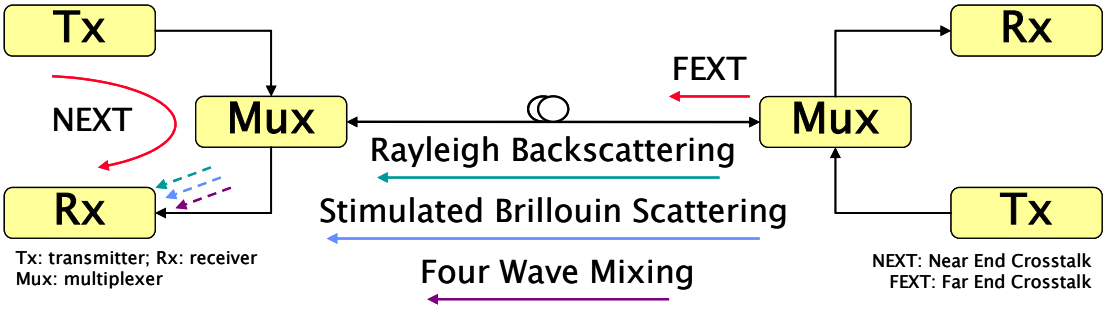

Fig.6.2 Schematic of limiting effects in bidirectional transmission

Near End Crosstalk (NEXT) and Far End Crosstalk (FEXT)

Bidirectional transmission requires an additional element within the transmitter and the receiver which separate up- and down- stream data. The multiplexer element can be a coupler, an optical circulator, a WDM coupler, or even an AWG, depending on the technique. In some configurations, transmission and reception can be performed by a single element, especially when regarding novel cost-effective devices to implement the ONU; then, the divider is not required.

The magnitude of the NEXT depends on the return loss (RL) of such components, which is usually higher than 40dB. FEXT refers to single reflections that occur throughout the transmission link and at the far end multiplexer; these, are guided backwards and detected by the near receiver. This crosstalk can be reduced by using high quality components, APC connectors or fibre splices in order to minimize the return losses.

Stimulated Brillouin Scattering

Stimulated Brillouin Scattering (SBS) is a nonlinear process of optical fibres. It takes place when the power is sufficiently high; then, part of the light propagating inside the fibre is backscattered at a shifted optical frequency, in the order of GHz (usually 11GHz at 1550nm). SBS becomes important for input power higher than 5dBm and for input power of 10dBm surpass to the Rayleigh Backscattered power. In CWDM systems, SBS would give an upper limit to the transmitted power [48].

Four-Wave Mixing

Four-Wave Mixing (FWM) is also a nonlinear process; it is caused due to the power dependence on the refractive index of the fibre. It occurs in multi-channel transmission, when two signals are injected into the fibre at frequencies f_1 and f_2, then additional signals are originated at $f_3=2f_1-f_2$ and $f_4=2f_2-f_1$. If there is an optical signal transmitted at one of those new frequencies, it experiences

crosstalk. In [48] it is demonstrated that FWM in bidirectional transmission is negligible in all practical cases because of the poor phase-matching condition.

Rayleigh Backscattering

Rayleigh scattering losses in fibre optics are caused by material density imperfections occurring during the fibre manufacture. The light is scattered in all directions, also in the back direction, which is denoted as Rayleigh Backscattering (RB). The backscattered signal will then overlap with the counter-propagating signal. RB is the most degrading effect in a bidirectional single-fibre single-wavelength system, for that reason it is analyzed in more detail afterwards.

6.3 Bidirectional Multiplexing

There are various techniques for bidirectional transmission over a single fibre through signals in the two directions can be differentiated. Those can be associated as multiplexing domains. The main ones, discussed below, are direction domain, time domain, electrical sub-carrier domain, optical wavelength domain, code domain, polarization domain.

Direction Division Multiplexing

The most straightforward is to transmit in full-duplex. Signals, at the same optical frequency are distinguished by their direction of propagation; it is named Direction Division Multiplexing (DDM). As a main advantage, it is easy to implement, as non-specific equipment is required; on the other hand, reflections and RB will produce direct crosstalk between the counter-propagating waves.

Time Division Multiplexing

A further option is Time Division Multiplexing (TDM), which consists on dividing the transmission in time-slots for uplink and downlink. In that case, signals do not suffer from bidirectional crosstalk as they are transmitted alternatively. TDM requires a signalling protocol to ensure the transmission in a half-duplex mode; there is also implicit a guard time to switch between the two directions. The inconvenient of time multiplexing is the half utilization of the channel. To achieve the same capacity as in a full-duplex system, the bit rate doubling would require at least 3dB more power budget.

Sub-carrier Multiplexing

A following technique is Sub-carrier Multiplexing (SCM). In SCM, up- and down- link signals are modulated and carried on a different electrical sub-carrier and same optical frequency. The channels are filtered out by electrical filters after the photo detection. It is simply to implement, as RF components, filters and mixers, is a mature technology, moreover part of the RB is moved out to the detection band.

Wavelength Division Multiplexing

The transmission techniques previously presented refer to employ a single wavelength for both ways of transmission. Wavelength Division Multiplexing (WDM) approach utilize different wavelength over a single fibre. This is an effective alternative especially for Coarse WDM and Dense WDM systems, where half of the wavelengths can be use for each direction. In a WDM system, signal and crosstalk remain in separated optical bands, so do not interfere each other; however, signals can suffer from intra-channel crosstalk. The magnitude of the interference will depend on the channel isolation of the WDM filter as well as on the channel spacing.

Code Division Multiplexing

As in mobile communication, Code Division Multiplexing (CDM) is an option to transmit signal over a single frequency. CDM employs different codes for the two transmission directions, which are spectrally adjacent. This technique is also referred as 'spread spectrum', as the spectra broad due to the code modulation that can be for beneficial for RB mitigation. Actually, there are two sorts of CDM. Code Division multiple access (CDMA) and Optical CDMA (OCDMA). In CDMA, the sequences are encoded and decoded in the electrical and then carried on the optical wavelength. OCDMA achieves the chip coding processing in the optical domain. The transmitted signal is encoded by an array of lasers; the decoder is based on Fibre Bragg Grating (FBG). DCM has been considered for application in PON because of its intrinsic security property, in addition to it avoids the signalling protocol that is required for TDM [49]-[50]. However, CDMA is only applicable for moderate bit rate (order of Mbit/s) and, in a FTTH network, OCDMA is not suitable for uplink transmission, as the source encoding is not a cost-effective solution to the end user, so it is not especially appealing.

Polarization Division Multiplexing

Polarization Division Multiplexing (PolDM) is based on transmitting two signals at the same wavelength but in orthogonal polarization states.

Bidirectional PolDM was first reported in [51]. Since the state of polarization of the light fluctuates in optical fibres, it is necessary to employ a polarization controller. Two separate the different polarized signals is used a Polarization Beam Splitter (PBS), which is a passive component and operates similar to a wavelength splitter but separating the two orthogonal polarizations instead. PolDM-based systems does not reduce the crosstalk from reflections respect to a DDM system, principally because a possible reflection would reverse its state of polarization, and thus interfere with the counter propagating signal. On the other hand, PolDM is often used for increasing the number of channels per wavelength by transmitting different polarized signals at one wavelength in one direction and thus double the number of possible end users [52].

For summarizing, this section reviewes the most relevant multiplexing alternatives, not all are suitable for bidirectional single-wavelength single-fibre transmission. Direction domain is simple and inexpensive but RB and reflections are presents at the system. Time domain requires burst synchronization and there are 3dB penalty for doubling bit rate. In sub-carrier domain, the RB is reduced but additional electrical components are required. Code domain has the complexity of implementation, but it also reduces RB. In polarization domain, the cost of component could be a disadvantage.

6.4 Bidirectional Modulations

Being the bidirectional single-fibre transmission over a single the preferred option, this section relates to the different modulation format alternative suitable to perform the SWSF transmission, that is how data is modulated at the uplink and downlink directions. From the perspective of the previous section, it can be understood as another domain: the 'modulation domain'.

Traditionally, the preferred modulation format for optical signals is intensity modulation (IM). Although it is not the best in terms of sensibility or robustness against noise, it is the simplest and the most cost effective to implement. However, as in the electric world, there are other ways of transmitting data, which offer better performance, but require more complex receiver schemes.

The general definition for describing the electromagnetic field in optical transmission is $E_s(t) = A_s(t)\cos\{\omega_0 t + \Phi_S(t)\}$. Where the amplitude is A_s, ω_0 is the optical frequency and $\Phi_S(t)$ is the phase of the signal. IM consist on transmitting data by varying the output power of the optical source, that is A_s, and keeping

ω_0 and $\Phi_S(t)$ constant. Optical FSK is based on transmitting each bit logical level using different frequencies hence, amplitude and phase are constant and information is contained on optical frequency. For binary digital signals, ω_0 takes two values: $\omega_0 + \Delta\omega$ and $\omega_0 - \Delta\omega$. The frequency deviation is defined as $\Delta f = \Delta\omega / 2\pi$. An important parameter in FSK modulations is the frequency spacing between '0' and '1', known as tone spacing, and defined as $2\Delta f = \Delta\omega / \pi$. Optical PSK modulation format is generated by keeping amplitude and frequency constant and adding the information at the phase $\Phi_S(t)$. For digital transmissions it takes two values, which are typically 0 and π.

In FTTH scenarios, where simplicity is always the most preferred property because of cost effectiveness, IM is the natural choice; however, FSK and PSK have interesting properties. As a main advantage, re-modulation of the upstream signal over the downstream one is transparent, as they are constant in amplitude. Re-modulation of an IM signal is also possible as long as the downstream signal has non-zero extinction ratio. On the other hand, such modulations present more robustness against RB impairments (experimentally tested in following sections).

At this point, we should remark the notations remote-modulation and re-modulation. In remote-modulation the signal for modulate with the uplink data is a continuous wavelength (CW) sent from the OLT to the ONUs. Here, up- and down data should be transmitted onto different wavelength or in a time multiplexing scheme instead. While so called re-modulation, is to reuse the downlink signal to imprint on it the uplink data. The essential combinations are following detailed.

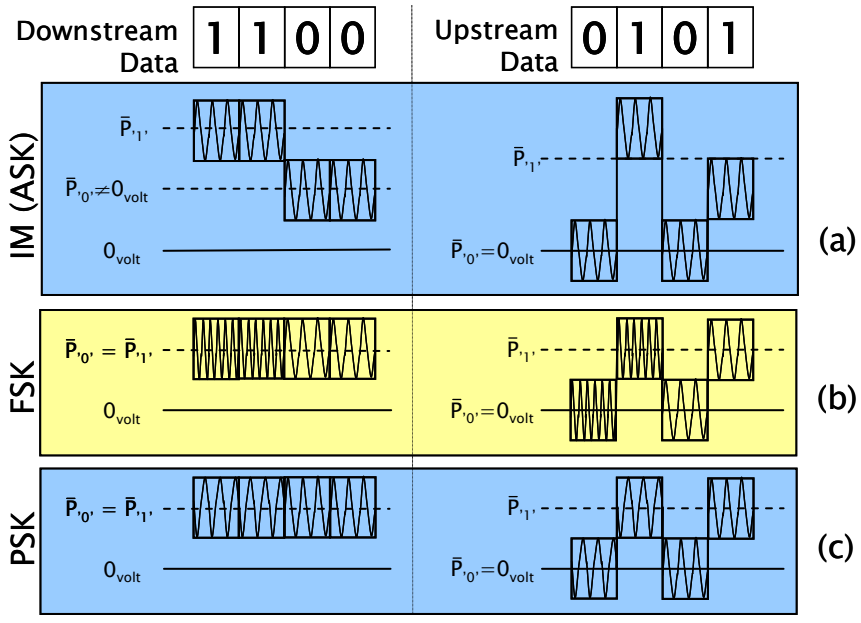

Fig.6.3 Basic re-modulation schemes

IM downlink / IM uplink

This re-modulation is based on reusing the IM downlink data to modulate the uplink data on it. This is possible when the downlink signal has a low extinction ratio (ER). Data reusing was first proposed in [16] and [17]. There, a semiconductor optical amplifier is used to saturate the incoming data and thus equalize the two levels. The resultant is a 'quasi' continuous wavelength, adequate to be modulated again. A graphical exemplification is depicted in Fig.6.3a. As a first consequence, the averaged optical power decreases (when no optical amplifier is used). Moreover, the signal is affected by a ripple that penalties the upstream BER. A trade off must be find for an optimal performance, since the downlink ER is also limited by the photo-detector.

An improvement is achieved by employing inverted Inverted-RZ coding (IRZ) [53]. The IRZ signal consist on inverting the intensity level of a normal return-to-zero (RZ) signal, thus it carries optical power at both the mark levels and the space levels in each bit period. Then half of the bit period carries the downstream data and the other, always 'ON', is use for modulating the upstream. Thus, is not necessary the process of saturating the downstream data and the ER of the downstream data can maintain high.

FSK downlink / IM uplink

In this configuration, the downstream data is modulated in optical FSK format. As the FSK signal is constant in amplitude, the upstream signal can be easily re-modulated over it, Fig.6.3b. The FSK modulation can be performed by a tuneable filter by direct modulation. FSK demodulation can be carried out by using an optical interferometer, a tuneable filter or an optical interleaver.

Our contribution to FSK down/IM up re-modulation is investigated in [28]. There, we reported an access topology based on FSK downlink and IM uplink modulation formats and remote modulation, which improves 4dB the sensitivity at BER=10^{-9} respect to send an un-modulated optical carrier. A Grating-assisted co-directional Coupler with rear Sampled Reflector (GCSR) is used at the OLT. The FTTH-PON scheme is detailed in Fig.6.4, with the proposed design of the OLT and the ONU.

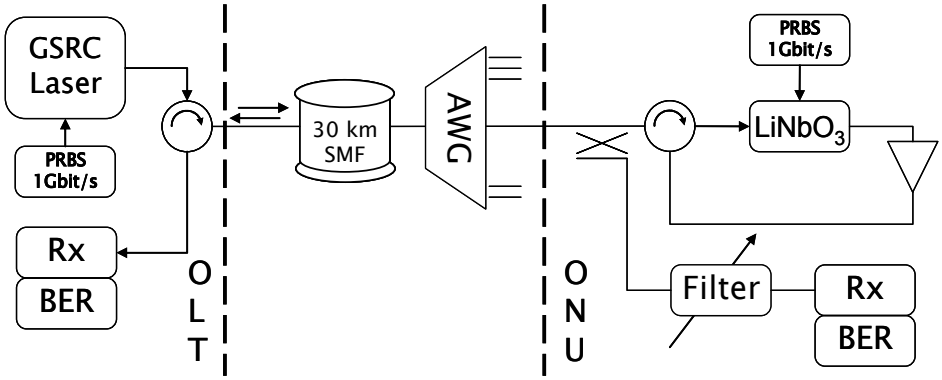

Fig.6.4 Setup for the FSK/IM re-modulation

In that scenario, the GCSR is used at the OLT for both FSK modulation and fast WDM tuning between the ONUs. An AWG routes the signals to different ONUs. At the ONU, a tuneable band pass filter at the reception branch selects the frequency corresponding to the '1' data; afterwards, the signal is photo-detected. The modulation is performed by a loop structure consisting on a $LiNbO_3$ modulator followed by an optical amplifier, to compensate the modulator insertion loss.

The transmission is tested at downstream and upstream for different conditions in order to verify the proposed topology feasibility. The GCSR was modulated at 1Gbit/s, the output power was -3dBm. The transmission was over a 30km standard fibre. The total loss of the link was 19dB. The sensitivity obtained of the downlink data with uplink transmission OFF was -23dBm, due to limitations of the laser electronics (-35.5dBm @622Mbit/s).

The optical spectrum and eye diagram for 1555.75 nm channel are shown in Fig.6.5. It can be distinguished three spectra: the signal without modulation (dotted line), the FSK signal before the filter (bold line), and the signal after filtering (normal line).

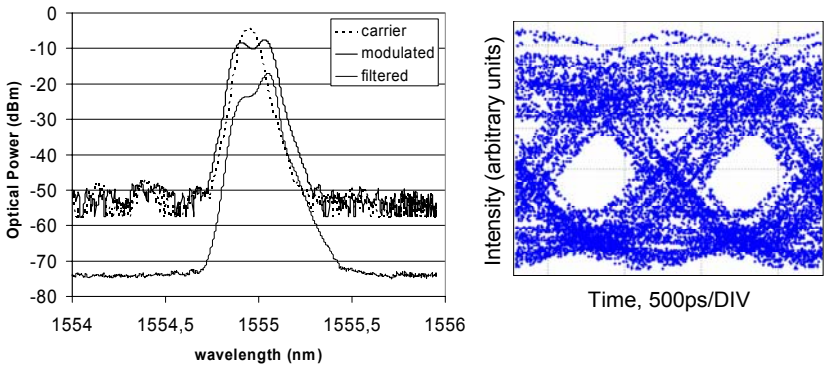

Fig.6.5 Optical spectra of unmodulated, 1Gbit/s FSK modulated, FSK after filtering and eye diagram @downlink

Results for uplink signal re-modulated and the eye at the sensitivity power are shown in Fig.6.6. The sensitivity (BER=10^{-9}) obtained for the FSK re-modulation was satisfactory, -26.5dBm. In order to compare, the downlink data was turned OFF, in that case the sensitivity was -22.5dBm, 4dB poorer due to the RB crosstalk.

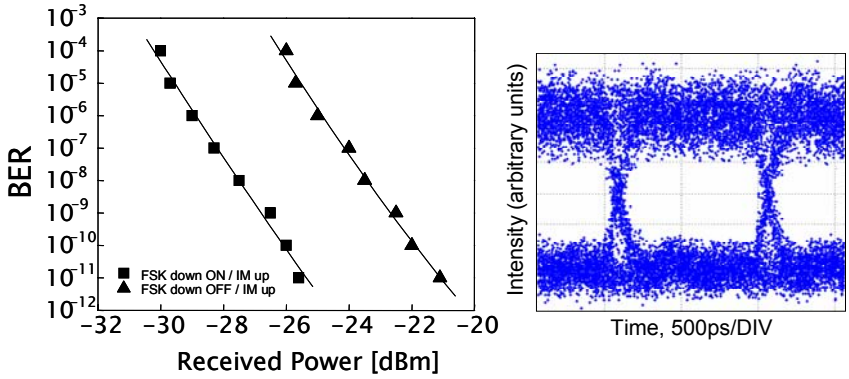

Fig.6.6 BER for FSK/IM re-modulation and IM re-modulation with FSK 'OFF'; eye diagram @uplink

PSK downlink / IM uplink

Phase modulation (PSK) is also a constant-amplitude modulation format that allows upstream re-modulation. In figure Fig.6.3c, there is a graphical exemplification. As it occurs in the FSK case, the averaged power of the downlink data should be different from zero in order to allocate the uplink signal. Re-modulation of a PSK signal was first reported in [28] where re-modulation of optical differential phase shift keying (DPSK) was successfully demonstrated, despite of a residual distortion in the uplink signal due to the phase-amplitude conversion.

The PSK signal at the OLT can be generated by an external modulator, or by an integrated electro-absorption modulator (EAM). The principal drawback of this technology is the cost of the detection components at the ONU. Demodulation of PSK can be performance by a Mach-Zehnder interferometer, an optical interleaver, or homodyne detection, for instance.

CW down / IM up –stream (remote modulation)

A straightforward solution to download a signal with continuous amplitude is directly sending a continuous wavelength (CW) carrier. This is denoted as remote modulation, since the optical signal is not modulated twice as in the previous solutions. To employ the same wavelength for both directions implies time-sharing at the optical packet level between up- and down- link in a TDM scheme.

Our input on this subject is reported in [20] where a bidirectional TDM IM-IM structure was tried out operating in burst mode. The downstream data and upstream carrier are sent from the OLT time multiplexed in a single burst. One burst section contains the downstream data and then, after a guard time, a CW is sent during the rest of the burst for upstream modulation purposes, Fig.6.7. The data source and receiver are synchronized in burst mode to the corresponding packet period (0.2μs).

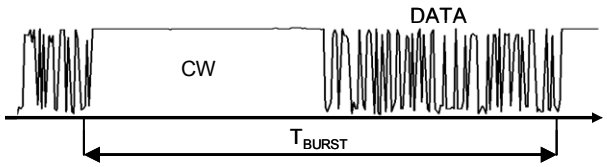

Fig.6.7 Burst of downlink signal for CW down/IM up remote modulation

The experimental setup for the experiments is represented in Fig.6.8. The light source at the OLT was a tuneable Fabry Perot-Laser InGaAsP (DFB). The output power was -6dBm. The downstream data was modulated at 1.25Gbit/s using a Mach-Zehnder modulator (MZM). The total link losses were 14dBm. The upstream data was remotely modulated at the ONU by a reflective SOA which was also employed as a photo-detector.

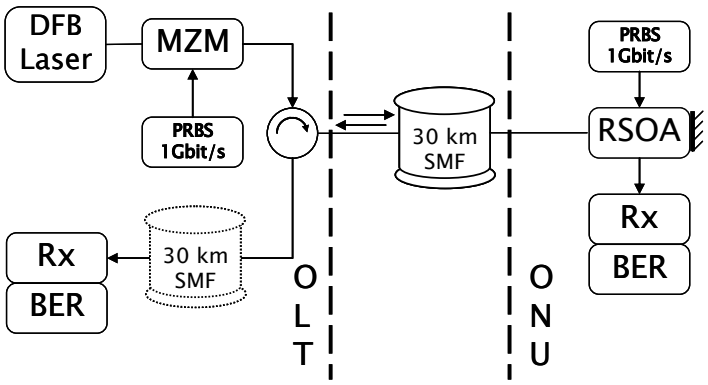

Fig.6.8 Setup for the CW/IM remote modulation

BER measurements were taken separately first in the uplink, then in the downlink. Tests were performed using, first, two separate fibres for upstream and, secondly, one a single fibre for both directions, in detection and in modulation modes. BER results are depicted in Fig.6.9. In the single-fibre configuration, the sensitivity (BER of 10^{-9}) at the downlink detection was -19dB and -17dB at the uplink. The fibre coil was then moved to the other port of the circulator, in order to emulate a two-fibre system. The sensitivity was considerably improved to -25dB. The degradation of sensitivity when a single fibre is used is caused by RB and residual reflections.

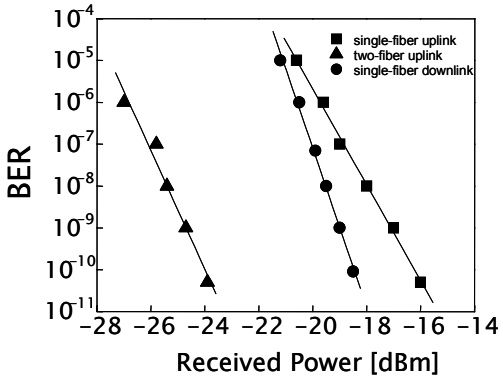

Fig.6.9 BER results for the CW/IM remote modulation

In principle, the performance of that system is worse with respect to the FSK/IM reported in [28]. Note, that the ONU is different in the two experiments and in particular, the RSOA adds as ASE noise to the signal so they cannot directly be compared.

Sub-Carrier Modulation (SCM)

In SCM, up- and down-link channels are transmitted simultaneously in a full-duplex operation on different electrical sub-carrier frequencies. In this way, optics is greatly simplified, at the expense of more complexity of electronics and SNR penalty. Besides, the method of transmitting the electrical sub-carrier admits a number of combinations. Referring to the spectral location of the sub-carriers, the alternatives are:

- Base Band down / RF sub-carrier up
- RF sub-carrier down / Base Band up
- RF sub-carrier down / RF sub-carrier up

The modulation inside the electrical channels, lets in the classical formats of the electrical RF domain like PSK, QPSK, QAM, OFDM or CDMA, for instance.

We begin investigating the SCM solution in [55] where we demonstrated for the first time full-duplex reception and modulation using an RSOA. SCM was experimentally proved to implement switched Ethernet services over a single fibre at 100Mbit/s (100Base-TX). In the experiments, a pattern generator at bit rate 125Mbit/s and PRBS=2^{-7}-1 sequence simulated the Ethernet traffic. The schematic of the test-bed is represented in Fig.6.10. The downstream data was transmitted using base band and upstream was multiplexed using a SCM channel at 500MHz. Both signals were pre-filtered using 125MHz low pass filters.

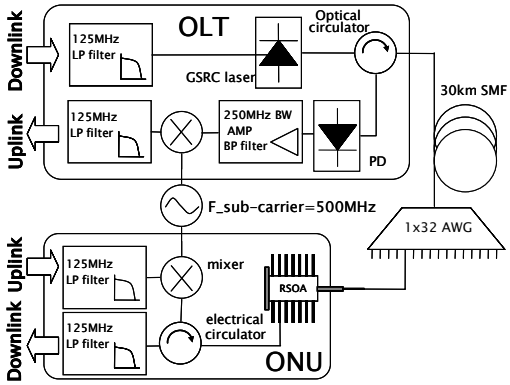

Fig.6.10 Experimental setup for SCM

The OLT was composed of a tuneable GSCR laser capable of tuning to pass through several of the 32 channels of the central AWG. The laser output power was -3dBm. It was tuned to 1543.73nm and modulated at 125Mbit/s. A circulator and photo-detector receive the upstream data. Once in the electrical domain, the signal should be down converted. At the ONU, the downstream-received data was detected by monitoring the bias current section of the semiconductor. Upstream modulation and detection using the RSOA were performed by biasing the RSOA at 60mA. The peak-to-peak excursion of the modulating data was 40mA. The transmitted upstream-data was modulated onto an electrical carrier. The line rate on each direction was 125Mbit/s, using an MLT-3 coding scheme. Since the bandwidth required for transmitting the signal is 125MHz, the SCM carrier frequency needs to exceed 250MHz in order to avoid spectrum overlay, therefore the selected sub-carrier frequency was 500MHz. Fig.6.11 contains the spectra of the downstream and upstream transmissions at the ONU side and upstream transmission at the OLT after down converting and filtering.

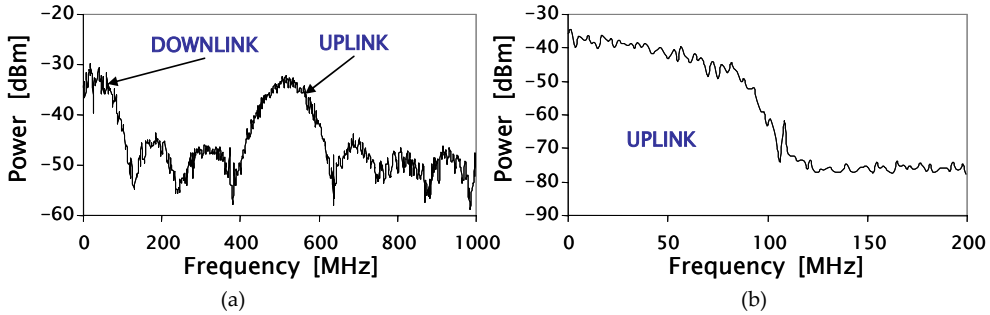

(a) (b)

Fig.6.11 (a)Spectra of the downstream and upstream at the ONU; (b)spectrum of the upstream at the OLT after down converting

The link was a 30km of single-mode fibre coil. Total loss of the link was 10dB. The achieved sensitivity (BER=10^{-9}) at the downstream reception was -29.8dBm when transmitting both, upstream and downstream and -28.5dBm

when transmitting downstream alone. This is consequence of part of the backscattered signal from the upstream is filtered at the ONU when receiving downstream data.

At the upstream, the transmission sensitivity was -25.2dBm. The degradation of the upstream-sensitivity is caused in part by the use of the RSOA as modulator, and the processes of up- and down- converting the signal to accommodate it on the SCM channel.

In [56] we also reported a similar SCM experience consisting on transmitting real VDSL data in a passive configuration.

Single-Side Band modulation (SSB)

The concept of SSB, as in the electrical domain, is based on eliminating half of the spectrum. In this technique, two double-sideband (DSB) signals are generated with carriers and modulated in quadrature, as described in the diagram of Fig.6.12. Then, the signals are added leading to the suppression of one of the modulation sidebands. The opposite operation should be performed at the remote part of the link, then two signals can travel along the same fibre without interfere each other.

An implementation of SSB in the optical domain uses a bidirectional Mach-Zehnder modulator (MZM) centred inside a Sagnac interferometer [57]. The two signals counter-propagating inside the loop interfere and generate thus a SSB signal. The modulated data is applied to the MZM simultaneously.

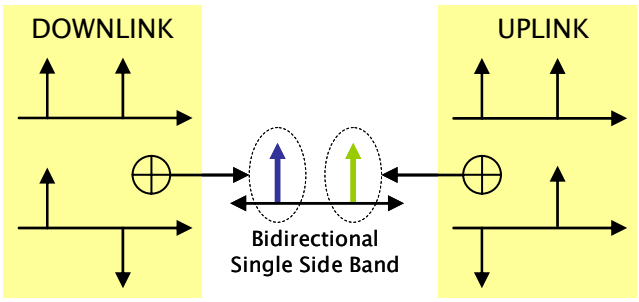

Fig.6.12 Schematic of Bidirectional SSB modulation

Chapter 7

Rayleigh Backscattering and Single Reflections

In this chapter we describe analytically the main impairments of bidirectional transmission: Rayleigh backscattering and single reflections. Although using a single fibre and a single wavelength to address each ONU in order to simplify the transmission equipment in the FTTH access network present many advantages, data signals are degraded due to the presence of Rayleigh backscattering of counter-propagating signals, as well as from crosstalk caused by possible reflections of passive components. Rayleigh backscattering represents an important limiting effect owing to signals propagating in opposite directions produce crosstalk between the signal travelling in one direction and the backscattering from the reverse directed signal. This causes both coherent and incoherent crosstalk as the signals overlap in the detection band. Back-reflections can be prevented by using angled connectors or splices nevertheless its influence should be also include on the analysis for a complete investigation.

As a remark, the systems considered in this dissertation are based on the direct-detection mechanism, that is, receivers detect only the optical power (the amplitude of the incoming signal squared) while coherent detection systems, which detects amplitude as well as frequency/phase different between the local oscillator, are out of the scope of this work.

7.1 Model of Rayleigh Backscattering in Optical Fibres

In section 6.2, Rayleigh backscattering was identified as one of the major problems in bidirectional transmission. In order to prevent from this effect, it is required a detailed analysis of its behaviour. In this section there are deduced the statistical properties of the backscattered signal and the implication on the transmission of a counter-propagating signal.

Rayleigh scattering loss in fibre is caused by material density imperfections occurring during fibre manufacture, so it becomes an unavoidable effect inner at the fibre. It is determined by the Rayleigh attenuation coefficient α_s, which is proportional to λ^{-4}. In a system with two signals at the same λ simultaneously in opposite directions, a beam travelling through the fibre from 'A' to 'B' (see Fig.7.1), causes the light scatter in all directions. The fraction scattered in the back direction, which is given by the recapture coefficient *S*, is known as the Rayleigh Backscattering noise (RB). Whenever a signal is sent from 'B' to 'A', it would be interfered by the RB noise.

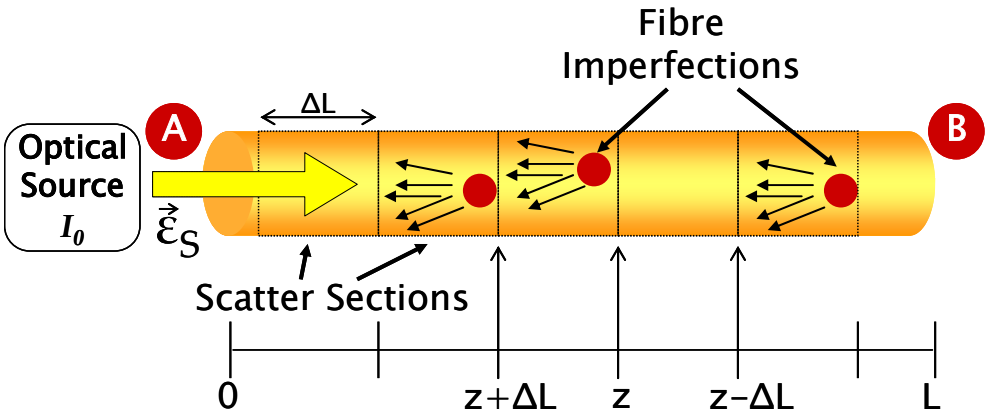

Fig.7.1 Fibre model for Rayleig Backscattering

For the deduction of the statistical properties of the RB signal, we use a two-dimensional model for the fibre represented in Fig.7.1. Where, *L* is the fibre length and it is divided by *N* scatter sections of length $\Delta L=L/N$. Considering the coherence of the source is larger than ΔL, the scattered field vectors are statistically independent.

Intensity noise of the Rayleigh Backscattering

Let us to consider a signal from a laser source launched at the beginning of the fibre (*A*). The electrical field linearly polarized at the source is expressed as

$$e_s(t) = \Re e\left[\vec{\varepsilon}_s(t)e^{j\omega_0 t}\right] \tag{7.1}$$

$$\vec{\varepsilon}_s(t) = \vec{p}_s\varepsilon_s = \vec{p}_s\sqrt{I_0}\gamma(t)e^{j\phi(t)}. \tag{7.2}$$

Where $\vec{p}_s$ is the Jones vector that indicates the source field polarization state; ω_0 is the optical carrier frequency; $\phi(t)$ is laser phase noise; I_0 is the amplitude of the field. $\gamma(t)$ represents the variations of the complex amplitude due to amplitude or angle modulation, $\gamma(t)=\sqrt{a(t)}e^{i\theta(t)}$. The field incident in a generic point *z* is then

$$\vec{\varepsilon}_i(t,z)=\mathbf{P}(z)\vec{\varepsilon}_s(t-z/v)e^{-\alpha z/2}e^{-j\beta z}. \tag{7.3}$$

With α, the intensity attenuation coefficient; β, the propagation constant; and v the group velocity at the fibre. **P** is the Jones matrix of the polarization state.

The fraction of the scattered field from a section located at *z*, which is guided backwards, is determined from the backscattering coefficient. The backscattering coefficient $\Delta\rho$ is assumed a time independent zero-mean circular complex Gaussian (ccG) random variable. Then, the backscattered signal at the beginning of the scatter section located at *z* is given by [58]

$$\Delta\vec{\varepsilon}_b(t,z)=\mathbf{M}(z)\vec{\varepsilon}_s(t-2z/v)e^{-\alpha z}e^{-j2\beta z}\Delta\rho(z), \tag{7.4}$$

M is the unitary Jones matrix, $\mathbf{M}(z)=\mathbf{P}^T(z)\mathbf{P}(z)$. The total backscattered field is the addition of all the contributions, that is

$$\vec{\varepsilon}_b(t)=\sum_{n=1}^{N}\Delta\vec{\varepsilon}_b(t,n\Delta l). \tag{7.5}$$

The total backscattered field can be calculated by integration making use of the differential form $\rho(z)=\lim_{\Delta L\to 0}\Delta\rho(z)/\Delta L$.

$$\vec{\varepsilon}_b=\int_0^L\mathbf{M}(z)\vec{\varepsilon}_s(t-2z/v)e^{-\alpha z}e^{-j2\beta z}\rho(z)dz. \tag{7.6}$$

The intensity noise that is in fact the power of the laser beam is $I(t)=\|\varepsilon(t)\|^2$. Then the backscattered intensity noise is

$$I_b(t)=\int_0^L\int_0^L\left(\mathbf{M}(z_1)\vec{\varepsilon}_s(t-2z_1/v)\right)\left(\mathbf{M}(z_2)\vec{\varepsilon}_s(t-2z_2/v)\right)^*e^{-\alpha(z_1+z_2)}e^{j2\beta(z_1-z_2)}\rho^*(z_1)\rho(z_2)dz_1dz_2. \tag{7.7}$$

To calculate the expectation of the backscattered intensity $\rho(z)$ is modelled as a delta correlated zero-mean ccG distribution [58], thus the averaged $\rho(z)$ is given by $\langle\rho^*(z_1)\rho(z_2)\rangle=2\sigma^2\delta(z_1-z_2)$. The Jones vector and the matrix **M** are unitary, then

$$\langle I_b(t)\rangle=\int_0^L\int_0^L\mathbf{M}(z_1)\vec{p}_s\mathbf{M}(z_2)\vec{p}_s e^{-j\phi(t-2z_1/v)+j\phi(t-2z_2/v)}\langle\rho^*(z_1)\rho(z_2)\rangle e^{-\alpha(z_1+z_2)}e^{j2\beta(z_1-z_2)}dz_1dz_2=$$

$$=2\sigma^2I_0\int_0^L\left\langle\left\|\mathbf{M}(z)\vec{p}_s\right\|^2\right\rangle e^{-2\alpha z}dz=2\sigma^2I_0\frac{(1-e^{-2\alpha L})}{2\alpha}$$

Finally, from [58] $\alpha_S S=2\sigma^2$, the averaged intensity is

$$\langle I_b \rangle = \alpha_S S I_0 \frac{(1-e^{-2\alpha L})}{2\alpha}. \tag{7.8}$$

In Fig.7.2 is depicted a graphical exemplification of the averaged intensity normalized. The backscattered intensity increases with the fibre length and converges after 20km approximately, depending of the fibre parameters. The convergence value is usually between -36dB and -32dB below the input power. In the represented example the normalized power achieves -35dB.

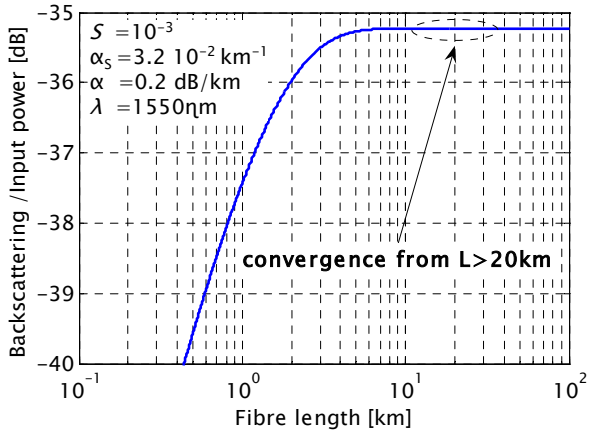

Fig.7.2 Normalized Rayleigh Backscattering intensity vs fibre length

Autocorrelation and Power Spectral Density

The Autocorrelation Function (ACF) and Power Spectral Density (PSD) of the RB signal can be calculated function of the statistical properties of the source field [59] as

$$R_b(\tau) = \langle I_b \rangle^2 \left(1 + |R_L(\tau)|^2\right) \tag{7.9}$$

$$S_b(f) = \langle I_b \rangle^2 \left(\delta(f) + S_L(f) \otimes S_L(f)\right). \tag{7.10}$$

Where R_L and S_L are the ACF and PSD functions of the laser, respectively. The spectrum of the laser linewidth usually follows a Lorentzian function with full-width at half maximum (FWHM) Δf and corresponding ACF and PSD as

$$R_L(\tau) = e^{-\pi \Delta f |\tau|}; S_L(f) = I_0^2 \frac{\Delta f}{2\pi\left(f^2 + (\Delta f/2)^2\right)}. \tag{7.11}$$

Substituting in (7.9) and (7.10), we can find the ACF and PSD of the RB intensity

$$R_b(\tau) = \langle I_b \rangle^2 \left(1 + e^{-2\pi \Delta f |\tau|}\right) \tag{7.12}$$

$$S_b(f) = \langle I_b \rangle^2 \left(\delta(f) + \frac{1}{\pi} \frac{\Delta f}{f^2 + \Delta f^2}\right). \tag{7.13}$$

We can calculate now the total power and the variance of the backscattered intensity, inside the detection band B.

$P_{RB} = R_b(0) = \int_0^B S_b(f)df = \int_0^B \langle I_b \rangle^2 \left(\delta(f) + \frac{1}{\pi} \frac{\Delta f}{\Delta f^2 + f^2} \right) df = \langle I_b \rangle^2 \left(1 + \frac{1}{\pi} tg^{-1} \frac{B}{\Delta f} \right)$. Then,

$$P_{RB} = \left(\frac{S\alpha_s I_0 \left(1 - e^{-2\alpha L}\right)}{2\alpha} \right)^2 \left(1 + \frac{1}{\pi} tg^{-1} \frac{B}{\Delta f} \right) \tag{7.14}$$

And therefore as $\sigma_{RB}^2 = R_b(0) - \langle I_b \rangle^2$, the variance is given by

$$\sigma_{RB}^2 = \frac{\langle I_b \rangle^2}{\pi} tg^{-1} \left(\frac{B}{\Delta f} \right). \tag{7.15}$$

The mean power is calculated as the square root of the variance, then the mean power of the RB noise received in detector at the beginning of the fibre, A is

$$\bar{P}_{RB} = \frac{S\alpha_s I_0 \left(1 - e^{-2\alpha L}\right)}{2\alpha} \frac{1}{\pi} tg^{-1} \frac{B}{\Delta f}. \tag{7.16}$$

The RB power depends on the electrical-optical bandwidth ratio and is proportional to the power emitted by the source. In Fig.7.3 is exemplified the normalized RB function of the laser linewidth for different data rate. The electrical bandwidth B_e=B, corresponds to the band of the electrical filter at the reception and it is associated to the bit rate so B_e=*data_rate*/2; and B_o corresponds to the laser linewidth. For example, for 3dB reduction of the RB power, it is required a relation of $B_e \approx B_o$, that is for a bit rate of 2.5Gbit/s, the laser linewidth should be wider than 1GHz.

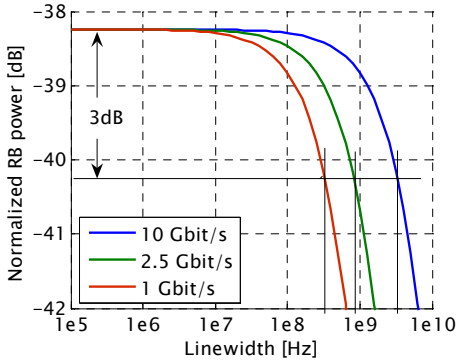

Fig.7.3 Normalized Rayleigh Backscattering power funcion of the souce linewidth

7.2 Performance Degradation due to Rayleigh Crosstalk

A measure of the performance degradation of a system is given by the crosstalk penalty, ΔP. It indicates how much the signal intensity should be increased in

order to achieve the same bit error probability as the system without crosstalk. The power penalty [dB] is given by [60]

$$\Delta P = -5\log\left(1-16Q^2\frac{\bar{P}_{RB}}{\bar{P}_S}\frac{1}{\pi}tg^{-1}\frac{B}{\Delta f}\right). \tag{7.17}$$

We performed experiments to measure the impact of the RB on the transmission. The setup is shown in Fig.7.4. The signal from a tuneable laser source is externally modulated by a Mach-Zehnder modulator (MZM) at with a PRBS-data at 1Gbit/s. Then it is spitted into the signal path and the crosstalk path via a 3dB coupler. The Part of the signal launched into the fibre coil generates the RB; a variable attenuator α_c is controls the relation crosstalk-to-signal (C/S) and the attenuator α_r adjusts the power at the reception. The power penalty obtained for a BER=10^{-9} is represented in Fig.7.5. The linewidth of the laser was varied by means of acting of the bias current. At the worst case (black line), the 1dB-penalty is achieved for a relation C/S=-21dB.

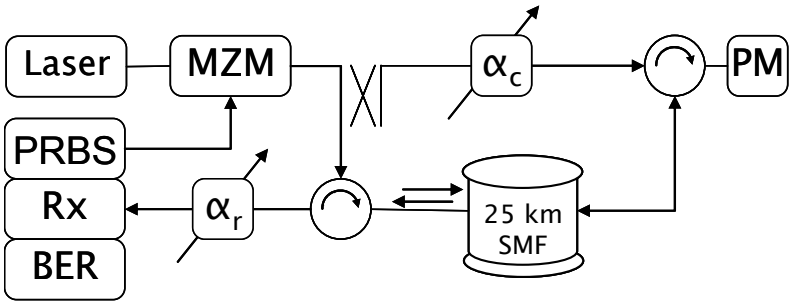

Fig.7.4 Setup for the RB Penalty measurement

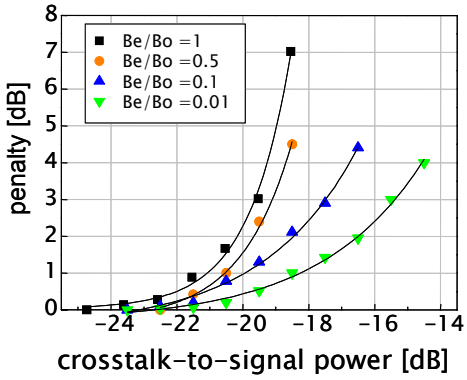

Fig.7.5 Penalty of the received power vs crosstalk-to-signal

7.3 Performance Degradation due to a Single Reflection

The second main problem to dealing with in bidirectional systems are Fresnel reflections (e.g. NEXT and FEXT). At the worst situation, depicted in Fig.7.6, signal and crosstalk are bit-synchronous and the product is a quaternary signal;

that fact degrades the system performance. The power penalty due to a single reflection is [61]

$$\Delta P = -10\log\left(1-\frac{\bar{P}_C}{\bar{P}_S}\right). \tag{7.18}$$

Figure 7.7 shows the result of comparing equation (7.18) with the case of Rayleigh Backscattering studied before, given by (7.17). For the same sensitivity penalty a lower crosstalk to signal is necessary for the Rayleigh backscattering than for a single reflection (10dB for a penalty of 1dB). Therefore, the effect of Rayleigh backscattering, which can be understood as the overlap of an infinite amount of single reflections along the fibre, is more problematic than the effect of a single reflection.

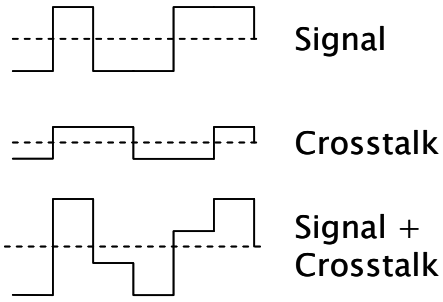

Fig.7.6 Signal, Crosstlak and quaternary sum waveform

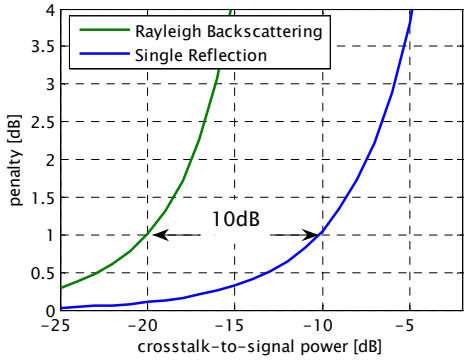

Fig.7.7 Comparison of penalty due to Rayleigh Backscattering and Single Reflection

7.4 Coherent and Incoherent Crosstalk

In the previous two sections, it was observed the influence of the laser linewidth at the bit error in terms of power penalty as well as the degradation produced by a single reflection. Here we examine what is in fact occurring with the spectra of the signals involved.

The detected current by a photodiode follows a square law characteristic according to equation (7.19)

$$i_{ph} = R\left[P_S(t)+P_C(t)+2\sqrt{P_S(t)P_C(t)}\cos 2\pi\left(f_{beat}t+\Delta\Phi(t)\right)\right], \tag{7.19}$$

where P_s and P_c are the optical powers of signal and crosstalk, respectively; R is the responsibity of the photodiode; f_{beat} is the difference of the frequencies of signal and crosstalk (the beat frequency); and $\Delta\Phi(t)$ is the optical phase difference.

The first two terms in (7.19) are the powers of the two interfering fields. The third term gives interferometric effects between the two fields, and determines the category of the crosstalk. If the beat frequency of the two fields, f_{beat}, is not within the electrical bandwidth of the receiver, then the crosstalk effects are removed at the receiver, and the crosstalk is denoted as heterodyne. Since only the first two terms in (7.19) remain, the effect of heterodyne crosstalk is to give additional optical power at the receiver. Homodyne crosstalk is then the case when the beat frequency of the two signals falls within the receiver bandwidth. That is to say, the named Optical Beat Interference (OBI) interference is the homodyne crosstalk.

Let us to define now the terms coherent and incoherent addressing to the homodyne crosstalk. The nature of incoherent and coherent homodyne crosstalk is very similar. Both types of crosstalk are due to interference between the co-polarised components of two or more optical fields at the same nominal wavelength, with a phase difference between them. The feature that distinguishes them from each other is the rate at which the optical phase difference $\Delta\Phi(t)$ changes, leading to different consequences when the fields are detected.

Coherent crosstalk occurs when the signals are phase-correlated. In other words, the phase difference between them is either constant, or changes on a much slower time scale than the coherence time of the optical sources. In order for coherent crosstalk to occur, the phase noise of the two fields must be the same over longer times than the coherence times of their sources. This condition only happens if the fields are generated by the same optical source. Therefore coherently interfering fields must have identical optical frequencies.

Incoherent crosstalk appears when the optical phases of the interfering signals are independent, or their phase difference is varying on a shorter time scale than the coherence time of the optical sources. That is when the difference between the two optical phases varies rapidly and randomly over $[0,2\pi)$. Therefore, incoherently interfering fields can be generated by either one or multiple optical sources, which corresponds with the single reflection situation.

In a single-wavelength system, homodyne crosstalk is always present, since signals have the same nominal optical frequency so directly overlap at the detection band, $f_{beat}=0$. Despite of remaining after detection, the second term in (7.19) influences slightly on the bit error-rate (BER) since it usually has low power compared to the data signal. However, the third term in (7.19) has a more severe effect due to the product P_sP_c. In the case of RB, the effect of the third term will depend on the nature of the source that generates it and may be somehow controlled. For example, a source with a narrow linewidth will produce coherent crosstalk (coherent Rayleigh crosstalk), but by increasing the

source linewidth the coherent crosstalk can be reduced provided that the linewidth is broad enough to fall part of the backscattered out of the reception band. The coherent Rayleigh can be also turned into incoherent, by forcing the phase difference $\Delta\Phi(t)$ to vary rapidly. Fig.7.8 gives an overview of crosstalk in a single-wavelength situation, in that case f_{beat}=0. After the photo-detection we find the three terms of equation (7.19): the desired signal (blue), the Rayleigh backscattering signal and the crosstalk which will be coherent crosstalk (striped), and then directly overlap with the desired signal or incoherent (red) and drifting over the detection band.

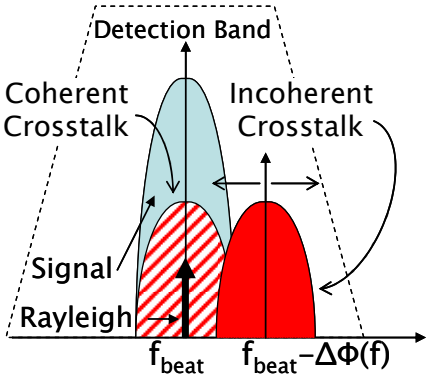

Fig.7.8 Spectra of homodyne crosstalk

Diverse modulation techniques can be applied to reduce these interferences, by proper broadening of the spectrum of the downstream signal and thus adding incoherence between the upstream data and the counter-propagating signal. Coherent and incoherent crosstalk can be also reduced or even eliminated if the signals are multiplexed in the electrical field. We treat them in the next chapter.

Chapter 8

Mitigation Techniques for Rayleigh Crosstalk

The increasing demand of the splitting at WDM-PON networks implies to increase the total power injected into the fibre, therefore RB power increases at the same time, becoming an important fact. When the same wavelength is used for both directions the temporally occurrence of coherent crosstalk should be handled to reduce the penalty due to crosstalk. In previous sections we learnt that in single wavelength systems we can prevent from crosstalk by taking out the interference signal from the detection band. Based on this idea, in this part we present several techniques and implement several of them in this section to mitigate the effect of Rayleigh Backscattering.

8.1 Laser Linewidth Broadening

As deduced in [58] and also demonstrated in section 7.1, the power spectral density function of the backscattered signal can be approximated by the source spectrum with twice the source linewidth. Therefore, the first practical issue to study is how the source linewidth influences on the reception of the upstream signal when it originates from remotely seeded light. The reduction of the coherent Rayleigh noise was first reported in [60] and [62] where it is shown that the spectrum of the RB noise tends to a more flat spectrum as decreasing the relation between the electrical and optical bandwidths, by means of either enlarging the linewidth of the source or slowing down the bit rate of the data

signal. We already notice such effect in terms of power the budget previously, in section 7.1 and contrast with the theory proposed in [60]. With the purpose of a deeper analysis we continue now with the developing of an analytical description for the BER function of the source linewidth.

Assuming Gaussian statistics for the RB signal, the bit error rate (BER) is given by

$$BER = \frac{1}{2} erfc\left(\frac{Q}{\sqrt{2}}\right). \tag{8.1}$$

By considering zero extinction ratio $I_0 = 0$ and P_1 the received power for the marks, the Q-parameter for the upstream detection can be approximated as

$$Q = \frac{I_1 - I_0}{\sigma_1 + \sigma_0} \approx \frac{RP_1}{\sqrt{\sigma_{S\_RB}^2 + \sigma_{RB}^2 + \sigma_T^2} + \sqrt{\sigma_{S\_RB}^2 + \sigma_{RB}^2 + \sigma_T^2}}. \tag{8.2}$$

Where $\sigma_{S\_C_{RB}}^2 = 4R^2 P_1 \bar{P}_{RB} \frac{1}{\pi} \arctan \frac{B_e}{B_o}$; $\sigma_{C_{RB}}^2 = 4R^2 \bar{P}_{RB}^2 \frac{1}{\pi} \arctan \frac{B_e}{B_o}$; $G_{coh} = \frac{1}{\pi} \arctan \frac{B_e}{B_o}$ and $B_0 = \Delta f$, i.e. the optical bandwidth twice of the laser linewidth.

It should also be taken into account the degree of polarization (DOP) of the Rayleigh backscattering. In [48] is reported that the state of polarization of the RB light is the same as the state of polarization of the incoming light and that the DOP of the RB is 1/3 of the DOP of the incoming light. Including the term *p* for denoting the DOP of the backscattered signal and substituting with the variances in equation (8.2), the Q-parameter leads to

$$Q = \frac{RP_1}{\sqrt{4R^2 P_1 \bar{P}_{RB} p G_{coh} + 4R^2 \bar{P}_{RB}^2 p G_{coh} + \sigma_T^2} + \sqrt{4R^2 \bar{P}_{RB}^2 G_{coh} + \sigma_T^2}}. \tag{8.3}$$

Where $\frac{C}{S} = \frac{\bar{P}_{RB}}{\bar{P}_S} = \frac{\bar{P}_{RB}}{P_1/2}$; $Q_{REF} = \frac{R\bar{P}_S}{\sigma_T}$. Thus,

$$Q = \frac{2Q_{REF}}{\sqrt{2(C/S) p G_{coh} (2Q_{REF})^2 + 2(C/S)^2 G_{coh} (2Q_{REF})^2 + 1} + \sqrt{2(C/S)^2 G_{coh} (2Q_{REF})^2 + 1}}. \tag{8.4}$$

Since the crosstalk to signal ratio is large than -10dB, the terms on $(C/S)^2$ can be simplified from equation (8.4). Then (8.4) changes into

$$Q \approx \frac{2Q_{REF}}{\sqrt{8(C/S) p G_{coh} Q_{REF}^2 + 1} + 1} \tag{8.5}$$

From (8.1) and (8.5) the BER is represented in Fig.8.1 as function of the laser linewidth. As predicted from the theory, the BER can be improved in some orders of magnitude by acting on the source. It is reflected that broadband light sources perform better respect to coherent light sources.

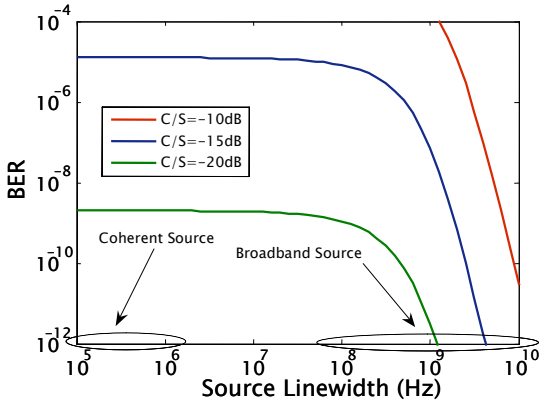

Fig.8.1 BER function of the laser linewidth for different (C/S), Q_{REF}=10

Experimental Results

In order to experimentally quantifying the theoretical results, BER measurements with three laser sources of different linewidth were performed. An external cavity (61600B), a DFB (CQF935) and a tuneable GCSR (NYW30) were used. The laser linewidth is defined as the full width at half-maximum (FWHM) of the spectrum. The FWHM of the three sources is measured with the method of heterodyne using a local oscillator, described in [63]. The measured FWHM were 150KHz, 1MHz and 30MHz, correspondingly. As an example, Fig.8.2 shows the Lorentzian shaped spectrum. It was captured from the spectrum analyzer after heterodyne with a narrow source.

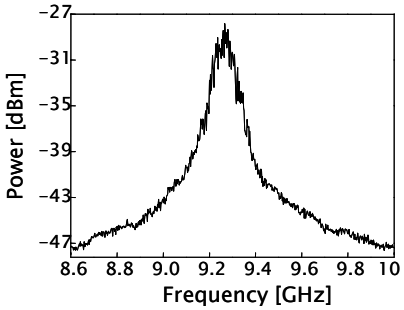

Fig.8.2 Example of Lorentzian spectrum. Laser GCSR (NYW30)

The experimental setup for the BER measurement is shown in Fig.8.3. At the OLT, the feeder signal for the ONU is generated by the laser source, which was exchanged by the different lasers to carry out the experiments; the transmitted power is 0dBm. The reception branch is composed of a variable attenuator, a 95/5 coupler to measure the received power, a PIN-TIA photo-receiver and the BER analyzer; an optical circulator separates both branches. The link consists of 25Km of SMF. The ONU is a loop-based structure placed between two ports of an optical circulator; the upstream data is generated by a 1Gbit/s PRBS 2^{11}-1 signal to a MZI Modulator (MZM) with zero chirp. Then, an EDFA amplifier, an

isolator and a filter compensate insertion losses of the modulator and ASE noise of the amplifier; a polarization controller is also included to control the launching conditions of the upstream signal.

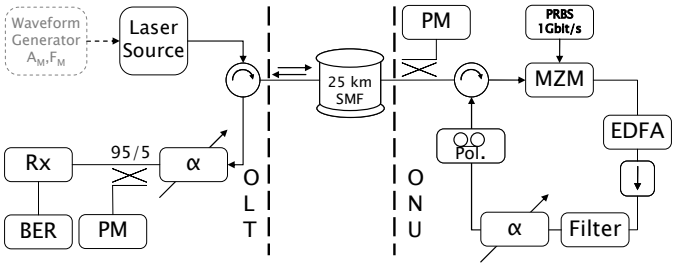

Fig.8.3 Experimental setup for source broadening and frequency dithering (dotted box)

Figure 8.4 shows the obtained sensitivity at BER=$10^{-9.}$ In the experiments, the FWHM laser linewidth ranked from 150KHz to 200MHz (they were broadened by adjusting the bias conditions). From results, it is deduced that the sensitivity is improved when optical sources with wider FWHM are employed transmission is easily tolerant to this effect if the laser linewidth; and with highly coherent light sources, there is a penalty of about 4dB.

As predicted from the theory, the bigger improvement is arisen when the frequency widening is in the order of the bit rate. Actually, two phenomena are the responsible: the fraction of the crosstalk which is fixed at the base band (7.19) is reduced due to the broadening; and the third term in (7.19) has broader spectrum and at the same time it moves along the detection band that is, it turns into incoherent.

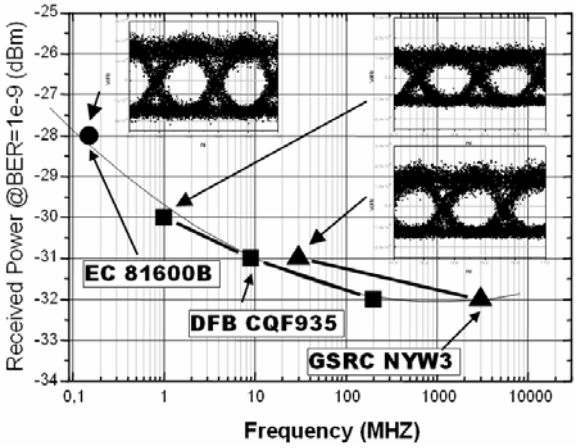

Fig.8.4 Receiver sensitivity power as a function of the laser linewidth (for different lasers)

8.2 Frequency Dithering

In the previous section is studied how source broadening is an effective method to add incoherence between counter-propagating signals involved in bidirectional transmission and thus mitigating the RB effect. However, sometimes this issue can be difficult because it means to employ different kind of laser to adjust the device to the required optical bandwidth; moreover, some applications would require a linewidth of GHz and maybe a laser with such is not available. In this direction, we propose an easier option which consists on applying an analogical RF signal to a direct modulated laser. That results into an optical FM spectrum; in this way, it is possible to achieve optical spectra in the order of GHz. The shape, the amplitude and the frequency of the modulating signal will determine the shape of the spectrum, hence the optical bandwidth. In order to avoid distortion on the signal, the spectrum of the RF modulated should be as flat as possible, for instance a triangular pilot tone generates a more homogeneous spectra than a sinusoidal one. A collection of FM signals with different amplitudes and frequencies was used to characterize the response of a grating-assisted coupler sampled reflector (GCSR) tuneable laser (NYW30) laser; an example is sketched in Fig.8.5. It shows the heterodyned Lorentzian spectrum of the laser and the result after introducing a triangular signal of 10KHz and 0.55mA of amplitude to the reflector tuning section. The measured FWHM of the spectrum reveals the laser linewidth was measured 30MHz; and a total of 15GHz frequency deviation was yield for the FM-modulated spectrum.

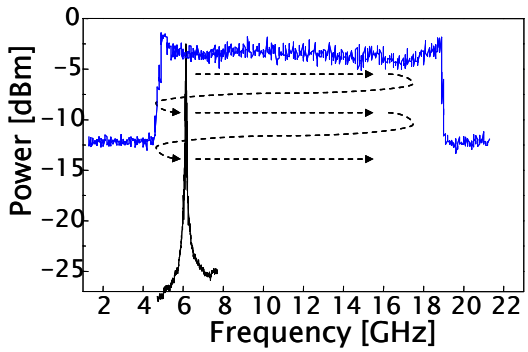

Fig.8.5 Laser spectra of a tuneable laser. Black line Lorentzian spectrum; blue line, FM spectrum with triangular modulation

In this situation, as the backscattered spectrum is no longer Lorentzian it should be treated in a similar way as if it was ASE noise detected by a receiver with an optical filter of the same width as the achieved in the frequency

deviation of the FM signal. Although (8.5) is still valid, the parameter G_{coh} should be changed as $G_{coh} = B_e / B_o$; with B_o the frequency deviation.

Experimental Results

The experimental setup is similar to previous section, represented in Fig.8.3, including now a function generator which generates the pilot tones. The GCSR laser is chosen at the OLT to generate the feeder signal for the ONU due to its flexibility for introducing the seeping modulation. It is modulated by an arbitrary waveform generator at the reflector section. The continuous-wave (CW) power transmitted from the OLT is 0dBm. The back-to-back sensitivity at BER of 10^{-9} is -32.5dBm. Then, the backscattering power is measured by placing the fibre coil and disconnecting the ONU, it is -35.5dBm. By means of the variable attenuator into the ONU-loop, the upstream power is then adjusted in order to obtain values of the crosstalk-to-signal ratio (C/S) that assures the systems is Rayleigh backscattering-limited. BER and C/S measurements are performed as a function of the FM frequency deviation, by varying the amplitude and the frequency of the pilot tone. A triangular waveform is first selected for a detailed analysis. The BER results are shown in Fig.8.6, for C/S if -13.5dB and -15.5dB. When introducing the optical FM pilot, a relevant improvement in the BER is obtained, between tree and four orders of magnitude, depending on the C/S. The improvement is around 2.4dB when increasing the optical bandwidth to 15GHz and the modulation frequency above 10KHz, where it stabilizes. The improvement is vanished for frequency deviation below 5GHz and modulation frequencies below 1KHz. Different waveforms for the pilot tone are also tested, the results are shown in Fig.8.7. The triangular signal performs 0.4dB better then sinusoidal and 1.7dB better than rectangular as it provides a more homogeneous spectrum. In all cases, a general improvement in the BER is shown when the frequency deviation is increased. The rectangular waveform behaves worst, as it may lead to laser mode hopping at the highest deviations of 15GHz.In terms of C/S, the triangular signal performs slightly better than the sinusoidal, and definitely better than rectangular one.

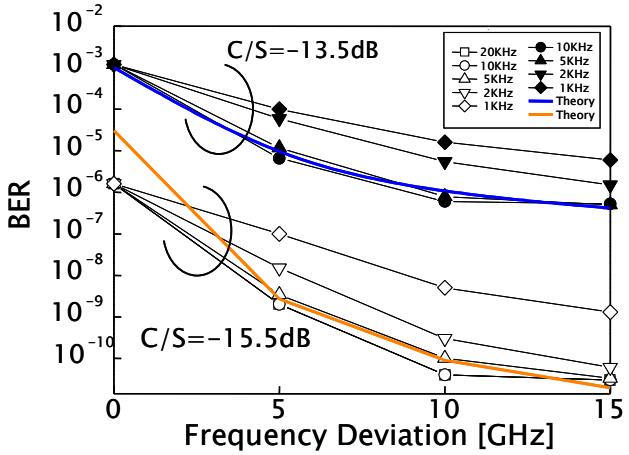

Fig.8.6 BER values as function of the fm frequency deviation and the modulating frequency

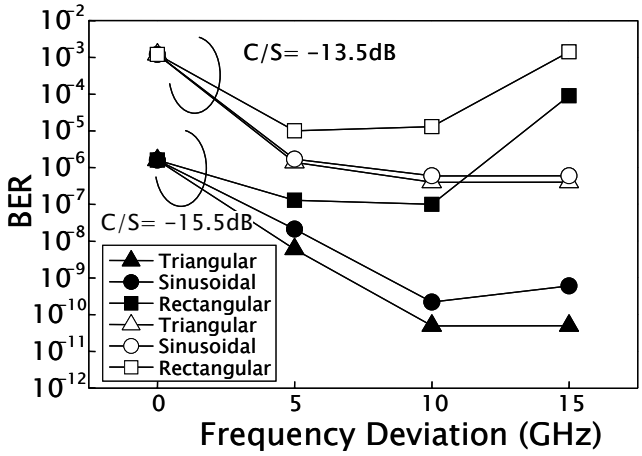

Fig.8.7 BER function of the FM frequency deviation, for different modulation waveforms, with modulation frequency of 10kHz

In conclusion, this approach consisting on introducing a RF tone to the laser source offers effectively and simplicity to combat Rayleigh backscattering effect. When broadening the laser linewidth presents a complexity, this proposal can be easily integrated in the WDM-PON system as only an electrical RF oscillator is required.

8.3 Forward Error Correction

FEC is an already experimented technique typically used to improve noise-limited long-transmission systems, but is also capable of mitigate the RB crosstalk notably using standard algorithms like two-dimensional (2D) Reed-Solomon (255, 239) coding [64]. In [2], it is reported a quantified performance in the gain due to FEC in a CWDM single-fibre single-wavelength transmission system limited by Rayleigh crosstalk. It is achieved a gain of 5.5dB in the presence of coherent crosstalk, Fig8.8. In [65] it was experimentally evaluated the maximum reach for a CWDM network and demonstrate that with the

employment of FEC the reach is enhanced by about 50%. More results on FEC performance, in combination with different modulation formats, is reported on the next issue.

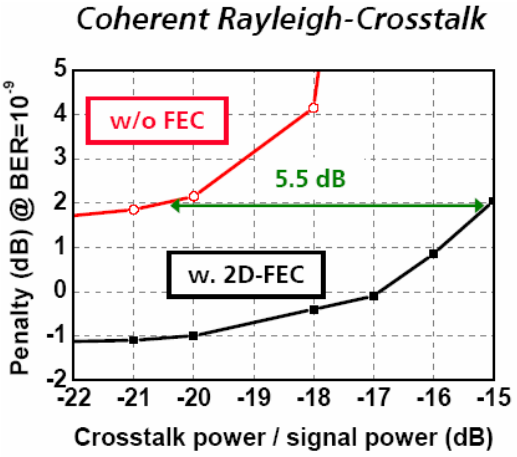

Fig.8.8 Efficiency of FEC on coherent RB mitigation. From [2]

8.4 Modulation Scheme-based Approaches

Different modulation formats are proposed and demonstrated for a single-fibre scheme. In such scenarios, the remote-ONU is usually implemented by a reflective structure or a device such as a reflective SOA (RSOA). In this situation, signal and Rayleigh crosstalk are completely coherent, since they originate from the same nominal optical frequency, therefore the way of sending the signal from the central office is a key issue and it should be carefully selected. Our experience reveals that employing signals with a modulation as a feeder signal perform better as a pure continuous wavelength tone. Moreover, constant-amplitude modulation format not only don't interfere on the transmission but also mitigate RB crosstalk.

Following the analysis of chapter 7, a similar deduction can be done for the backscattered generated by ASK and FSK modulated signals. The ACF PSD of the RB signal can be calculated again function of the statistical properties of the source field, from equations (7.9) and (7.10); now the denoted as source field, should be substituted by the field of ASK or FSK signals. An analysis of the BER could be developed by following the process of the previous chapters; nevertheless, in this part we point out a more qualitative analysis of the RB spectra.

From [59], the PSD of the backscatter of the ASK and FSK modulated signals is respectively is given by

$$S_{ASK}(f) = \frac{B^2}{T^2}\left(I_0^2\delta(f) + T^2 \frac{\sin^2 \pi f 2T}{(\pi f 2T)^2} \right) \tag{8.6}$$

$$S_{FSK}(f) = \frac{B^2}{T^2}\left[I_0^2\delta(f) + \frac{T^2}{2}\left(\frac{\sin^2(\pi(f-f_0)2T)}{(\pi(f-f_0)2T)^2} + \frac{\sin^2 \pi(f-f)_1 2T}{(\pi(f-f_1)2T)^2} \right)\right]. \tag{8.7}$$

Where $T=1data\_rate$; and $B = \alpha_S S \frac{(1-e^{-2\alpha L})}{2\alpha}$.

Regarding the expression (8.6), the bandwidth of the backscattered-ASK after detection is the double bandwidth of the ASK, that is twice the electrical bandwidth, $BW_{ASK}=2B_e$. By analogy, from (8.7), the bandwidth of the FSK function is two times the addition of the ASK bandwidth and the frequency deviation $f_D=f_1-f_0$, $BW_{FSK}=2(B_e+f_D)$. Now, comparing with the Lorentzian case, i.e. when sending a continuous wavelength $BW_{CW}=2\Delta f$ and taking as a premise that the three signals have same energy then it is clear that the amount of crosstalk within the detection band is considerable minor in the ASK and FSK situations.

How good performs FSK with respect to ASK would depend in part on the frequency deviation. Moreover, the FSK situation can be theoretically seen as a kind of sweeping, hence the crosstalk becomes more incoherent. The degree of incoherence will be given by the bit rate. Even though the crosstalk maintains coherent for the backscattered ASK, the spectrum spreading also helps to mitigate the RB effect, since the major part of the power is out of the detection band.

Following we experimentally determine the performance of thee basic scenarios where the element at the ONU is an RSOA. The implementations are outlined and evaluated by analyzing the effects of Rayleigh backscattering. The experiments focus on the uplink direction, as it is more interesting from the perspective of re-modulation. Furthermore, the uplink direction is more critical concerning Rayleigh crosstalk. In the first scenario (indicated as ASK-ASK), uplink and downlink signals are modulated by intensity modulation (IM) and multiplexed in the time domain, providing half-duplex transmission. In the second scenario, FSK for the downstream data is combined with IM for the upstream data (indicated as FSK-ASK). Finally, in the third scenario, SCM in the electrical domain is used for both, upstream and downstream channels. Full-duplex transmission in the time domain is performed in the latter two systems.

Further, Forward Error Correction (FEC) has been applied to these systems in order to increase the power budget.

8.4.1 ASK–ASK Configuration using Time Division Multiplexing

Figure 8.9 shows the setup for the ASK-ASK system. At the OLT, the downstream bursts are separated into two time slots, one slot for sending the downstream data and the other for feeding the ONU with an optical signal for

upstream re-modulation. Note that for this purpose, modulated light with an adequate offset is equally suitable. At the ONU, an electrical switch is used to select either the modulation or the detection operation. In our experiments, the bursts were generated by an ECL with an external MZI modulator, followed by an EDFA and a FBG to compensate the MZI insertion losses.

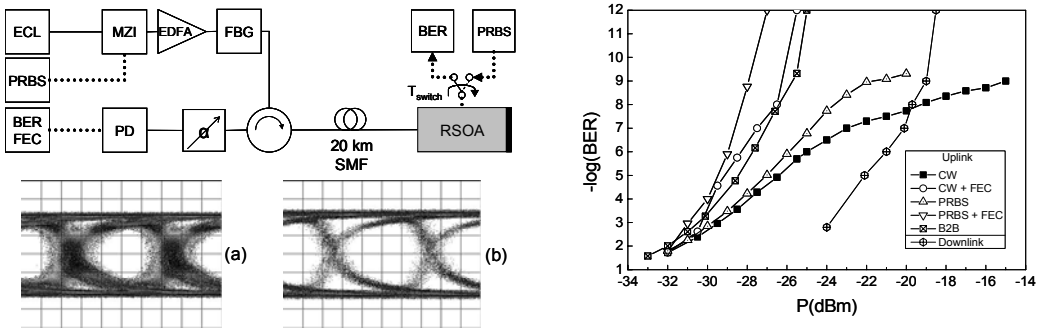

Fig.8.9 Setup and BER measurements for the ASK-ASK scheme. Eye diagram of received 1.25Gbit/s upstream signal for different downstream signals: (a)CW; (b)ASK

To analyze the effect of crosstalk on upstream transmission, we compare the uplink sensitivities resulting from the downstream transmission of an un-modulated carrier and a 1.25Gbit/s ASK modulated optical signal (in half-duplex mode). The back-to-back case is also included for reference, and the performance results are shown in Fig.8.9. The uplink sensitivity (BER=10^{-9}) is -15dBm when the upstream data is modulated onto a pure optical carrier (CW). A sensitivity of -20dBm is observed when using a 1.25Gbit/s PRBS signal with an optical power offset for upstream re-modulation. Hence, there is 5dB sensitivity improvement when the feeder signal is intensity modulated. In the experiments, different reasons contribute to the reduction of the Rayleigh crosstalk. Firstly, the modulation makes the spectrum of the downlink signal wider, so that less crosstalk power falls within the electrical detection bandwidth. Secondly, when toggling between the CW and the PRBS signal, the average launched power is lesser in the PRBS case. Consequently, the backscattered power is also reduced, resulting in a better signal to noise ratio at the OLT. This in turn improves the uplink sensitivity.

In Fig.8.9 it is also depicted the eye diagram of the received upstream signal for two different downstream feeder signals: (a), a continuous wavelength (CW) and (b), a intensity modulated (ASK). In the first case, there is an error floor at BER=10^{-9}, which corresponds to the CW curve. In the second case, where the feeder signal is intensity modulated, better sensitivity is achieved and the error floor is reduced to BER=10^{-10}.

As mentioned before, another way to improve the power budget in systems with Rayleigh crosstalk is to use FEC. To this end, the effects of FEC on the receiver sensitivity of the described system are quantified. FEC is emulated using an appropriate BER analyser. A one-dimensional (standard Reed-Solomon) FEC code with block size of 255 (n) and content size of 239 (k) is applied, introducing a transmission overhead of 6.275% and offering a correction strength of 8 bits. As a result, effective bit rate is reduced from 1.25GBit/s to 1.171GBit/s. Since the error floor is removed on the application of FEC, the sensitivity is improved by 11.4dB in the CW case (Fig.8.9, CW+FEC), and by 8dB in the PRBS case (Fig.8.9, PRBS+FEC). If the CW and PRBS curves in Fig.8.9 are to be extrapolated without the error floor, the increased sensitivity would be approximately 7dB in both situations.

The detection capabilities of the RSOA are tested by sending an ASK modulated signal at 1.25GBit/s from the OLT. As is also shown in the figure, -19dBm of optical input power is required at the ONU to achieve a detectable variation of voltage.

8.4.2 FSK-ASK Configuration using Modulation Format Multiplexing

The FSK-ASK configuration is depicted in Fig.8.10. In the experiments, a four-section GCSR laser is used to generate the FSK downstream data at 1Gbit/s. The optical frequency deviation is 10GHz and the resultant residual amplitude modulation was 0.4dB. The ONU here is divided into the downstream demodulating section and the upstream re-modulation part by an optical coupler. For FSK detection, a tuneable band pass filter converts the FSK modulation into intensity modulation by suppressing the transmission frequency corresponding to the zero data. A PIN photo-detector is used to receive the downstream data. As the FSK signal is constant in amplitude, the upstream data can simply be intensity modulated by the RSOA in the re-modulation branch.

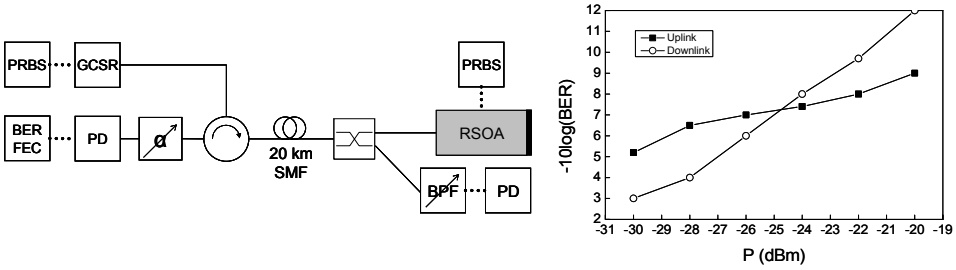

Fig.8.10 Setup and BER measurements for the FSK-ASK scheme

Figure 8.10 also illustrates the BER curves of the downlink FSK signal detected at the ONU and the upstream signal modulated over the FSK signal. In the

uplink, the sensitivity is -20dBm, as in the PRBS case of the ASK-ASK system. However, the dependency of the BER on the optical input power is weaker than that in the ASK-ASK system. Once again, there is an improvement compared to the CW system, since the FSK spectrum is broader than the spectrum of a pure tone. A downlink sensitivity of -23dBm is achieved in this setup.

8.4.3 SCM Configuration using Electrical Frequency Multiplexing

The setup for sub-carrier multiplexing is depicted in Fig.8.11. Upstream and downstream signals are multiplexed on different electrical frequencies. Since the electrical bandwidth of the employed RSOA is 1.2GHz, a bit rate of 155Mbit/s is chosen. This is the highest GPON data rate that could be accommodated in the system for testing various downstream schemes within the available bandwidth. The sub-carrier frequencies are selected with a spacing of 3 x 155MHz to prevent interference between uplink and downlink signals. The uplink SCM oscillator is locked at 852.5MHz and the uplink information is electrically modulated onto this sub-carrier. Three different tests were carried out by varying the downlink signal. First, a CW signal without downstream data is sent; second, a base band ASK-modulated downstream signal is transmitted and finally the downstream signal is up-converted and transmitted on a sub-carrier at 387.5MHz.

The results illustrated in Fig.8.11 show that there is no significant difference between the sensitivities of the back-to-back configuration and the 20km SMF transmission, when upstream data is multiplexed in the electrical domain using SCM. This result, which is consistent for each of the three downlink experiments, reveals that the Rayleigh crosstalk is greatly reduced whenever upstream and downstream data are transmitted on different electrical frequency bands.

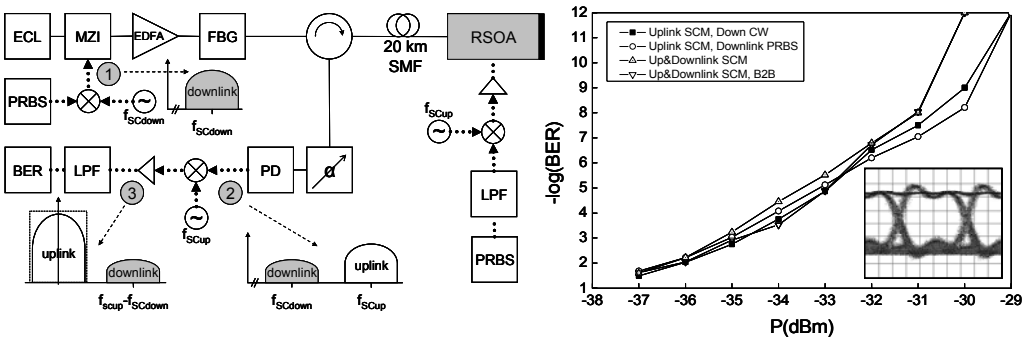

Fig.8.11 SCM setup, electrical spectrum along the link and BER measurements. Eye diagram of received 155Mb/s upstream signal @BER=10-12 for SCM downstream modulation

A graphical explanation can be seen in Fig.8.11, by considering the evolution of the electrical spectrum. At point 1, the electrical spectrum is formed only by the downlink signal, which is intensity modulated at 155 Mb/s and up-converted to 387.5 MHz. The signal travelling to the ONU is partly reflected due to Rayleigh backscattering and combines with the counter-propagating upstream signal centred on a different sub-carrier frequency (852.5MHz). At point 2 in the OLT, both the upstream signal and the crosstalk are detected by the photo-detector, and after down-conversion (point 3), the desired upstream signal is selected by final base band filtering. As the backscattered downlink signal is located in a different frequency range than the uplink signal, the related crosstalk is hardly relevant.

FEC is also applied in this scenario using the same parameters as in the ASK-ASK case. The results were similar, improving the system sensitivity by about 7dB, while reducing the effective data rate by 6.275%.

Fig.8.11 (inset) shows the eye diagram of the detected signal after filtering at a BER value of 10^{-12}. The eye diagram is clearly open. The peak at the beginning of the bit period is due to the time response of the RSOA at the lower data rate.

8.4.5 Modulation Schemes Performance Summary

In summary, a modulated downstream signal offers better performance for upstream transmission as compared to an un-modulated optical carrier, and FSK modulation behaves better than ASK modulation. Furthermore, Rayleigh backscattering is almost negligible if both the downstream and upstream data are multiplexed in the electrical domain by means of SCM, as electrical filtering during the reception process spectrally isolates these signals.

In addition, FEC techniques enhance reception by adding code redundancy protection to the transmission link, even in systems limited by Rayleigh crosstalk. This also enhances the power budget, crucial for such networks, where the upstream signal suffers twice the link loss due to the lack of a light source at the ONU.

Table 2 summarizes the characteristics of the three systems discussed in this section. The measured sensitivities shown therein correspond to the uplink direction. From the complexity point of view, the ASK-ASK and the SCM systems are remarkable options, as only one or two optoelectronic (o/e) devices are required as key ONU elements. The drawback of the SCM system is the lower bit rate, limited by the available electrical bandwidth of the RSOA. This bandwidth however, is sufficient for many purposes, including Fast Ethernet transmission. When using a photo-detector for detection and the RSOA for modulation, the bit rate can be increased to up to half of the RSOA's electrical bandwidth. Nowadays new RSOA devices allow higher bit rate.

	ASK-ASK		FSK-ASK	SCM
Sensitivity (dBm)	CW -15 PRBS -20	CW+FEC -26.4 PRBS+FEC -28	-20	-30
Bit rate (Gbit/s)	1.25		1.0	0.155
ONU o/e devices	RSOA		Optical filter, PIN-PD, RSOA	PIN-PD, RSOA
Transmission	Half-duplex (TDM)		Full-duplex	Full-duplex

Table 2 Summary of modulation combinations

8.5 Wavelength Shifting

Wavelength shifting of the optical carrier is a type of Single Side Band modulation (SSB) with carrier suppression. SSB modulation can be employed not only as a full-duplex transmission method but also as a way of removing part of the coherent RB crosstalk. A novel implementation of this method is presented in [66]. It is based on the combination of single side band (SSB) modulation and phase modulation (PM) at the ONU, which produces a wavelength shifting of some GHz over the downstream carrier, generating a new wavelength which is then modulated with the upstream data. At the ONU, a dual-arm MZM is driven in phase and quadrature. A RF generator is connected to the two arms of the MZM by through a power divider. A delay line is inserted in one of the arms to control the differential phase. The power of the RF frequency is then adjusted to reach the cancellation of the carrier; the shifted frequency is determined by the RF generator. The resultant signal can be then modulated with the upstream data by a single-arm MZM, for instance. An improvement of 7dB of the sensitivity power for a BER=10^{-9} at the OLT reception is reported in [66].

8.6 Chirped Modulation

The chirp phenomenon in direct modulated lasers as well as in Mach-Zehnder modulators (MZM) leads to an increment of the laser linewidth by a factor $(1+\alpha^2)$ [67], also named linewidth enhancement factor and Henry factor, determined by the parameter α. Therefore, it is reasonable to expect that the chirp of direct modulated MZM or RSOA might influence the transmission. In that sense, acting on the chirp of the modulator element can be also thought as a mitigation technique.

Chirp is a measure of how the optical output frequency changes with the current modulation. While the classical effect of chirping is to impose penalty in BER, in a bidirectional single-wavelength system it can help in the fashion of

adding incoherence between signals. Chirp can occur when directly driving a laser, the change in the carrier density changes the effective index of refraction, and thus the oscillation optical frequency. This is interpreted as a phase or frequency modulation. Despite the nature of chirp in external modulators is different as in direct modulated lasers, the definition of chirp is still valid. In the case of the MZM the chirp is induced by difference in the arms of the modulator.

However in both cases the outcome is an enhancement of the spectra in $(1+\alpha^2)$, the magnitude of the parameter α in direct modulated lasers and external modulators differs. The parameter α is between 2 and 10 in semiconductor lasers; in external modulators it reaches lower values, between -1 and 1. In consequence, in a direct modulated semiconductor, the spectrum could be 5-100 times broader, by acting on the alpha parameter.

The chirp of the modulator at the ONU does not affect the RB in upstream direction, since it is given directly by the source at the OLT, as already demonstrated. However, it influences the RB of the upstream data signal. In a structure with reflective-ONU configuration with amplification, the RB of the upstream signal is amplified once it reaches the ONU and reflected-backwards again. The backscattered re-amplified signal directly interferes with the upstream data becoming thus the most dangerous crosstalk in such configurations. The above methods of RB mitigation are centred on the backscatter signal in the uplink direction; nevertheless we realized that the chirp of the modulator at the ONU is at the same time a decidable variable for an effective performance of a bidirectional system.

Simulations performed using the *VPItransmissionMaker™* tool verify the previous dissertation. The simulated schematic consists of an ONU composed by a laser diode, emitting a continuous wavelength (CW), and a modulator device. An interference signal with the properties of a backscatter signal is added to the data signal. Experiments are performed at 10Gbit/s. Two modulator devices are simulated. First, a semiconductor amplifier (SOA) is directed modulated with the data signal. In the second setup the modulator device is a Mach-Zehnder modulator (MZM); an ideal amplifier is included to this set up in order to adjust the same output power in both cases. The results are shown in Fig.8.12a and Fig.8.12b. In both two different crosstalk-to-signal ratio (C/S) are simulated for illustrating as well. In the case of a direct modulated SOA (Fig.8.12a) there is and improvement at the BER of one order of magnitude when chirp is present (*alpha=10* in the experiments), moreover, the error floor is removed from the BER curves with worse (C/S).While, in contrast, for the MZM (Fig.8.12b) the curves maintain practically together when varying the alpha factor.

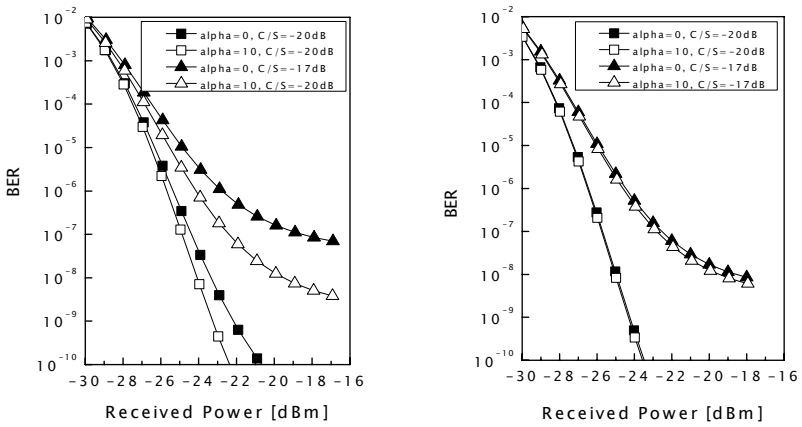

(a) (b)

Fig. 1 Effect of the alpha factor in the BER in a ONU composed by (a) Directly modulated SOA and (b) MZ Modulator

8.7 Summary of Techniques for Rayleigh Crosstalk Mitigation

To summarize, in this chapter there are reported several solution for Rayleigh crosstalk mitigation. In bidirectional single-wavelength single-fibre communication, the crosstalk provoked by Rayleigh backscattering is the most important limiting effect. For that reason, it must be dealt with any solution for alleviating such effect in order to reach feasibility a competent performance of the SWSF system in front of a two-wavelength or two-fibre proposals.

Which technique to use, will be determined in part by the modulation employed for the up and down data transmission and also by the devices available and the structure of the whole system. It is confirmed that re-modulate a signal which is already intensity modulated helps in reducing the RB effect. The same occurs with the re-modulation of FSK, and SCM signals. Adding incoherence between the desired signal and the interference signal is possible by means of novel approaches as optical frequency dithering of the feeder source or by using a modulator seemly chirped. Proper broadening of the spectrum of the feeder signal (by acting on the laser linewidth) and applying a correction code, FEC, are also demonstrated to improve the system efficiency.

Those techniques are experimented and proved in reflective-ONU configuration; in a generic ONU formed by loop with a MZM and an optical amplifier, as well as in RSOA-based ONU.

Chapter 9

Influence of the Gain in Reflective-amplified ONUs

Recent developments in WDM-PON technology propose to employ a reflective structure at the Optical Network Unit (ONU). The main requirement for the ONU is wavelength independency in order to yield uniform and therefore cost-effective FTTH solutions. In seeded-light WDM-PONs, carrier signals for the ONUs (usually CW light) are generated at the central office (CO) and injected towards the ONUs. There, the carrier is modulated with the corresponding upstream data and sent back to the Optical Line Termination (OLT). The wavelength supplier at the OLT can be not only a coherent light source (DFB, ECL, GCSR lasers) [68], but also a broadband or multimode source, in combination with the spectrum slicing technique [69]. The reflective structure at the ONU may consist, for instance, of a Reflective SOA (RSOA), a loop consisting of an optical amplifier and an external modulator, or a self-injected FP laser [70]-[71].

In optical full-duplex transmission, three main signals are travelling through the fibre: the downstream data and the carrier, in the downlink direction; and the upstream data in opposite direction. In that case, data signals are exposed to crosstalk interference due to Rayleigh backscattering (RB) and because of back-reflections from passive elements along the optical distribution network (ODN), defined as the network interconnecting OLT and ONU. The upstream signal is the most critical one as it suffers twice the fibre length and other component issues. In large ODNs that supply a high number of users,

amplification may be required. Within the ODN, the amplification is performed at the remote nodes, by means of doped fibre, and at the ONUs by employing reflective semiconductor devices [72].

When dealing with bidirectional transmission impairments, the ONU gain cannot be chosen arbitrarily. As reported in [73], an optimal value for the gain at the ONU must be properly selected depending on the link losses. The ONU gain increases the uplink signal but also the level of back reflected and backscattered light in a non-linear fashion. For instance, by applying the recommendation ITU-T G.984 to the bidirectional transmission scheme, the ONU gain should cover the ODN losses, which might be up to 30dB for a Class C network. This high level may be critical in presence of a reflection point; therefore, the ONU gain becomes an important parameter for designing the network.

In the literature, RB and crosstalk in bidirectional communication have been intensively discussed but the previous work treats the impairments separately. The study presented in [73] focuses on back-reflections from two sources, the continuous wave light at the OLT and the modulated signal at the ONU, and [74]-[76] analyze beat interferences and RB.

In the next steps of this chapter, we develop a rigorous investigation of the effect of the ONU gain and the position of the distribution node in a PON with centrally seeded-light configuration. Furthermore, we simplify the expressions considering the system exempt of reflections and only affected by RB; and study the influence of the location of the network distribution element. We deduce an expression for the Q-parameter function of the gain at the ONU and finally, the theoretical results are experimentally demonstrated.

9.1 Interferences in Reflective-ONU Configuration

In a WDM-PON with reflective-ONUs two principal signals form the upstream transmission, the carrier supplier (downstream) and the modulated data (upstream). But in fact, there are additional signals inside the fibre, consequence of the Rayleigh backscattering (RB) effect and due to potential reflections from passive components along the distribution network. At the same time, there is one group of signals deriving directly from the carrier and a second one, which comes from the modulated data. Fig.9.1 illustrates the entire scenario; the indices RB and RE denote whether the interference has RB nature or stems from a discrete reflection point. The whole set of interferences is listed below,

- Carrier_{RB}: backscattering of the downlink carrier feeding the ONU
- Carrier_{RE}: possible reflection of the downlink carrier
- Carrier_{RB_RE}: reflection of the upstream backscattering

- $Data_{RB}$: backscattering of the upstream data
- $Data_{RE}$: possible reflection of the upstream data
- $Data_{RB\_RE}$: possible reflection of the downstream backscattering

In the first group, $Carrier_{RB}$ is the backscattering of the feeder signal to the ONU. This is always present in the transmission, for a link longer than 20km it achieves a constant value of typically -34dB (normalized), depending on the type of fibre and the selected wavelength.

If the carrier finds a discontinuity affecting the downlink course, $Carrier_{RE}$ appears. In the same way, a discontinuity in the uplink direction will produce a reflection of the backscattering of the carrier signal, denoted as $Carrier_{RB\_RE}$.

In the second group, derived from the data signal, $Data_{RB}$, the backscattering of the upstream data, is the most harmful one, since it is amplified by the ONU. $Data_{RE}$ is a possible reflection of the upstream data and it may have high influence when a reflection point occurs at the ONU vicinity, due to a non-proper antireflection-coated face of a reflective-SOA, for instance. $Data_{RB\_RE}$ is a potential reflection of the backscattered upstream data; it, jointly with $Carrier_{RB\_RE}$ this is the less critical one, as reflected signals have a low level from the beginning.

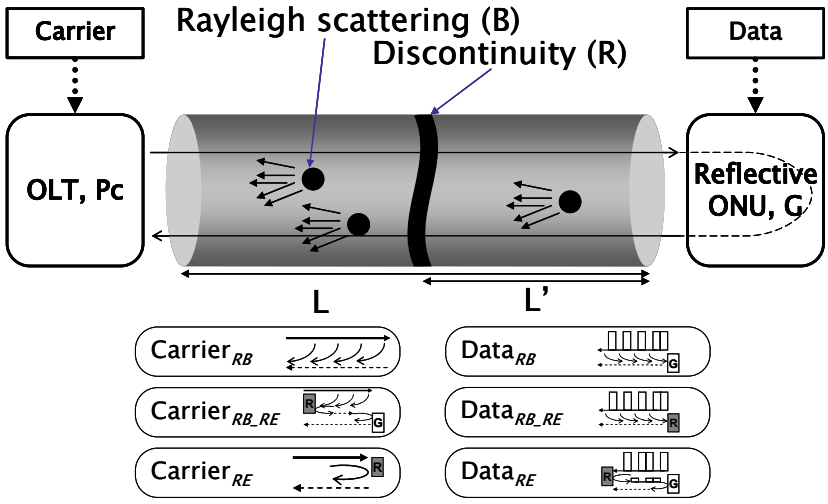

Fig.9.1. Link model and interference signals of upstream path in remote-seeded transmission

Rayleigh Backscattering of the Carrier ($Carrier_{RB}$)

The downstream carrier signal generates RB in the uplink direction. In [63], the mathematical expression for $Carrier_{RB}$, is given as

$$P_{C_{RB}} = P_C B(1-e^{-2\alpha L}), \tag{9.1}$$

where P_C is the initial power injected into the fibre; and $B = S\alpha_s / 2\alpha$, with S the fibre recapture coefficient (dimensionless), $\alpha_s[km^{-1}]$ the fibre scattering

coefficient and $\alpha[km^{-1}]$ the attenuation coefficient. Moreover, L indicates the fibre length.

Reflection of the Carrier (Carrier$_{RE}$)

Return loss in optical components causes single reflections. In our particular case, NEXT and FEXT refer to a reflection point located at the OLT or at the ONU, respectively. Reflections can also occur along the link, due to splices and distribution elements. For a generic reflection point, the signal Carrier$_{RE}$ is given by

$$P_{C_{RE}} = P_C \, \mathrm{R} \, e^{-2\alpha(L-L')}, \tag{9.2}$$

where L' is the distance from the reflection point to the ONU and R is the corresponding return loss.

NEXT should be taken into account when transmitter and receiver are directly connected to a coupler, especially for data signals with poor extinction ratio as it happens in direct modulated SOAs. However, regarding typical OLT configurations, the up- and down-link paths are merged by means of an AWG and therefore a possible reflection is strongly attenuated. By analogy, FEXT is not significant in the case of a link with high loss because the reflection suffers twice the attenuation.

Reflection of the RB of the Carrier (Carrier$_{RB_RE}$)

In the reflective-ONU configuration, a gain element is present at the ONU. Thus, the input signal is amplified, modulated and redirected to the OLT. A reflection in the direction of the ONU can cause a reflection of Carrier$_{RB}$ due to its amplification, resulting in the term Carrier$_{RB_RE}$ in uplink direction. This circle is never ending and, depending on the distance and the value of the return loss, leads to a re-amplification re-modulation feedback. By considering all the infinite reflections, the power of Carrier$_{RB_RE}$ is given by

$$P_{C_{RB\_RE}} = P_C B \left(\frac{l}{l'}\right)^2 (1-R)(1-l'^2)\sum_{n=1}^{\infty}(Rl'^2 g)^n = \frac{P_C B l^2 (1-R)(1-l'^2)Rg}{1-Rl'^2 g}. \tag{9.3}$$

For simplification, the exponential terms have been substituted by $l = e^{-\alpha L}$ (the entire loss in one direction) and $l' = e^{-\alpha L'}$ (the loss between the reflection point and the ONU).

Rayleigh Backscattering of the Upstream Data (Data$_{RB}$)

The second group of interferences derives from the modulated data itself. As it occurs with the carrier there is a backscattered fraction, which reaches the ONU, is amplified and joins the uplink signal. Named as Data$_{RB}$, it is given by

$$P_{D_{RB}} = P_C B(1-l^2)l^2 g^2 . \tag{9.4a}$$

It has to be taken into account both subsequent backscattered and upstream-amplified terms. This noise again will create RB; and the process will continue iteratively. Thus, (9.4a) develops into

$$P_{D_{RB}} = P_C l^2 \sum_{n=1}^{\infty} B^n (1-l^2)^n g^{n+1} = \frac{P_C l^2 B(1-l^2)g^2}{1-B(1-l^2)g} . \tag{9.4b}$$

It has to be noted that under normal conditions this expression depends on the squared gain, which may lead to systems limitations.

Reflection of the Upstream Data (Data$_{RE}$)

This is potentially one of the most damaging signals in reflective-ONU systems; since it also depends on squared g. Data$_{RE}$ appears as the consequence of a reflection in the direction of the ONU, as Carrier$_{RE}$. It can also lead to a re-alimented loop which is still worse in this case due to the signal that reflects has larger power. Equation (9.5) represents the power of Data$_{RE}$.

$$P_{D_{RE}} = P_C l^2 (1-R) g \sum_{n=1}^{\infty} (Rl'^2 g)^n = \frac{P_c (ll')^2 (1-R) R g^2}{1-Rl'^2 g} . \tag{9.5}$$

Reflection of the RB of the Data (Data$_{RB_RE}$)

By the same mechanism that creates Carrier$_{RE}$, the backscattering of the data signal might also be reflected to the OLT. However, in this situation, it depends directly on the gain of the ONU. Data$_{RB_RE}$ follows

$$P_{D_{RB\_RE}} = P_C B l^2 \left(1-\left(\frac{l}{l'}\right)^2\right) Rg . \tag{9.6}$$

Effect on the Downlink Transmission

A similar analysis can be done for the downlink data. The ONU is composed of a photo-detector and the reflective device; up- and down-stream transmission are separated by an optical filter (in the case of employing two different wavelengths) or by an optical coupler. Signals affecting the downlink data are the backscattering and a possible reflection (Data$_{RE}$) of the upstream data at the ONU. The first one will increase linearly with g (9.7) while Data$_{RB}$ increases with squared g. Therefore, by optimizing the gain to minimize the impact of Data$_{RB}$ we assure a low effect of the gain in the downlink detection (assuming the downlink power to be sufficient for an adequate signal to crosstalk ratio at the downlink). Moreover, in the situation of using two different wavelengths, the problem becomes independent of the gain parameter, as Carrier$_{RB}$ is in a

different band and $Data_{RE}$ would not reach the photo-detector after filtering. The expression of the backscattered signal of the downlink data is given by

$$P_{Dup_{RB}} = P_C B(1-l^2)lg\ . \tag{9.7}$$

9.2 Evolution of the Upstream Interferences

To have a range and magnitude for the required amplification factor we can base on the ITU-T standard for GPON (G.984). There are defined three network classes, depending on the ODN loss. The extreme values are 5dB and30 dB for a Class A and Class C network, respectively. The ranges for each network class and the necessary gain at the ONU side can be calculated as detailed in Table 3. The recommended margins vary between 1-27dB, depending on the network class. Thus, for our further examinations values of 0-30dB are considered.

	Class A	**Class B**	**Class C**
ODN loss (dB)	5 to 20	10 to 25	15 to 30
OLT_TX (dBm)	-4 to +1	+1 to +6	+5 to +9
ONU_TX (dBm)	-3 to +2	-2 to +3	+2 to +7
ONU_gain (dB)*	1 to 21	2 to 24	8 to 27

Table 3 Loss of the optical distribution network

(*)ONU_gain,min = ONU_tx,min – OLT_tx,max + ODN loss,min
ONU_gain,max = ONU_tx,min – OLT_tx,min + ODN loss,max

9.2.1 Influence of the Total Loss of the Link

Now we study the effect on the total loss of the link (ODN loss) when varying at the same time the gain value. In Fig.9.2.a, b, is represented the family of interference signals, defined by the expressions (9.1)-(9.6). For the representation, the return loss for a generic reflection (*R*) is set to 50dB (typical RL for a passive component); a Class A link, with minimum ODN loss and a Class C link, with maximal ODN loss are considered. For both cases, the reflection is considered at the ONU (*l'=1*).

As shown in Fig.9.2.a, increasing the gain in a link with low loss can lead to a critical crosstalk as the crosstalk signals are insufficiently attenuated. Regarding Fig.9.2, as the loss increases, the system is more relaxed in the range of values of the gain. While the carrier backscattered maintains constant, the influence of the upstream data, backscatter as well as a possible reflection of it, are not sufficient attenuated and become the most significant ones when in a link with low losses.

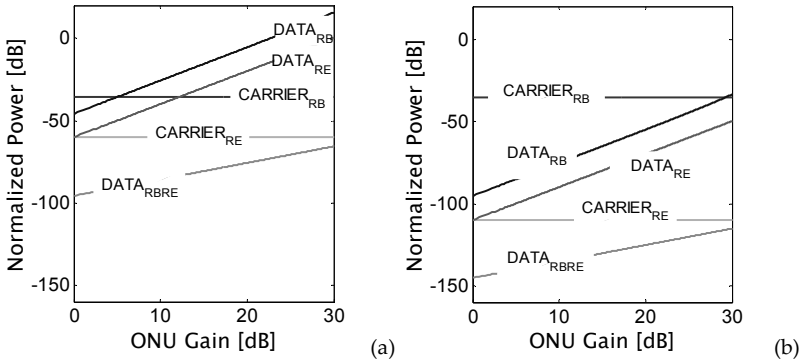

Fig.9.2. Evolution of the interferences. (a)ODN loss=5dB; (b)ODN loss=30dB. Reflection point at the ONU, R=60dB.

9.2.2 Variation with the Position of a Reflection

At this point, the aim is to examine the influence of the position where the reflection is generated. It is reasonable to expect that it is the most adverse situation if this location is at the extremes of the link because signals have extreme power values. By regarding Fig.9.3a, in a reflection deriving from the OLT in the upstream direction, a reflection of the carrier ($Carrier_{RE}$) gets importance over the rest of the signals. Moreover, a reflection of the upstream data ($Data_{RE}$) in the downlink direction may lead to a re-alimented loop due to the reflected ONU, also $Data_{RB\_RE}$. Thus, these two are more relevant when the reflection is originated at the ONU and for high values of the gain, Fig.9.3b.

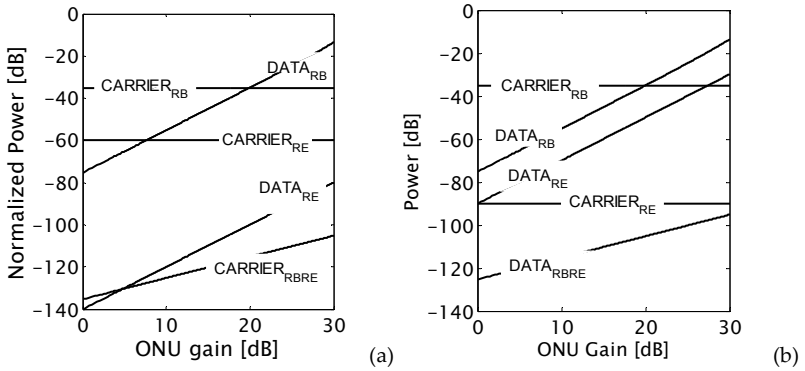

Fig.9.3 Evolution of the interferences. ODN loss=20dB, R=50dB. (a)Reflection point at the OLT; (b)Reflection point at the ONU.

9.2.3 Effect of the Return Loss of Devices

Return losses of passive components in the PON are typically in the range of 40-70dB (i.e., circulator: 40-60dB; AWG 40-45dB; coupler/splitter/filter: 40-60dB; APC-connector >60dB, fibre splice >70dB). A high reflection at the ONU side, e.g. from a defect connector, would increment considerably both, a reflection of the upstream data and the related backscattering ($Data_{RE}$ and $Data_{RB\_RE}$),

anyhow $Data_{RB\_RE}$ is quite low with respect to the upstream data. In Fig.9.4 the evolution of them is depicted for two intermediate values of reflection loss. Note that a reflection in the downlink direction, $Data_{RE}$ could develop higher order terms owing to a loop-back effect, as shown in the curve R=30dB. In the case of an ONU formed by a reflective amplifier, a reflection nearby can lead to a laser effect which could damage the equipment seriously.

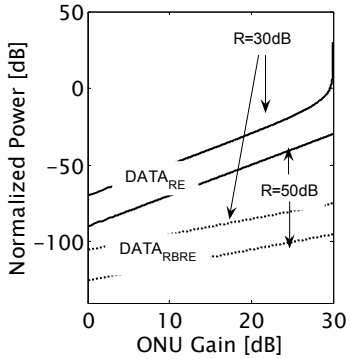

Fig.9.4. Power of interferences $Data_{RE}$ and $Data_{RB\_RE}$ for two values of return loss R=50dB and R=30dB. ODN loss=20dB.

9.3 Total Crosstalk to Signal Ratio

The total sum of all the interferences affecting the upstream transmission, i.e., expressions (9.1)-(9.6), leads to an optical crosstalk to signal ratio in the uplink direction (C/S) expressed by

$$\left(\frac{C}{S}\right)=\frac{\Sigma P_i}{P_C l^2 g}=\frac{B}{g}\left(\frac{1}{l^2}-1\right)+\frac{\mathrm{R}}{g}\left(\frac{1}{l'}\right)^2+\frac{(1-R)R[(1-l'^2)B+g]}{1-Rl'^2 g}+\frac{B(1-l^2)g}{1-B(1-l^2)g}+B\left(1-\left(\frac{l}{l'}\right)^2\right)R \quad (9.8)$$

We observe a clear dependency of the system on the amplification factor at the ONU. Specifically, the total crosstalk to signal ratio depends on the following characteristics of the network:

- The coefficient of Rayleigh Backscattering, *B*
- The ONU gain, *g*
- The total loss of the link, *l*
- The position of a reflection point, *l'*
- The return loss of passive devices, *R*

Note that increasing the gain improves the C/S, whereas an excessively large gain makes it worse. The descent and rise in the curve is because the signal increases linearly with *g* and crosstalk augments with a power of *g*.

9.3.1 Impact of a Reflection

In a previous paragraph, we have already described the evolution of the interferences owing to the reflection value, in concrete $Data_{RE}$ and $Data_{RB\_RE}$.

Nevertheless, it is useful to study the effect of a potential reflection on the total crosstalk-to-signal ratio of the system.

A graphical example of expression (9.8) is illustrated in Fig.9.5. We consider the reflection located at the ONU premises, as a most dangerous situation. The curves in the figure correspond to several values of the ODN loss, defined as the total loss of the link, that is, *l* in the formulas expressed in [dB]. As well, two representative values of the reflection are chosen for representing each situation. In a normal situation, where the components have been carefully selected to avoid reflections, we consider a minimum return loss *R* of 60dB; and as a worst case, a value of 35dB is chosen, following the ITU-T standard for GPON (G.984), which recommends a maximum of 32dB for the total return loss of the link.

It is a general tendency of the curves that high gains can make C/S worse. The C/S reaches a minimum value, obtained after the optimization of equation (9.8). It should be numerically solved due to the complexity of (9.8). Of course, the influence of reflections is negative, and the C/S gets worse by almost 2dB in presence of a strong reflection. On the other hand, for a small reflection, a gain equal to the link loss is a good approximation to the optimum value. Consequently, in order to ensure a correct performance in case of eventual reflections, it is reasonable to adjust the gain at the ONU about 3dB below the total loss of the link.

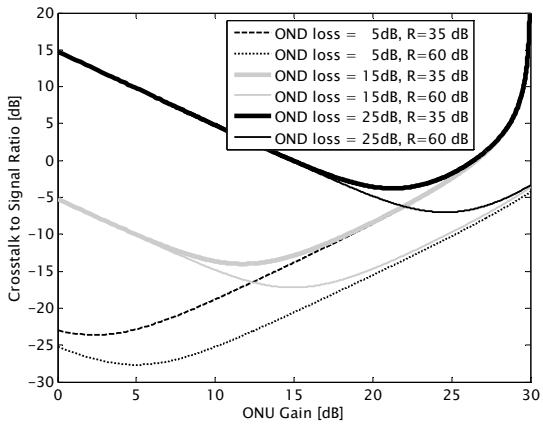

Fig.9.5. (C/S) function of the ONU gain for different values of the link loss and reflection situated at the ONU (*l'=1*).

9.3.2 Simplification by Considering Rayleigh Backscattering-only

In case of having only the effect of RB, the problem reduces to the interferences Carrier_{RB} and Data_{RB}. Considering these two, and calculating the derivative of (C/S) in (9.8) with respect to g, $\partial(C/S)/\partial g = 0$, we find that $g_{opt} = 1/l$.

In order to verify the findings, simulations were performed using the *VPItransmissionMaker™* tool. The simulated schematic consists of a CW-laser with output power 0dBm and a PIN photo-detector, forming the OLT. The link

consists of a 25km fibre coil and a 5dB attenuator, which emulate the losses from passive devices. The ONU is formed by a Mach-Zehnder modulator and an ideal amplifier. A bidirectional model for the fibre was employed which simulates the Rayleigh effect and supports full-duplex bidirectional transmission. Simulations were performed at data rates of 1.25Gbit/s. The result of the simulations is represented in Fig.9.6. The analytical curves are deduced from (9.8), simplified for the two interferences mentioned above. It can be seen that the larger separation of the signals is given for a gain equally to the reciprocal link loss. Beyond a certain point, the interference reaches higher values as the desired signal, because the data signal increases linearly with the gain, while the sum of the two interferences depends on the squared g.

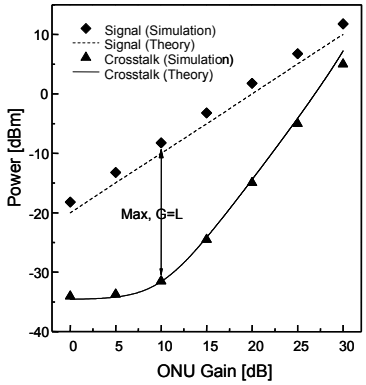

Fig.9.6 Signal and Crosstalk powers considering RB interferences (PC_{RB} and PD_{RB}). Link loss= 10dB.

9.3.3 Variations of the RB Crosstalk on the position of the distribution element

Up to this point, the analysis referred to a point-to-point link even though in a practical PON, there are distribution elements along the ODN in order to cover a certain number of users with a common OLT. Then, another relevant variable to analyse, continuing with the premise that the system is only affected by RB, is the evolution of the backscattering signals versus the position of the distribution element. Fig.9.7 depicts plain examples of a WDM-PON, formed by a single distribution element (i.e., an AWG). The distribution element can be also a splitter in a WDM/TDM-PON. The multiplexer may be found at the central office (CO) or close to it (Fig.9.7a); but also somewhere in the field (deep split), in order to reduce the total amount of fibre (Fig.9.7b).

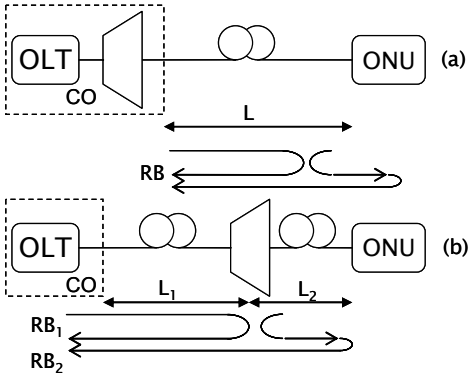

Fig.9.7 Schematic of a plain WDM-PON with different locations of the distribution element.

The distribution element introduces a fixed attenuation (usually 6-8dB) and splits the RB analysis in two zones, the distribution section (at the ONU side) and the feeder section (at the OLT side). A considerable reduction of the backscattering from the carrier signal ($Carrier_{RB}$) at the ONU side can be expected. Likewise, the backscattering of the upstream data ($Data_{RB}$) would be reduced at the link between the distribution element ant the OLT. In a situation where the distribution element is in the middle, the RB at the OLT side (RB_1) will be determined by the backscatter of the carrier and at the ONU side (RB_2) by the backscatter of the upstream data. By taking into account both, $Carrier_{RB}$ and $Data_{RB}$, and dividing the link into two zones, the expression of C/S yields

$$\left(\frac{C}{S}\right) = B\frac{(1-l_1^2)+(l_1 l_2 a)^2(1-l_2^2)g^2}{(l_1 l_2 a)^2 g}, \tag{9.9}$$

where, l_1 is the attenuation in the link OLT-multiplexer, l_2 is the attenuation in the link ONU-multiplexer; and a is the insertion loss of the multiplexer (or distribution element). Calculating the derivative in (9.9) with respect to g, $\partial(C/S)/\partial g = 0$, the optimum value for the gain is now

$$g_{opt} = \frac{1}{L_{tot}}\sqrt{\frac{(1-l_1^2)}{(1-l_2^2)}}. \tag{9.10}$$

Equation (9.10) reveals that, if the distribution element is near the OLT ($l_1 \to 1$), the gain should be low for optimizing; and on the contrary, when the distribution element is near the ONU ($l_2 \to 1$), then the optimum is for high gains.

Considered from a different side, for a given value of the gain it is useful to think of the position that enhances the system performance. For illustrating, equation (9.9) is represented in Fig.9.8 for a 50km link with 10dB loss and a distribution element with insertion loss a=5dB. Regarding Fig.9.8 (dotted line), for a gain value equals to the total loss of the link (15dB in the example), it is recommendable to avoid placing the multiplexer in the centre between the OLT

and the ONU. However, when the gain is higher than the optimum value (Fig.9.8, black line), a better crosstalk to signal ratio is achieved if the multiplexer is close to the ONU ($l_1 \rightarrow L$), as $Data_{RB}$ increases considerably with the gain. In this situation, the new optimum, given from (9.10) is 18dB. In contrast, if the multiplexer is in the OLT vicinity ($l_1 \rightarrow 0$), the best performance is obtained for a lower gain (Fig.9.8, grey line); the optimal value is now 10dB.

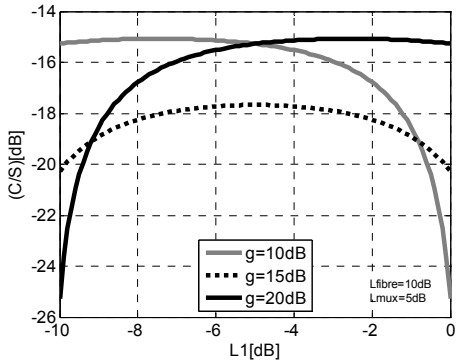

Fig.9.8 (C/S) depending on the distance between the multiplexer and the ONU. l_1=0 is at the OLT side and l_1=L is at the ONU side.

9.4 Derivation of the Q-Parameter

In order to evaluate the influence of the interferences in the system performance, appendix A presents the derivation of the Q-parameter function of the gain at the ONU. From the analysis of the previous section, we identify the most significant interferences as $Carrier_{RB}$, $Data_{RB}$ and $Data_{RE}$. It should also be taken into account the degree of polarization (DOP) of the Rayleigh backscattering. In [48] is reported that the state of polarization of the RB light is the same as the state of polarization of the incoming light and that the DOP of the RB is 1/3 of the DOP of the incoming light. Including in equation (A.3) the term p expressions (9.1) and (9.4) for denoting the DOP of the backscattered signal, then introducing these two together with (9.5) (simplified to a single round trip) and simplifying and rearranging terms, the Q-parameter leads to

$$Q \approx \frac{2Q_{REF}}{\sqrt{G_{coh}\,8\left(B\left(\frac{1+g^2}{lg}\right)p+(l')^2 R_e g\right)Q_{REF}^2+1}+1}, \tag{9.11}$$

where Q_{REF} is the Q-parameter in a system which only includes thermal noise. B is the RB coefficient, l is the total loss of the link, l' is the loss between the reflection point and the ONU, p is the degree of polarization of the Rayleigh signals, Re is the return loss value of the reflection and, for Lorentzian power spectra of the source signal, $G_{coh} = (1/\pi)\arctan(B_e / B_o)$.

Equation (9.11) illustrates the dependency of the system performance on the amplification factor. The Q-value increases for small values of *g*, however, as reflected by the crosstalk-to signal ratio analyzed previously, high values of the gain cause a reduction of the Q. In particular, the most dominant term in the denominator is the backscatter of the upstream data, as it varies with squared g. The term related to the reflection, which varies with g becomes significant for a high values of return loss.

For a more accurate estimation of the Q-parameter, ASE noise due to spontaneous emission should be included. When the ONU is based on a semiconductor amplifier, this parameter is comparable to the magnitude of the terms due to the RB. The Q-parameter, developed in appendix A is now given by (A.5)

$$Q = \frac{1}{\sqrt{G_{coh}\,2(C/S) + \frac{2P_{ASE}G_{coh}}{\bar{P}_S}}}, \tag{9.12}$$

where $P_{ASE} = (G-1)n_{sp}hvB_o$, with *G* the gain of the amplifier. Note that $G = g$ when the ONU is composed by a single amplifier device, therefore there are no insertion losses at the ONU side. It is useful to express (9.12) in terms of the noise factor (F_n). According to [42] the noise factor is described as $F_n = 2n_{sp}(G-1)/G$ and then $P_{ASE} = 0.5F_nGhvB_o$. Note that the ASE noise that arrives at the OLT is affected by the link loss, as it occurs with the rest of interferences; moreover it depends directly on the gain factor. The spontaneous emission affects the denominator in (9.12) in such way that when increasing the gain by small values, the rising of the Q-value is slower and thus the maximum value of *Q* is also smaller.

So, regarding equations (9.11) and (9.12), for high gains, the denominator increases in both cases and the interference level arrives at values in the order of the desired signal which implies a reduction on the Q-value and thus on the system performance, as it occurs when analyzing the (C/S).

9.5 Experimental Verification

With the aim to experimentally quantifying the influence of the ONU gain and, verifying the theoretical results deduced in the previous sections, we performed BER measurements to obtain sensitivity values of the system. Moreover, in a final experiment, we analyze the influence of the position of a multiplexer element.

9.5.1 Influence of the gain

Two different reflective ONUs are tested. ONU_1 is designed as a loop formed by an external modulator (MZM) and an EDFA optical amplifier (Fig.9.9). The gain is directly controlled by acting on the EDFA pump. This configuration emulates an ideal case, which is not affected by chirp (since the MZM has low chirp) and where the modulated signal is not distorted by gain variations. ONU_2 consists of an RSOA (Fig.9.10). Here, the achieved gain depends on the current applied to the RSOA. In direct modulation with RSOAs, the current modifies the power of the output signal but also adds distortion on the resultant modulation, as the working point of the semiconductor changes. ONU_2 stands for a more realistic ONU proper of a cost-effective FTTH solution.

The carrier is supplied at the OLT by a DFB laser, with an output power of 0dBm; the CW light at 1550nm is sent through a link of 25km SMF. At the ONU, the carrier is modulated and reflected backwards to the OLT.

The experimental results show the influence of the gain on the power sensitivity (for BER=10^{-9}). According to theory, a better sensitivity is reached for certain gain values.

What can be seen from the gain curves of ONU_1 (Fig.9.9) is that the power sensitivity is kept constant in a ONU gain margin of 0-8dB. The total link loss is 7dB (without including connectors). All connectors are APC, so no significant reflections are expected, so that the system is RB-limited. As estimated in our theoretical analysis, for values above the total loss, the system sensitivity gets worse. This behaviour responds to a system limited by Rayleigh Backscattering interferences, which is not affected by any strong reflection.

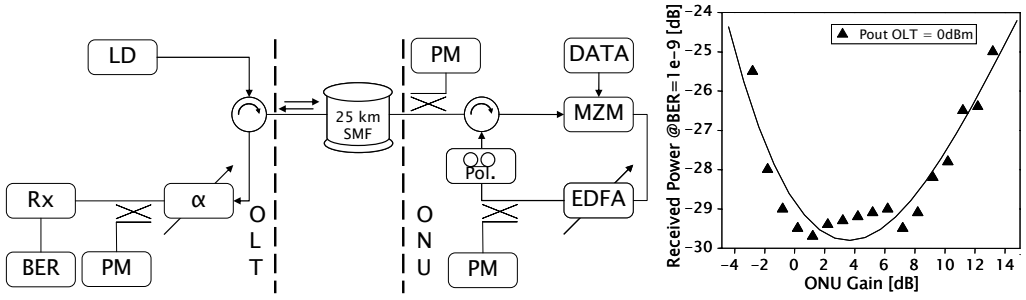

Fig.9.9 Experimental setup for ONU_1 and sensitivity results.

For ONU_2, the best performance is observed for a bias current in the amplifier of 70mA, which corresponds with a narrower gain margin of 6-8dB, depending on the optical input power (Fig.9.10). The curves in Fig.9.10 get narrower in presence of a reflection point; deducted from (9.8). In particular, for the case of the RSOA, reflections of the output signal are generated at the anti-

reflection (AR) face of the amplifier, the reflection parameter is estimated as $R=10^{-3}$. As well, ASE noise is high in such amplifiers. Notice that no optical filter is in the setup, with the aim of maintaining the philosophy of a low-cost ONU. Consequently, all the generated ASE noise is added to the modulated signal. Hence, a more accurate explanation for the curves in Fig.9.10 is given by equation (9.12).

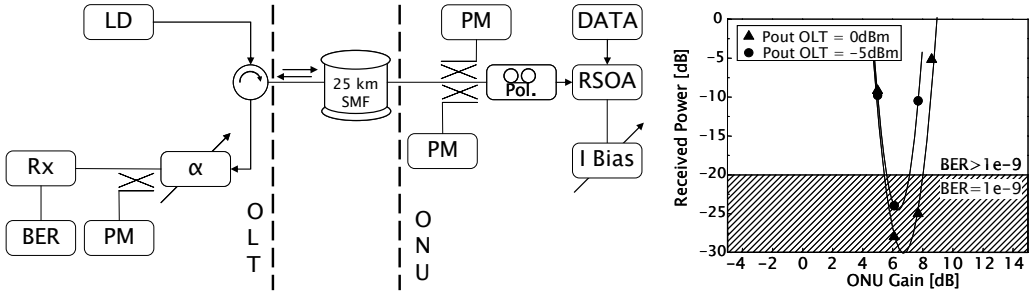

Fig.9.10 Experimental setup for ONU_2 and sensitivity results

9.5.2 Influence of the distribution element

Following, we analyze the evolution of the penalties due to RB signals versus the position of the distribution element in order to establish the most adequate location for it to be placed on. Moreover, the amplification at the ONU is analyzed in order to determine the optimum gain on each situation.

The setup of the experiments is sketched in Fig.9.11. At the OLT a tuneable GCSR laser was used to feed the ONU with a constant wavelength at 1549.32nm, matching the selected channel according with the multiplexer. The output power was 0dBm. The upstream reception was carried out by an APD photo-detector; an optical amplifier followed by an optical filter, to select the wavelength corresponding with the selected ONU was introduced before the photo-detection. The received power was measured at the entrance of the OLT, before the optical amplifier. The link was formed by several fibre coils; two sections of 25km and two of 5km, placed as shown in Fig.9.11. The total attenuation introduced by the fibre was 11.5dB. An add drop multiplexer with 3.5dB insertion loss was employed as a distribution element, so the total loss of the link was 15dB. The multiplexer was placed in different positions between the fibre sections (dotted in Fig.9.11).

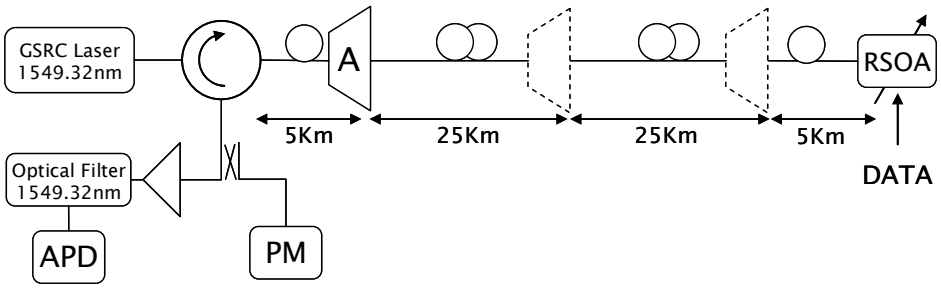

Fig.9.11 Experimental setup for the measurements varying the multiplexer position

The ONU was formed by a Reflective Semiconductor Optical Amplifier (RSOA), which was directly modulated with the upstream data at 1.25Gbit/s. The gain at the ONU was adjusted by acting on the RSOA bias current. The RSOA response to the bias current was characterized in order to find the adequate values of the gain, the results are shown in Table 4.

I_{BIAS} [mA]	50	60	75
RSOA Gain [dB]	10.1	14.7	18.5

Table 4 Gain of the RSOA function of the Bias current, Pin RSOA=-15dBm.

A first measurement was performed without the multiplexer. The BER results are represented in Fig. 9.12. The best performance of the system was for a current of the RSOA of 60mA that corresponds with 15dB (the gain matching the link losses). Theoretically, in this situation the optimum gain would be 11.5dB, between 50mA and 60mA, which requires a finer tune of the current. The back-to-back sensitivity was also measured and, in contrast, it revealed an improvement of the sensitivity at BER=10^{-9} when increasing the bias current, which confirms the strong dependence of the upstream data backscattered on the gain value.

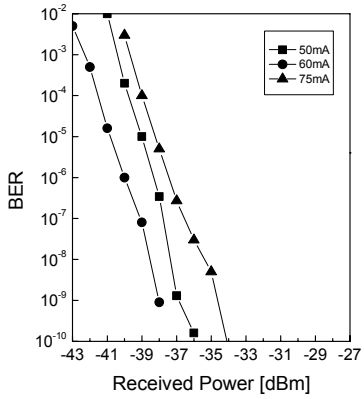

Fig.9.12 BER measurements before introducing the distribution element

Afterwards several measurements were carried out for different positions of the multiplexer. First, at the OLT side (L_1=5km, L_2=55km); second, at the ONU premises (L_1=55km, L_2=5km); and last, at the halfway of the link (L_1=30km, L_2=30km). The BER measurements for the three configurations are represented in Fig.9.13; the results agree with the theoretical approaches.

Near the OLT, the current bias of 50mA corresponding with the gain of 5dB performs the best (Fig.9.13a) and the worse case is for the larger current with a sensitivity penalty of 5dB; moreover, an error free operation is not achievable and there is an error floor at BER=10^{-9}. At the ONU side, higher amplification improves the system (Fig.9.13b). In that case, there is an error floor in the order of BER=10^{-7} for the lowest current, due to the (C/S) is not large enough to assure a BER=10^{-9} which verifies the theoretical approach, also depicted in Fig. 9.8. The worst condition occurs when the multiplexer is located in the middle of the link (Fig.9.13c), because of when placing the multiplexer in the mid-point; the 30km of fibre on each part are long enough for the RB generation in both of the sections. Here, an error floor was detected for each of the currents and error free operation is not possible in any case. The order of the error floor was 10^{-9}, 10^{-8}, 10^{-6} for currents 60mA, 50mA and 75mA correspondingly. In that case, a moderate amplification is an adequate solution.

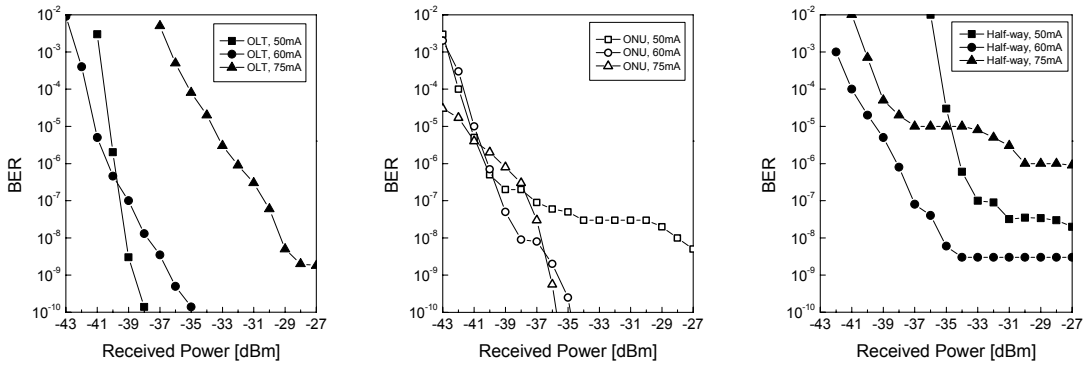

(a) (b) (c)

Fig.9.13 BER measurements with the distribution element at (a)5km from the OLT; (b)5km from the ONU; (c)half-way between the OLT and the ONU

9.6 Conclusions on the effect of the Gain

In this chapter, the influence of the gain in remotely seeded ONUs on upstream transmission is studied and evaluated. Theoretical and experimental results point up to an optimum value for the ONU gain (g). For high values of g, the interference originated from backscatter of the modulated signal becomes a term of relevance on the optical signal-to-interference ratio in upstream direction. Moreover, small reflections in passive components at the ONU or in

its vicinity are re-alimented and re-modulated and can degrade the transmission seriously. Hence, more transmission power does not necessarily imply a better performance. Preferably, the PON should be quantified in terms of loss and reflections for optimally adjusting the gain value and thus minimizing the Rayleigh backscattering effect.

We also studied the effects on the system when varying the position of a multiplexer situated in the access network between the OLT and the ONU. In such circumstances, the limitation is mainly caused by the Rayleigh backscattering crosstalk from both the carrier signal and the upstream data. The loss introduced by the multiplexer modifies the backscatter signals and the power of the crosstalk is decreased when the distribution element is placed near one of the extremes of the access network. The results also reveal that moderate values of the gain perform better, as the backscatter of the upstream data increases with the amplification introduced at the ONU.

In networks, which require large values of gain, these statements seem to be an impediment in the network design; nevertheless, it should be noted that this study is related to a point-to-point model. In a real WDM-PON network, where multiplexers and splitters attenuate signal and interference, the gain restrictions represented by the above given results are more relaxed. On the other hand, g could be increased without penalty by jointly applying techniques to mitigate the impairments of bidirectional transmission such as proper spectrum broadening of the feeder signal (by means of the laser line-width), by using hybrid FSK/IM modulation or electrical sub-carrier modulation, or by optical frequency dithering of the feeder source.

In order to ensure a proper performance in case of eventual reflections, a general recommendation is to adjust the gain at the ONU to 3dB below the total link loss. In addition, components with return loss of less than 30dB should be avoided in the ONU and OLT premises.

General Conclusions

WDM-PONs encompasses promising approaches to realise fibre-optic access networks with wavelength-agnostic ONUs, so called colourless ONUs. However, further R&D has to be conducted with respect to network architectures, key components and cost reduction. Up to now, several CWDM and DWDM-PON architectures have been reported based on colourless ONUs with uniform designs using SOAs, RSOAs or directly modulated, injection-locked FP lasers as well as VCSELs operating in a wide wavelength range; however, the semiconductor amplifier solution is the most scalable one. To form the upstream signal, these components are fed by light that is generated remotely at the OLT by individual lasers or by broadband light sources in combination with spectrally slicing AWGs, or the light is generated by local configurations e.g. by means of self-seeding SOAs. Up- and down-stream signals are (usually) transmitted at data rates up to 1.25Gbit/s within one wavelength channel or alternatively within different channels, via the same physical port of a cyclic AWG.

An RSOA featuring the optical network unit is established as a potential cost effective solution for a FTTH passive optical platform with bidirectional operation along single fibre outside plant. Being wavelength independent, this ONU design is able to achieve the high bit rates for a triple play environment, up to 1.25Gbit/s in the experiments collected on this thesis. Semiconductor optical amplifiers are then potential candidates for modulation and detection tasks at the ONU, as they perform both functions efficiently, and provide adequate amplification.

Modulation and photo-detection tests have been implemented in order to demonstrate the architecture feasibility. Results show that bidirectional communication using one single fibre is possible with proper bias levels. ASE noise and Rayleigh backscattering can constrain system performances but a reasonable sensitivity is achieved.

The proposed system designs show reasonable sensitivity levels and validate the bidirectional single-fibre single-wavelength (BSFSW) design for an

optical access network. The bidirectional strategy is, at the same time, very attractive for FTTH architectures owing to the reduction of the capital expenditure (CAPEX) per customer. However, such architectures require novel ONU designs that take into account crosstalk effects that can seriously degrade transmission performance.

Different test-beds have been implemented to analyze the effect of backscattering on a reflective ONU based on an RSOA, with a single fibre to transmit both upstream and downstream signals. They show that the Rayleigh crosstalk can be significantly reduced and the system sensitivity therefore improved, by broadening the optical spectrum of the downstream signal when transmitting base band data. Thus, a modulated downstream signal offers better performance for upstream transmission as compared to an un-modulated optical carrier; optical FSK modulation behaves better than ASK modulation, for instance. Furthermore, Rayleigh backscattering is almost negligible if both, the downstream and upstream data, are multiplexed in the electrical domain by means of sub-carrier multiplexing, as electrical filtering during the reception process spectrally isolates these signals. In addition, FEC techniques enhance reception by adding code redundancy protection to the transmission link, even in systems limited by Rayleigh crosstalk. This also enhances the power budget, crucial for such networks, where the upstream signal suffers twice the link loss due to the lack of a light source at the ONU.

We also highlight the importance of the position of the distribution element inside the access network. With the premise of that the gain applied at the ONU can not be arbitrarily selected, the results show an optimum value for the gain, different on each situation (or of the bias current when employing an RSOA); as well as a dependency on the position of the element and the introduced insertion loss. As a general reference, the gain applied at the ONU side, should not exceed the total loss of the link. The experimental results regarding this issue agree with the theoretical approaches. For high gains, the interference originated from backscatter of the modulated signal becomes a term of relevance on the optical signal-to-interference ratio in upstream direction. Then, low values of the gain are better when the multiplexer is situated at the OLT side and in contrary higher values of the gain are more adequate if the distribution is done at the ONU side.

Therefore, as a general conclusion, is a preferred moderate gain at the ONU and placing the multiplexer in one of the extremes of the link. The distribution network should be quantified in terms of loss and location distances of fibre and components for optimally adjusting the gain value and thus minimizing the RB effect.

As an important remark, the modulation performance of the RSOA would also vary depending on the operating point, that is the bias current and amplitude. For that reason, to vary the current can be a handicap and can also differ from one amplifier to another.

Future research

As a recommendation for further research we propose to deep with de design of integrated structures as a RSOA-EAM or a RSOA-SOA. Thus, the RSOA section will deal with the amplification and the electro-absorption or the SOA section with the modulation. The amplification could be tuned then without interfere in the modulation response of the device.

The major inconvenient presented in actual devices as the noise factor and polarization dependent gain should be improved in order to offer a robust solution for the final user.

And finally, an important issue yet to be resolved is the operating temperature range of semiconductor amplifier devices which should cover the restrictive range of –40 to 85 degrees.

Last Remarks

One of the key questions of the national governments and telecom companies is whether FTTH should be driven by deploying a fibre infrastructure or by creating new services which demand higher bit rate and therefore, since the copper pair has nearly arrived to its limit, fibre solutions. Other key question, and not less important, is if the development of the telecommunications should be let to private companies or there must be some actuation from the governments by deploying fibre to the municipalities or by creating new services like solving administrative issues online, for instance. Some fibre services are already in development as HDTV, and there are plenty of new possibilities as a high definition voice service, for instance.

There are several barriers for the development of FTTH in Europe. The market liberalization was not as successful as it was supposed to be and now it seams that the administration should take part. Companies do not trust in an early investment because they consider that the revenue will come in decades and not in a few years as a company pursues. However, there are more optimistic companies who calculate the revenue for 4 years. Other inconvenient seam to be the technology but it is really not. 1Gbit/s and 10Gbit/s prototype

devices have been tested in the lasts years in labs around the world and most of them are ready to be installed in the field. A clear example illustrating that this problem can be cost-solved is the company *Giga,* from Denmark that offers 10Gbit/s for free connection to everyone. *Cisco* prediction is 1Gbit/s to the home for 2016; we have now 9 years more to accomplish it.

Appendix A

Deduction of the Q-Parameter

A.1 Q-Parameter in Presence of Rayleigh Backscattering and Reflections

By considering zero extinction ratio, $I_0 = 0$, and $I_1 = RP_1 = 2R\bar{P}_S$, the received power for the marks, the Q-parameter is given by

$$Q = \frac{I_1 - I_0}{\sigma_1 + \sigma_0} = \frac{2R\bar{P}_S}{\sqrt{\sum_i \sigma_{Si}^2 + \sum_i \sigma_i^2 + \sigma_T^2} + \sqrt{\sum_i \sigma_i^2 + \sigma_T^2}}, \quad \text{(A.1)}$$

where the sum refers to all the interferences present in the system. σ_{Si}^2 is the covariance of the signal with an interference, σ_i^2 is the variance of the interference and σ_T^2 is the thermal noise of the receiver. For large values of the signal with respect to crosstalk, one can approximate $\sum_i \sigma^2 \approx (\sum_i \sigma)^2$, if we consider that the interferences are independent in between. Thus, we estimate the Q-parameter as function of the (C/S) as

$$Q \approx \frac{2Q_{REF}}{\sqrt{G_{coh} 2(C/S)\left(2Q_{REF}\right)^2 + G_{coh} 2(C/S)^2 \left(2Q_{REF}\right)^2 + 1} + \sqrt{G_{coh} 2(C/S)^2 \left(2Q_{REF}\right)^2 + 1}}, \quad \text{(A.2)}$$

where $(C/S) = \sum_i \sigma_i^2 / \bar{P}_S$; and $Q_{REF} = R\bar{P}_S / \sigma_T$, is the Q-value in a system limited by thermal noise. For a crosstalk to signal ratio larger than 10dB, the terms of $(C/S)^2$ in equation (A.2) can be ignored. This modifies (A.2) into

$$Q \approx \frac{2Q_{REF}}{\sqrt{G_{coh}2(C/S)(2Q_{REF})^2 + 1} + 1}. \tag{A.3}$$

A.2 Q-Parameter in Presence of Rayleigh Backscattering and ASE Noise

When ASE is present in a system, it is dominant compared to thermal noise. Most significant in (A.1) are the terms beating with the data signal, and the interferences. Thus, we can omit also the thermal noise. Then (A.1) transforms into

$$Q \approx \frac{2R\bar{P}_S}{\sqrt{\sigma^2_{S\_C_{RB}} + \sigma^2_{S\_D_{RB}} + \sigma^2_{S\_ASE}}}. \tag{A.4}$$

According to [42] we have $\sigma^2_{SIG-ASE} = 4R^2 2\bar{P}_S P_{ASE} G_{coh}$, where P_{ASE} is the ASE noise. After application to A4 we arrive at a new expression of the Q-parameter, namely

$$Q \approx \frac{1}{\sqrt{G_{coh}2(C/S) + \frac{2P_{ASE}G_{coh}}{\bar{P}_S}}}. \tag{A.5}$$

Appendix B

List of Acronyms

APD	avalanche photo-diode
APON	asynchronous passive optical network
ASE	amplified spontaneous emission
ASK	amplitude shift keying
AWG	arrayed waveguide grating
BER	bit error rate
BLS	broadband light source
BPF	band pass filter
BPON	broadband passive optical network
BSFSW	bidirectional single-fibre single-wavelength
BWDM	band-wise direction division multiplexing
CAPEX	capital expenditures
CDM	code division multiplexing
CDMA	code division multiple access
CO	central office
CPE	customer premises equipment
CW	continuous wavelength
CWDM	coarse wavelength division multiplexing
DDM	direction division multiplexing
DFB	distributed feedback

DWDM	wavelength division multiplexing
EAM	electro absorption modulator
ECL	external cavity laser
EDFA	erbium doped fibre amplifier
EDFA	erbium doped fibre amplifiers
EPON	Ethernet passive optical network
ER	Extinction Ratio
FEC	forward error correction
FEXT	far end crosstalk
FP	Fabry-Perot
FSAN	full service access network
FSK	frequency shift keying
FTTB	fibre to the Building
FTTC	fibre to the Curb
FTTCab	fibre to the Cabinet
FTTH	fibre to the home
FWHM	full width half-maximum
FWM	four-wave mixing
GCSR	grating-coupled sampled reflector
GPON	gigabit-capable passive optical network
IM	intensity modulation
ITU	International Telecommunications Union
LD	laser diode
LED	light emitting diode
MZI	Mach-Zehnder interferometer
MZM	Mach-Zehnder modulator
NEXT	near end crosstalk ()
OBI	optical beat interference
OCDMA	optical CDMA
ODN	optical distribution networks
OLT	optical line termination
ONU	optical network unit
OPLL	optical phase locked loop
p2p	point-to-point
PBS	polarization beam splitter

PDG	polarization dependent gain
PolDM	polarization division multiplexing
PON	passive optical network
PRBS	pseudo random bit sequence
PSK	phase shift keying
RB	Rayleigh backscattering
RL	return loss
RN	remote node
RSOA	reflective semiconductor optical amplifier
SBS	stimulated Brillouin scattering
SCM	sub-carrier multiplexing
SLED	super-luminescent light emitting diode
SMSR	side-mode suppression ratio
SOA	semiconductor optical amplifier
SOA-SA	semiconductor optical amplifier saturated absorber
SSB	single side band modulation
TDM	time division multiplexing
TDMA	time-division multiple access
VCSEL	vertical cavity surface-emitting laser
WDM	wavelength division multiplexing

Appendix C

Research Publications

International Conference publications

[1] C. Arellano, V. Polo, J. Prat, "Effect of the Multiplexer Position in Rayleigh-limited WDM-PONs with Amplified-reflective ONU", Proc. ICTON'07, Rome (Italy), Mo22, July 2007

[2] C. Arellano, K-D. Langer, J. Prat, "On the influence of ONU-Gain on Transmission in Centrally Seeded-Light WDM-PONs", Proc. OFC/NFOEC'07, OTuG4, Anaheim (CA), March 2007

[3] K-D Langer, C. Arellano, J. Vathke, K. Habel, "Recent Developments in WDM-PON Technology", Proc. ICTON'06 Nottingham (UK), invited MoB1-2, July 2006

[4] C. Arellano, C. Bock, K-D. Langer and Josep Prat , "RSOA-based Optical Network Units for WDM-PON", Proc. OFC/NFOEC'06, OTuC1, Anaheim (CA), March 2006

[5] C. Arellano, C. Bock, K-D. Langer and J. Prat, "Optical Network Unit based on Semiconductor Optical Amplifier in single-wavelength single-fiber access network", ITG Fachkonferenz 189, pp.63-68 ,Berlin (Germany), October 2005

[6] C. Arellano, "PONs using reflective optical network units", MUSE Workshop on Optical Access Networks, Heinrich-Hertz-Institut, Berlin (Germany), October 2005

[7] K-D. Langer, K. Habel, J. Vathke, C. Paul, C. Arellano, "Single-fibre passive optical network using full duplex wavelength channels", ITG Fachkonferenz 189, pp.99-104, Berlin (Germany), October 2005

[8] C. Arellano, C. Bock, M. Seimetz, K-D. Langer and J. Prat, "Crosstalk mitigation using Subcarrier Multiplexing and Forward Error Correction in reflection-mode ONU systems", Proc. NOC'05, pp. 271-276, London (UK), July 2005

[9] C. Arellano, J. Prat, "Semiconductor Optical Amplifiers in access networks", Proc. ICTON'05, We.A1.4, Barcelona (Spain), July 2005

[10] C. Arellano, J. Prat, V. Polo, C. Bock, "Bidirectional Single Fiber Transmission Based on a RSOA ONU for FTTH Using FSK-IM Modulation Formats", Proc. OFC/NFOEC'05, JWA46, Anaheim (CA), March 2005

[11] J. Prat, C. Bock, C. Arellano, J. Gené, J. Segarra, G. Junyent, J. Comellas, V. Sales, V. Polo, M. C. Santos, "Redes Avanzadas de Fibra Óptica hasta el Hogar (RAFOH)", Proc. URSI '04

[12] J. Prat, C. Arellano, V. Polo, C. Bock, "Optical Network Unit Based on a Bidirectional Reflective Semiconductor Optical Amplifier", Proc. OpNeTec'04, Pisa (Italy), A5.1, October 2004

[13] J. Prat, C. Bock, C. Arellano, "Bidirectional transmission strategies with Reflection-mode ONUs", Fiber-to-the-Home 2004 Conference, Orlando (FL), October 2004

[14] C. Arellano, C. Bock, J. Prat "Reflective ONUs and modulation schemes for bidirectional transmission", Summer School 2004 of the e-Photon/One NoE on Optical Access Technologies, Mons (Belgium), September 2004

Journal Publications

[15] J. Lázaro, C. Arellano, V. Polo, J. Prat, "Rayleigh Scattering Reduction by Means of Optical Frequency Dithering in Passive Optical Networks with Remotely Seeded ONUs", IEEE Photon. Technol. Lett., vol.19, no. 2, pp.64-66, February 2007

[16] J. Prat, V. Polo, C. Bock, C. Arellano, J.J.Vegas-Olmos, "Full-duplex Single Fiber Transmission using FSK Downstream and IM Remote Upstream Modulations for Fiber-to-the-Home", IEEE Photon. Technol. Lett. vol. 17, no. 3, pp. 702 – 704, March 2005

[17] J. Prat, C. Arellano, V. Polo, C. Bock, "Optical Network Unit Based on a Bidirectional Reflective Semiconductor Optical amplifier for Fiber-to-the-Home Networks", IEEE Photon. Technol. Lett., vol.17, no.1, pp. 250 – 252, January 2005

References

[1] Full Service Access Networks (FSAN), G.x Initiative Documents Collection on World Wide Web, http://www.fsanweb.org

[2] K.-D. Langer, K. Habel, F. Raub, M. Seimetz, "CWDM access network and prospects for introduction of full-duplex wavelength channels" Proc. NOC'05, pp. 68-75, London (UK), July 2005

[3] C. Arellano, M. Seimetz, C. Bock, K. Habel, K-D. Langer, J. Prat, "Crosstalk mitigation using subcarrier multiplexing and forward error correction in reflection-mode ONU systems", Proc. NOC'05, pp. 271-276, London (UK), July 2005

[4] ITU-T, "Broadband Optical Access Systems Based on Passive Optical Networks (PON)", ITU-T Recommendation G.983.1, October 1998

[5] IEEE 802.3ah Ethernet in the First Mile Task Force, "Part 3: Carrier Sense Multiple Access with Collision Detection (CSMA/CD) Access Method and Physical Layer Specifications Amendment: Media Access Control Parameters, Physical Layers, and Management Parameters for Subscriber Access Networks", IEEE Standard 802.3ah-2004, 2004

[6] ITU-T, "Gigabit-capable Passive Optical Networks (GPON)", ITU-T Recommendations G984.x, March 2003

[7] G. Krammer, "Advances in Optical Access Networks", OFC'05, OThG1, Anaheim (CA), March 2005

[8] H. Suzuki, H. Nakamura, J-I Kani, K. Iwatsuki, "A wide-area passive optical network (WDM-PON) accommodating 10 Gigabit Ethernet-based VPN services", ECOC04, Tu4.6.3, Stockholm (Sweden), September 2004

[9] D.P. Shea, J.E. Michel, R.P. Davey, A. Lord, "Analytical Upstream Modelling of A,plified 10Gb/s x 1024 split, 100km Super PON", Proc. LCS'03, session 21, London (UK), 2003

[10] G. Talli, Paul D. Townsend, "Feasibility Demonstration of 100km Reach DWDM Super PON with Upstream Bit Rates of 2.5Gb/s and 10Gb/s", Proc. OFC'05, OFI1, Anaheim (CA), March 2005

[11] J.A. Lázaro, R.I. Martinez, V. Polo, C. Arellano, J. Prat, "Hybrid Dual-Fiber-Ring with Single-Fiber-Trees Dense Access Network Architecture Using RSOA-ONU", Proc. OFC 2007, OTuG2, Anaheim (CA), March 2007

[12] M. Feuer, J. Wiesenfeld, J. Perino, C. Burrus, G. Raybon, S. Shunk, N. Dutta, "Single-port laser-amplifier modulators for local access", IEEE Photon. Technol. Lett., vol.8, no.9, pp.1175-1177, September 1996

[13] N. Buldawoo, S. Mottet, F. Le Gall, D. Sigonge, D. Meichenin, S. Chelles, "A Semiconductor Laser Amplifier-Reflector for the future FTTH Applications", Proc. ECOC'97, p196-199, Edinburgh (UK), September 1997

[14] N. Buldawoo, S. Mottet, H. Dupont, D. Sigogne, D. Mechenin, "Transmission Experiment using a laser amplifier-reflector for DWDM access network", Proc. ECOC'98, pp.273-274, Madrid (Spain) September 1998

[15] J.J. Koponen, M.J. Söderlund, "A duplex WDM passive optical network with 1:16 power split using reflective SOA remodulator at ONU", Proc. OFC'04, MF 99, Los Angeles (CA), March 2004.

[16] H. Takesue, T. Sugie, "Data rewrite of wavelength channel using saturated SOA modulator for WDM Metro/Access networks with centralized light sources", Proc. ECOC'02, 8.5.6, Copenhagen (DE), September 2002

[17] H. Takesue, N. Yoshimoto, Y. Shibata, T. Ito, Y. Tohmori, T. Sugie, "2.5-Gbit/s wavelength channel data rewriter using semiconductor optical saturator/modulator for drop-and-rewrite WDM networks, Proc. ECOC03, 2.3.3, Rimini (Italy), September 2003

[18] T. Rampone, Hong-Wu Li, A. Sharaiha, "Semiconductor Optical Amplifier Used as an In-Line Detector with the Signal DC-Component Conservation", IEEE J. Lightwave Technol., vol.16, no.7, pp.1295-1301, July 1998

[19] J O'Carroll, M.J. Connelly, "Signalling information detection using a semiconductor optical amplifier", Proc. Third International Symposium on Communication Systems and Digital Signal Processing, pp. 132-135, July 2002

[20] J. Prat, C. Arellano, V. Polo, C. Bock, "Optical network unit based on a bidirectional reflective semiconductor optical amplifier for fiber-to-the-home networks, IEEE Photon. Technol. Lett., vol.17, no.1, pp.250-252, January 2005

[21] C. Arellano, V. Polo, C. Bock, J. Prat, "Bidirectional Single Fiber Transmission based on a RSOA ONU for FTTH using FSK-IM Modulation Formats", Proc. OFC05, JWA46, Anaheim (CA), March 2005

[22] A. Houghton, "Research in the IST programme: Broadband for all", Proc. ECOC03, Mo3.1.1, Rimini (Italy), September 2003

[23] R. Sananes, C. Bock, J. Prat, "Techno-Economic Comparison of Optical Access Networks", Proc. ICTON'05, Th.A1.8, Barcelona (Spain), July 2005

[24] K. Iwatsuki, J. Kani, H. Suyuki, M. Fujiwara, "Access and Metro Networks Based on WDM technologies", IEEE J. Lightwave Technol., vol.22, no.11, pp.2623-2630, November 2004

[25] C. Bock, J. Prat, S.D. Walker, "Hybrid WDM/TDM PON using the AWG FSR and featuring Centralized Light Generation and Dynamic Bandwidth Allocation", IEEE J. Ligthwave Technol., vol.23, no.12, December 2005

[26] A. Borghesi, I. Lealman, D.W. Smith, "Semiconductor optical amplifier for CWDM metro and access networks", Proc. NOC'05, pp.99-106, London, (UK), July 2005

[27] M. Seimetz, "Bidirectional Transmission for Optical Access Networks-Conventional Techniques and Novel Alternatives", Proc. NOC'04, pp.170-179, Eindhoven (NL), June 2004

[28] J. Prat, V. Polo, C. Bock, C. Arellano, J.J.Vegas-Olmos, "Full-duplex single fiber transmission using FSK downstream and IM remote upstream modulations for fiber-to-the-home", IEEE Photon. Technol. Lett., vol.17, no.3, pp. 702-704, March 2005

[29] J. Prat, J. M. Fábrega, "New homodyne receiver with electronic I&Q differential demodulation", Proc. ECOC'05, We4.P.104, Glasgow (UK), September 2005

[30] S. Narikawa, H. Sanjo, N. Sakurai, K. Kumozaki, T. Imai, "Coherent WDM-PON using directly modulated local laser for simple heterodyne transceiver", Proc. ECOC'05, We 3.3.2, Glasgow (UK), September 2005

[31] H-C Kwon, W-S Jang, S-K Han, "WDM-PON downstream optical link using wavelength-locked FP-LD by spectrally-sliced FP-LD", IEICE Trans. Communications, vol.E88-B, no.1, pp. 384-387, 2005

[32] H-C Kwon, W-S Jang, S-K Han, "Optimisation of remote seeding optical source in wavelength-locked FP-LD bidirectional WDM access optical link", IEE Proc. Optoelectron., vol.152, no.5, pp. 247-249, October 2005

[33] S-M Lee, S-G Mun, C-H Lee, "Consolidation of a metro network into an access network based on long-reach DWDM-PON", OFCNFOEC'06, NWA2, Anaheim (CA), March 2006

[34] D.J. Shin, D.K. Jung, H.S. Shin, J.W. Kwon, S. Hwang, Y.J. Oh, C.S. Shim, "Hybrid WDM/TDM-PON for 128 subscribers using λ-selection-free transmitters", Proc. OFC'04, PDP4, Los Angeles (CA), March 2004

[35] D. J. Shin et al., "C/S-band WDM-PON employing colorless bidirectional transceivers and SOA-based broadband light sources", Proc. OFC'05, PDP36, Anaheim (CA), March 2005

[36] E. Wong, X. Zhao, C.J. Chang-Hasnain ,W. Hofmann, M.C. Amann, "Uncooled optical injection-locked 1.55 μm VCSEL for upstream transmitters in WDM-PONs", Proc. OFC'06, PDP50, Anaheim (CA), March 2006

[37] Y. Wen et al., "2.5 Gb/s WDM-PON upstream transmission scheme using Fabry-Perot laser diodes injection-locked by a spectrum sliced supercontinuum pulse source without polarization control", Proc. OECC/COIN'04, 13B2-3, 2004

[38] Z. Xu, Y. Jing Wen, C-J Chae, Y. Wang, C. Lu, "10 Gb/s WDM-PON upstream transmission using injection-locked Fabry-Perot laser diodes", OFCNFOEC'06, JThB72, Anaheim (CA), March 2006

[39] P. Healey et al. "Spectral slicing WDM-PON using wavelength-seeded reflective SOAs", IEEE Electronics Lett., vol.37, no.19, pp. 1181-1182, September 2001

[40] S. Hann et al. "Bi-directional transmission using a self-tuned Fabry-Perot laser diode at the subscriber in WDM-PON", Proc. ECOC'04, We 4.144, Stockholm (Sweden), September 2004

[41] E. Wong et al. "Directly-modulated self-seeding reflective SOAs as colorless transmitters for WDM passive optical networks", Proc. OFC'06, PDP49, Anaheim (CA), March 2006

[42] G. P. Agrawal, *Fibre-Optic Communication Systems*, 3rd ed. New York: Wiley, 2002

[43] T. Rampone, H-W Li, A. Sharaiha, "Semiconductor Optical Amplifier Used as an In-Line Detector with the Signal DC-Component Conservation", J. Ligthwave technol., vol. 16, no. 7, July 1998

[44] E. P. Burr, J. B. Song, A. J. Seeds, C. C. Button, "28 ps recovery time in an InGaAsP/InGaAsP multiple-quantum-well saturable absorber employing carrier sweepout", J. Applied Physics, vol.90, no.7, October 2001

[45] Z. Bakonyi, G. Onishchukov, C. Knöll, M. Gölles, F. Lederer, R. Ludwig, "In-Line Saturable Absorber in Transmission Systems with Cascaded Semiconductor Optical Amplifiers", IEEE Photon. Technol. Lett., vol.12, no.5, May 2000

[46] I.T. Monroy, F. Öhman , K. Yvind, R. Kjær, C. Peucheret, A.M.J Koonen, P. Jeppesen, "85 km long reach PON system using a reflective SOA-EA modulator and distributed Raman amplification", Proc. LEOS'06, WEE4, Montreal (CA), October 2006

[47] A.Garreau, J.Decobert , C. Kazmierski, M-C. Cuisin, J-G. Provost, H.Sillard, F.Blache, D. Carpentier, J.Landreau, P.Chanclou, "10Gbit/s Amplified Reflective Electroabsorption Modulator for Colorless Access Networks", Indium Phosphate and Related Materials Conference Proceedings, TuA2.3, May 2006

[48] M. Oskar van Deventer, *Fundamentals of Bidirectional Transmission over a Single opticalFibre*, Kluwer Academic Publishers, 1996

[49] B-G Ahn, Y. Park, "A Symmetric-Structure CDMA-PON System and its Implementation", IEEE Photonic. Technol. Lett., vol.14, no.9, September 2002

[50] C. Zhang, K. Qiu, B. Xu "Multiple-access technology based on optical code-division multiple access for passive optical networks", SPIE Optical Engineering vol.45, no.10, October 2006

[51] S. Yamazaki, T. Ono, H. Shimizu, K. Emura, "A bidirectional common polarization control method for coherent optical FDM transmission system", Photonic. Technol. Lett., vol.2, no.2, pp.135-138, February 1990

[52] I. Tsalamanis, E. Rochat, S.D. Walker, "Experimental demonstration of cascaded AWG access network featuring bi-directional transmission and polarization multiplexing", Optics Express, vol.12, no.5, pp.764-769, May 2004

[53] G-W. Lu, N. Deng, C-K. Chan, L-K Chen, "Use of downstream inverse-RZ signal for upstream data re-modulation in a WDM passive optical Network", Proc. OFC'05, OFI8, Anaheim (CA), March 2005

[54] W. Hung, C-K Chan, L-K Chen, C. Lin, "System characterization of a robust re-modulation scheme with DPSK downstream traffic in a WDM access network", Proc. ECOC'03, We3.4.5, Rimini (Italy), September 2003

[55] C. Bock, M.P. Thakur, C. Arellano, J.J. Lepley, S.D. Walker, J. Prat, "Wavelength Independent RSOA-based ONU for FTTH PON Implementation of Switched Ethernet Services", Proc. ECOC05, Glasgow (UK), Mo4.3.3, September 2005,

[56] M.P. Thakur, C. Bock, J.J. Lepley, C. Arellano, J. Prat, S.D. Walker, "Passive VDSL Transmission over Single Fibre using Reflective Technique at Customer Premises", Proc. ECOC'05, Glasgow (UK), Mo4.3.6, September 2005

[57] A. Loayssa, D. Benito, M. J. Garde, "Single-Sideband Suppressed-Carrier Modulation Using a Single-Electrode Electrooptic Modulator", IEEE Photon. Technol. Lett., vol.13, no.8, August 2001

[58] P. Gysel, R. K. Staubli, "Statistical Properties of Rayleigh Backscattering in Single-Mode Fibres", IEEE J. Lightwave Technol., vol.8, no.4, pp.561-567, April 1990

[59] P. Gysel, R. K. Staubli, "Spectral properties of Rayleigh backscattered light from single-mode fibres caused by a modulated probe signal, IEEE J. Lightwave Technol., vol.8, no.12, December 1990

[60] R. K. Staubli, P. Gysel, "Crosstalk penalties due to coherent Rayleigh noise in bidirectional optical communication systems" IEEE J. Lightwave Technol. vol.9, no.3, March 1991

[61] P. P. Bohn, S. K. Dass, "Return Loss Requirements for Optical Duplex Transmission", IEEE J. Lightwave Technol., vol.5, no.2, February 1987

[62] T. H. Wood, R. A. Linke, "Observation of Coherent Rayleigh Noise in Single-Source Bidirectional Optical Fiber Systems", IEEE J. Lightwave Technol., vol.6, no.2, February 1988

[63] D. Derickson, "*Fibre optics test and measurement*" Hewlett-Packard Professional Books, Ed. Prentice Hall, 1997

[64] S. Radic, N. Vukovic, S. Chandrasekhar, A. Velingker and A. Srivastava, "Forward Error Correction Performance in the Presence of Rayleigh-Dominated Transmission noise", Photonic. Technol. Lett., vol.15, no.2, February 2003

[65] K.-D. Langer, K. Habel, J. Vathke, C. Paul and C. Arellano, "Single-fibre passive optical network using full duplex wavelength channels", ITG Fachbericht 189, pp.99-104, Berlin (Germany), October 2005

[66] J. Prat, M. Omella, V. Polo, "Wavelength shifting for colorless ONUs in single-fiber WDM-PONs", Proc. OFC/NFOFC'07, OTuG6, Anaheim (CA), March 2007

[67] Charles H. Henry, "Theory of the linewidth in Semiconductor Lasers", IEEE J. Quantum Electronics, vol.QE-18, no.2, February 1982.

[68] F. Payoux, P. Chanclou, T. Soret, N. Genay, R. Brenot, "Demonstration of a RSOA-based Wavelength Remodulation in 1.25 Gbit/s Bidirectional Hybrid WDM-TDM PON", Proc. OFC/NFOFC, OTuC4, Anaheim (CA), March 2006

[69] P. Healey, P. Townsend, C. Ford, L. Johnston, P. Townley, I. Lealman, L. Rivers, S. Perrin, R. Moore "Spectral slicing WDM-PON using wavelength-seeded reflective SOAs", IEEE Electronic Lett., vol.37, pp.1181-1182, 2001

[70] Z. Xu, Y.J Wen, C-J Chae, Y. Wang, C. Lu, "10 Gb/s WDM-PON Upstream Transmission Using Injection-locked Fabry-Perot Laser Diodes", Proc. OFC/NFOFC'06, JThB72, Anaheim (CA), March 2006

[71] F. Payoux, P. Chanclou, M. Moignard, R. Brenot, "Gigabit optical Access using WDM PON based on Spectrum Slicing and Reflective SOA," Proc. ECOC'05, We3.3.5, Glasgow (UK), September 2005

[72] J. A. Lázaro, R. I. Martinez, V. Polo, C. Arellano, J. Prat, "Hybrid Dual-Fibre-Ring with Single-Fibre-Trees Dense Access Network Architecture Using RSOA-ONU", Proc. OFC/NFOFC'07, OTuG2, Anaheim (CA), March 2007

[73] M. Fujiwara, J-I. Kani, H. Suzuki, K. Iwatsuki, "Impact of Backreflection on Upstream Transmission in WDM Single-Fibre Loopback Access Networks", IEEE J. Ligthwave Technol., vol.24, pp.740-746, 2006

[74] S. K. Das, "Beat Interference Penalty in Optical Duplex Transmission", IEEE J. Lightwave Technol. vol.20, no.2, pp. 213-217, February 2002

[75] M. Sumida, T. Kubo, T. Imai, "Limitations Imposed by Rayleigh Backscattering in closely Interleaved, Bidirectional WDM Transmission Systems," IEEE Photon. Technol. Lett., vol.15, pp.150-152, 2003

[76] Peter P. Bohn, Santaku, 'Return Loss Requirements for Optical Duplex Transmission', IEEE J. Ligthwave Technol, vol.5, pp.243-254, 1987

Biography

Cristina Arellano was born in Barcelona, Spain, in 1976. She received the M.Sc. degree in telecommunications engineering from the Technical University of Catalonia (Universitat Politècnica de Catalunya - UPC), in 2002. In 2003 she joined the Optical Communications Group of the Department of Signal Theory and Communications of the UPC where she finish her Ph.D research in 2007. Her work is centered on optical access networks and is mainly focused on bidirectional communication, semiconductor optical amplifiers and their applications for Fibre-to-the-Home networks.